AEDC-TR-77-67

cy.1

A STUDY OF ACOUSTIC DISTURBANCES AND MEANS OF SUPPRESSION IN VENTILATED TRANSONIC WIND TUNNEL WALLS

PROPULSION WIND TUNNEL FACILITY
ARNOLD ENGINEERING DEVELOPMENT CENTER
AIR FORCE SYSTEMS COMMAND
ARNOLD AIR FORCE STATION, TENNESSEE 37389

October 1977

Final Report for Period July 1, 1975 to June 30, 1976

Prepared for

ARNOLD ENGINEERING DEVELOPMENT CENTER
AIR FORCE SYSTEMS COMMAND
ARNOLD AIR FORCE STATION, TENNESSEE 37389

and

NATIONAL AERONAUTICS AND SPACE ADMINISTRATION
AMES RESEARCH CENTER
MOFFETT FIELD, CALIFORNIA 94035

NOTICES

When U. S. Government drawings specifications, or other data are used for any purpose other than a definitely related Government procurement operation, the Government thereby incurs no responsibility nor any obligation whatsoever, and the fact that the Government may have formulated, furnished, or in any way supplied the said drawings, specifications, or other data, is not to be regarded by implication or otherwise, or in any manner licensing the holder or any other person or corporation, or conveying any rights or permission to manufacture, use, or sell any patented invention that may in any way be related thereto.

Qualified users may obtain copies of this report from the Defense Documentation Center.

References to named commercial products in this report are not to be considered in any sense as an endorsement of the product by the United States Air Force or the Government.

This report has been reviewed by the Information Office (OI) and is releasable to the National Technical Information Service (NTIS). At NTIS, it will be available to the general public, including foreign nations.

APPROVAL STATEMENT

This technical report has been reviewed and is approved for publication.

FOR THE COMMANDER

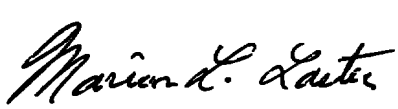

MARION L. LASTER
Director of Test Engineering
Deputy for Operations

ALAN L. DEVEREAUX
Colonel, USAF
Deputy for Operations

REPORT DOCUMENTATION PAGE		READ INSTRUCTIONS BEFORE COMPLETING FORM
1 REPORT NUMBER AEDC-TR-77-67	2. GOVT ACCESSION NO.	3. RECIPIENT'S CATALOG NUMBER
4 TITLE (and Subtitle) A STUDY OF ACOUSTIC DISTURBANCES AND MEANS OF SUPPRESSION IN VENTILATED TRANSONIC WIND TUNNEL WALLS		5 TYPE OF REPORT & PERIOD COVERED Final Report - July 1, 1975 - June 30, 1976 6 PERFORMING ORG. REPORT NUMBER
7 AUTHOR(s) N. S. Dougherty, Jr., ARO, Inc.		8 CONTRACT OR GRANT NUMBER(s)
9 PERFORMING ORGANIZATION NAME AND ADDRESS Arnold Engineering Development Center Air Force Systems Command Arnold Air Force Station, Tennessee 37389		10. PROGRAM ELEMENT, PROJECT, TASK AREA & WORK UNIT NUMBERS Program Element 65807F
11 CONTROLLING OFFICE NAME AND ADDRESS Arnold Engineering Development Center (XRFIS) Arnold Air Force Station, Tennessee 37389		12 REPORT DATE October 1977 13. NUMBER OF PAGES 101
14 MONITORING AGENCY NAME & ADDRESS (if different from Controlling Office)		15 SECURITY CLASS. (of this report) UNCLASSIFIED 15a. DECLASSIFICATION/DOWNGRADING SCHEDULE N/A

16 DISTRIBUTION STATEMENT (of this Report)

Approved for public release; distribution unlimited.

17 DISTRIBUTION STATEMENT (of the abstract entered in Block 20, if different from Report)

1. Porous wall wind tunnels -- Noise
2. Noise -- Damping

18 SUPPLEMENTARY NOTES

Available in DDC

19. KEY WORDS (Continue on reverse side if necessary and identify by block number)

disturbances (acoustic)	wind tunnel
noise	walls (ventilated)
suppression	Mach numbers
transonic flow	

20 ABSTRACT (Continue on reverse side if necessary and identify by block number)

An experimental investigation of acoustic disturbances and means of suppression from ventilated transonic wall samples was performed in a low-background-noise research tunnel at AEDC. Configurations for ventilation investigated were longitudinally slotted walls, with and without baffles in the slots, slats versus round rods, and perforated walls with normal or inclined circular holes with varied hole sizes and varied diameter/wall thickness

DD FORM 1 JAN 73 1473 EDITION OF 1 NOV 65 IS OBSOLETE

20. ABSTRACT (Continued)

ratio. Comparative acoustic data were acquired over a broad range of subsonic Mach numbers. Several of these wall configurations were found to emit intense, discrete whistling noise with overall root-mean-square amplitudes as large as five percent of the free-stream dynamic pressure. In all cases except one, suppressed noise levels not exceeding 0.75 percent of the free-stream dynamic pressure were achieved compared to a background noise level for the tunnel of approximately 0.47 percent with solid test section walls. Noise suppression was accomplished by means of appropriate devices added to the wall samples which could have application to actual transonic wind tunnel test sections.

AFSC
Arnold AFS Tenn

PREFACE

The work reported herein was jointly sponsored by the Arnold Engineering Development Center (AEDC), Air Force Systems Command (AFSC), and the NASA-Ames Research Center, and the work was conducted by AEDC under Program Element 65807F. The results were obtained by ARO, Inc., AEDC Division (a Sverdrup Corporation Company), operating contractor for the AEDC, AFSC, Arnold Air Force Station, Tennessee. This experimental research was conducted under ARO Projects No. P32A-B2A and P34A-H4A. The author is N. S. Dougherty, Jr., ARO, Inc. Alexander F. Money is the Air Force project manager. The manuscript (ARO Control No. ARO-PWT-TR-77-36) was submitted for publication on May 11, 1977.

CONTENTS

ILLUSTRATIONS

Page

TABLES

1.0 INTRODUCTION

The use of ventilated test section walls is the standard practice for establishing flows near Mach 1.0 in wind tunnels. Guidelines for choosing the configuration of the ventilated test section walls and the relative aerodynamic performance of various configurations are discussed in Ref. 1. However, most of the configurations produce intense aerodynamic noise in the test section, e.g., Refs. 2 through 6, in some cases exceeding 152 db (Ref. 0.0002 dynes/cm^2) or about three percent of the free-stream dynamic pressure of the flow. In these cases, the test section walls were found to be the predominant source of overall aerodynamic noise.

There is growing concern that aerodynamic noise found in transonic wind tunnels can have potentially deleterious effects on test data. Two investigations which have shown effects to exist are the boundary-layer transition data correlation in Ref. 7 and the buffet and vibration data studies in Ref. 8.

With this in mind, the reduction of aerodynamic noise in transonic tunnels has been an objective of experimental research at AEDC for several years. One of the results of this research has been the "splitter plate"* modification for perforated walls (Ref. 9). This "splitter plate" modification is a proposed device for suppressing edgetones in perforated walls which have 60-deg inclined holes such as the test section walls in the Arnold Engineering Development Center (AEDC) transonic wind tunnels.

*United States Patent No. 3,975,955.

A recently developed technique giving effective suppression of edgetones in variable-porosity perforated walls having 60-deg inclined holes is wire screen overlay. The screen overlay was demonstrated in the NASA/Marshall Space Flight Center 14-In. Transonic Wind Tunnel and is described in Ref. 12. Both the "splitter plate" and the wire screen overlay noise suppression schemes have been used with success on experimental wall samples in the ONERA 6- by 6-ft S-2 tunnel at Modane, France, which also has 60-deg inclined-hole, variable-porosity walls (see Ref. 13).

The research reported herein is a continuation of a previous investigation (Ref. 9). The present investigation included an extension of the wire screen overlay concept (Ref. 12) to walls other than the variable-porosity walls with 60-deg inclined holes and an extension of the "splitter plate" to a particular configuration of normal-hole perforated walls. The purpose of this report is to present the results obtained in comparative tests of these various types of walls and to show the effectiveness of the noise suppressive measures tried.

2.0 APPARATUS

2.1 ACOUSTIC RESEARCH TUNNEL

The 6-in. Acoustic Research Tunnel (ART, Fig. 1) is a continuous flow, atmospheric indraft tunnel capable of being operated over the Mach number range from 0.05 to 1.10. For most of the present experiments, the Mach number was limited to < 1.0 by a minimum in cross-sectional area at the diffuser entrance flaps which were used to obtain as low as possible background noise in the test section. (Removal of the flaps introduces a separated region from a rearward-facing step at the diffuser entrance and an undesirable noise source.)

The ART is equipped with acoustic silencers in the diffuser and plenum exhaust ducts which have 46-db maximum attenuation rating at

1,200 Hz. Operation at Mach numbers above the choking limit is provided by the flow removal through the ventilated wall samples. The wall angle (top and bottom) may be adjusted from 0 to 0.5-deg divergence as necessary for setting a flat axial Mach number distribution (constant velocity) along the test section. There are mechanical vibration-isolation expansion joints for minimizing structural vibrations of the test section.

The ART is remotely powered by the Tunnel 16T Plenum Evacuation System (PES) through a large-volume reservoir. Flow straightening and turbulence suppression are provided in the tunnel intake by a honeycomb and damping screen. All of these features were provided in the ART to achieve a minimum of background noise for acoustic experiments. The tunnel has a fixed nozzle with a 16:1 geometric contraction ratio. The test section is 6 by 6 in. square at the nozzle exit and 24 in. in length.

There is a removable test section extension channel 6 by 6 in. square, 24 in. in length, which may be placed between the nozzle and test section of the ART. This channel was used in the present experiments for changing boundary-layer thickness on certain wall samples.

2.2 WALL SAMPLES

Four basic wall configurations were studied: longitudinally slotted walls, longitudinally slotted walls with slot baffles, perforated walls with normal circular holes, and perforated walls with inclined circular holes. These configurations represent, in general, the four distinct concepts in transonic wind tunnel test section design found in practice. The evolution of each is traced in part in Ref. 1. Variations on the slotted-wall concepts investigated in the present research included longitudinal tapered slots with slats that formed the wall structure versus flat-to-round transitioning longitudinal rod walls, which have a variable-porosity feature. The second slotted-wall

variation was the baffled-slot versus open-slot concept. Variations on the circular-hole perforated-wall concept were hole size/wall thickness ratio, inclined versus normal holes, and a variable-porosity feature for perforated walls having inclined holes. Three different hole sizes were selected for the inclined-hole perforated walls.

The rationale for choosing the particular configurations to be investigated was that these are all configurations found in some particular presently operating wind tunnel with one exception, the longitudinal rod wall which is a new concept recently proposed for possible application to transonic tunnels.

2.2.1 Slotted Walls

Longitudinal Tapered Slots

Slotted walls were initially developed and are in use at the NASA/Langley Research Center. The percentage open area is usually about five percent in the region of the test section where models are placed, and the slots are tapered in width to give gradual axial increase in open area in order to compensate for the boundary-layer growth. There are tunnel-to-tunnel variations in slot taper tailored to the needs of a particular tunnel to achieve flat axial Mach number distribution.

Slot samples were fabricated for the subject test with six-percent maximum open area and linear rate of increase in open area. These samples are shown in Fig. 2 and were fitted into 4-in.-wide wall frames giving six slots spanwise. Some distinguishing features of these slots were the rounded edge and 45-deg bevel angle of the slot cross section. These features of the wall were patterned from the NASA/Langley Research Center tunnels.

Longitudinal Rods

A slotted-wall configuration formed by precision-honed, polished rods of circular cross section, laid adjacent to one another and parallel to the test section axis is a novel concept for test section design. Interest in this concept stemmed from the possibility that such walls might produce lower test section noise levels than present slotted walls as well as provide better attenuation of shock and expansion waves from models because of the rounded surfaces. An additional advantageous feature of such a wall would be a capability for porosity variation by depressing alternate rods, zero porosity being obtained with all the rods pressed together with contact between rods.

The samples of walls investigated in the ART were specially fabricated by the National Bureau of Standards. Details of the samples are shown in Fig. 3. The rod diameter was 0.125 in. A larger version of walls with 0.25-in.-diam rods was investigated for tunnel flow quality and wave attenuation characteristics in the 1-ft Aerodynamic Wind Tunnel (1T) at AEDC, Ref. 14. The configuration of walls investigated included a region of transition in geometry from flat to round in the forward portion of the test section where the porosity was gradually increased from zero to a uniform value. The porosity (percent open area) was adjustable from zero to ten percent using a technique where every other rod could be depressed a distance sufficient to provide the desired open area as shown in Table 1 (also see Fig. 3b).

Longitudinal Baffled Slots

Finely spaced baffled slots are used in the transonic tunnels at the NASA/Ames Research Center. As discussed in Ref. 1, there is the advantage with this type of wall that the baffle breaks up longitudinal communication beneath an impinging shock wave from a model, reducing the strength of the reflected wave.

The walls are formed by structural steel channels laid side by side. A small gap is left between channels in which corrugated metal inserts are tack welded to form baffled slots. The configuration tested in these experiments was an actual sample of wall from the NASA/Ames Research Center 11-Ft Transonic Wind Tunnel. Details of the slot-baffle configuration are given in Fig. 4.

2.2.2 Perforated Walls

Normal Holes

Two configurations of normal-hole perforated walls were investigated, both having the same hole pattern as shown in Fig. 5 with 0.50-in.-diam holes. The difference in configurations investigated was plate thickness and, thus, the aspect ratio of the hole.

The porous open area of this wall is 22.5 percent. Characteristics of the normal-hole wall at 22.5-percent porosity in regard to shock and expansion wave attenuation are described in Ref. 1.

Inclined Holes

Motivation for improving the attenuation of shock and expansion waves in transonic test sections to minimize the interferences on test models led to the inclined-hole wall. As described in Refs. 1 and 10, best results on a 20-deg cone-cylinder calibration body were obtained with 60-deg hole inclination and six-percent porosity. This type of wall has differential resistance between inflow and outflow (more outflow for a given differential pressure than inflow for the same negative differential pressure). Differential resistance characteristics are required to improve attenuation of both shock and expansion waves from models. This particular wall was found to be most effective for a 20-deg cone-cylinder model tested at Mach numbers close to 1.2 (Ref. 10).

Actual samples of this type wall from Tunnel 16T were tested in the ART. The hole diameter is 0.75 in. in Tunnel 16T. Details of the wall sample configuration are shown in Fig. 6a.

In addition to these samples of Tunnel 16T wall, wall samples taken from Tunnel 1T, which has a 1- by 1-ft-square test section modeled after the 16-ft tunnel, were also tested. This sample, which has 0.125-in.-diam holes, is shown in Fig. 6b. Wall thickness in both full- and model-scale tunnels (16T and 1T) is the same as the hole diameter. The criterion for hole size selection is based on tunnel size as discussed in Ref. 11.

Inclined Holes - Variable Porosity

A later development of the 60-deg inclined-hole perforated wall was to add variable porosity capability. The wall is formed by two plates match drilled to the same hole pattern. The configuration tested in ART was that used in the AEDC 4-ft Aerodynamic Wind Tunnel (4T). Details of this wall configuration are shown in Fig. 6c. The sliding backup plate is moved forward relative to the fixed airstream surface plate to partially close the holes. The plates have 0.50-in.-diam holes, which give a porosity variation in Tunnel 4T from zero- to ten-percent open area.

For normal operation in Tunnel 4T, porosity is fixed for all Mach numbers $\leq$ 1.0 at nominally five or six percent. Porosity is varied only in the range of M_∞ from 1.0 to 1.2 as described, for example, in Ref. 15.

2.3 INSTRUMENTATION

2.3.1 Sensor Placement

A single microphone was used to measure pressure fluctuations in the test section with various wall samples installed. The microphone

was a Bruel and Kjaer Model 4136 condenser-type, 0.25 in. in diameter. The microphone was flush mounted in the test section sidewall using a teflon sleeve for vibration and electrical insulation from the wall as shown in Fig. 7.

The location of the microphone was on the test section sidewall centerline 18.75 in. from the throat (see Fig. 8). There was an array of static pressure orifices in the nozzle and test section sidewall. Tunnel total pressure was derived from a pitot probe in the inlet immediately upstream of the start of nozzle contraction, downstream of the honeycomb and screens. Plenum chamber pressure was measured through a static pressure orifice installed on the plenum forward wall. All of the pressure measurements were recorded on a precision balance, strain-gage-type pressure transducer through a sequenced stepping switch. The tunnel total temperature was measured by a thermocouple in still air ahead of the nozzle intake.

2.3.2 Signal Conditioning - Calibration

The microphone signal was conditioned through a matched set of preamplifier, amplifier, and power supply electronics manufactured by Bruel and Kjaer. The signal was recorded on a true root-mean-square voltmeter with an overall system frequency response estimated to have been from approximately 10 Hz to 30 kHz. The signal was also recorded on a real-time Fourier spectrum analyzer capable of recording signals from 5 Hz to 20 kHz.

The microphone was calibrated in place by application of a 140 ± 0.5-db sine wave from a pistonphone at 1-kHz frequency. The steady-state pressure transducer used for measuring tunnel flow conditions was calibrated using a vacuum-referenced Ideal mercury manometer.

2.3.3 Flow Visualization

A spark schlieren system was employed for flow visualization through the 8-in.-diam optical sidewall access ports. The spark illumination was of 2-μsec duration. Simple adjustment of knife-edge cutoff provided shadowgraph views instead of schlieren when desired.

3.0 PROCEDURES

3.1 TESTING

The basic test procedure was to take measurements at varied Mach numbers for each wall sample, measured noise levels having dependency upon the Mach number. The procedure was as follows:

1. Perform a background noise calibration with solid test section wall inserts. This background was the reference level to which all ventilated-wall sample data would be compared.

2. Test each basic ventilated-wall configuration, top and bottom wall samples installed.

3. Test each wall sample with the particular noise suppressive measure installed.

In this way, directly comparable acoustic data could be acquired with a defined reference base level.

In all cases, test section wall divergence, in combination with plenum suction, was used to set as near constant a static pressure distribution as possible in the test section for flat Mach number distribution. Example Mach number distribution data are shown in Section 4.1. In general, increased divergence angle was required for increasing Mach number, and plenum suction was added for Mach numbers greater than or equal to 0.7.

One of the sidewall static pressure orifices, at 16 in. from the throat, was used as the reference to which the others at different axial stations were compared. This orifice was the one upon which calculations of relevant flow parameters were based, e.g., Mach number, dynamic pressure, and wall pressure differential.

3.2 DATA REDUCTION

The reference wall static pressure together with the tunnel total pressure was used to compute Mach number, M_∞ , by

$$\frac{p_t}{p_s} = \left(1 + \frac{\gamma - 1}{2} M_\infty^2\right)^{\gamma/(\gamma-1)} \tag{1}$$

and the dynamic pressure of the flow by

$$q_\infty = \frac{\gamma}{2} p_s M_\infty^2 \tag{2}$$

An average wall differential pressure coefficient (between test section and plenum chamber) was computed by

$$C_{p\ wall} \equiv \frac{p_s - p_c}{q_\infty} \tag{3}$$

where p_c was the measured plenum chamber pressure.

Time-averaged rms fluctuating pressure level recorded on the microphone was computed from instantaneous p'(t) by

$$\tilde{p}_{rms} = \frac{1}{T} \int_0^T \sqrt{p'^2(t)}\ dt \tag{4}$$

These readings were then normalized to fluctuating pressure coefficient, ΔC_p, defined as follows

$$\Delta C_p \equiv \frac{\tilde{p}_{rms}}{q_\infty} \times 100\ , \text{percent} \tag{5}$$

These were overall rms levels of fluctuations. Certain predominant frequency components identified by Fourier analysis of the microphone spectra were read directly in Hz. Acoustic velocity in the test section free-stream flow was computed from

$$c_\infty = \sqrt{\gamma R T_s} \tag{6}$$

where T_s was derived from

$$\frac{T_t}{T_s} = 1 + \frac{\gamma - 1}{2} M_\infty^2 \tag{7}$$

Then free-stream velocity was computed from

$$U_\infty = c_\infty M_\infty \tag{8}$$

Nondimensionalized frequency in the form of Strouhal number, S, was computed from

$$S = \frac{hf}{U_\infty} \tag{9}$$

where f is a frequency component of interest and h is a particular representative length dimension of the perforation assumed to be the contributing source of noise at that frequency.

4.0 RESULTS

A summary of the ventilated-wall configurations investigated is given in Table 2. Results of the experiments performed will be discussed in an order of increasing difficulty in achieving noise suppression among the various configurations investigated. Data are presented first for the solid wall background calibration. Results are then presented for the longitudinal tapered slot, the longitudinal rod wall, the perforated wall with normal holes, the perforated wall with inclined holes, and, finally, the baffled longitudinal slot.

4.1 SOLID WALL

The ideal case of a minimum background noise level in a wind tunnel having turbulent boundary layers on the test section walls is the case where smooth solid walls are employed. Tunnel flow quality of the particular wind tunnel in which experiments are to be performed is germane to acoustical experiments of the type performed herein, inasmuch as boundary-layer characteristics and axial flow uniformity in the test section are significant parameters.

Mach number as a function of axial distance from the start of nozzle contraction in the ART is shown in Fig. 9a. Mach number is a significant parameter with regard to resonance characteristics of a test section of particular length and cross-sectional dimensions when discrete aerodynamic noise is present above the broadband background noise (see Ref. 16). Shown in Fig. 9b are representative boundary-layer data (Ref. 17) for the bottom test section wall of the ART at $M_\infty = 0.5$. Typical Mach number distribution data are shown in Fig. 9c for every inch along the test section from a calibration test performed with a specially instrumented sidewall in place of the normally used sidewall fitted with the optical port. Local Mach number was based at each station on sidewall measurement of local static pressure. The data presented in Fig. 9c with open symbols denote results with solid top and bottom wall inserts. Data given for Mach numbers above the choking limit were obtained in this calibration by using Tunnel 1T perforated-wall samples in place of the solid wall inserts, and the results are indicated in Fig. 9c by data points with closed symbols.

The solid wall background noise data are presented in Fig. 10. The measured levels of $\tilde{p}_{rms}$ in db (Ref. 0.0002 dynes/cm^2) are shown in Fig. 10a. The normalized levels in the form of ΔC_p are shown in Fig. 10b. The reader is referred to Refs. 18 and 19 for representative levels of expected pressure fluctuations from turbulent boundary-layer flow. The microphone used in the present experiments was larger with respect to

the boundary-layer thickness than what would be desired for the study of a turbulent boundary layer. The ΔC_p data are compared with an often-cited empirical correlation at adiabatic wall conditions given in Ref. 20 for compressible turbulent boundary layers

$$\Delta C_p = \frac{0.6}{\left(1 + 0.14\ M_\infty^2\right)} \tag{10}$$

General agreement is to be noted of the data in Fig. 10b with Eq. (10) at higher M_∞ but poor agreement at lower M_∞.

The experimental uncertainty in the measurements are:

$\tilde{p}_{rms} \cong \pm 8.5$ percent

$p_s \cong \pm 0.4$ percent

$p_t \cong \pm 0.4$ percent

Computed $M_\infty \cong \pm 1.0$ percent, Eq. (1)

Computed $q_\infty \cong \pm 2.5$ percent, Eq. (2)

Computed $\Delta C_p \cong \pm 11$ percent, Eq. (5)

4.2 LONGITUDINAL TAPERED SLOTS

The results obtained with the longitudinal tapered-slotted walls are shown in Fig. 11 in the form of ΔC_p versus M_∞. These data are compared with the solid wall background. For approximately the range $0.2 \leq M_\infty \leq 0.6$, the longitudinal tapered-slot data indicate an average value for ΔC_p to be approximately 0.47 percent. These slotted-wall data were actually lower in amplitude than the solid wall background. No case will be made here that the slotted-wall data should be lower because the uncertainty in the calibration could easily account for the difference.

There is a slight peak in ΔC_p to 0.6 percent at $M_\infty = 0.78$ for the longitudinal tapered-slotted walls. This is a low value for ΔC_p, and the contribution to test section noise level from either the slots or the communication with the plenum chamber for this configuration was thus small. Therefore, no attempts at noise suppression were made for these walls, the noise level having been found to be so low. The wall pressure coefficient, $C_{p\ wall}$, is shown in Fig. 12.

4.3 LONGITUDINAL RODS

The portion of the investigation concerning the longitudinal rod walls has been reported by Gilliam (Ref. 21). For the purpose of this report, only the acoustic data will be discussed for comparison of the results with the other type walls.

The porosity, τ, was varied from zero to approximately ten percent. The results are presented in Fig. 13 as a function of M_∞ for varied τ. Comparing these data with the solid wall background reveals that the levels for the rod walls for $M_\infty \leq 0.87$ were essentially the same as the solid wall case for all porosities.

Selected wall differential pressure coefficient data are shown in Fig. 14, and it can be seen that slightly greater wall differential pressure occurred at higher M_∞ for reduced τ. Above $M_\infty = 0.92$, there were increased levels of ΔC_p associated with the presence of a low-frequency "buzz" shown at these Mach numbers. Lowest amplitude levels of the "buzz" were found at τ = four percent. The "buzz" frequency varied with M_∞ as shown in Fig. 15 and was also a function of τ. That the frequency should have dependency on τ suggests that the acoustic mechanism responsible for the "buzz" was somehow related to the flow between rods. Rod vibration was considered as a possible contributor to the "buzz" pnenomenon but was ruled out after an inplace dynamic shaker test (see Ref. 21 for description) revealed no natural vibration frequencies in the range of "buzz" frequencies observed.

The low-frequency levels of "buzz" appeared to be related to the geometry of the plenum chamber instead of the test section. This conclusion was verified by an experiment which revealed that the "buzz" frequency could be changed by changing the volume of the plenum chamber. The experiment was performed at τ = two-percent porosity using a 2-in.-thick layer of Styrofoam.® The amplitude in ΔC_p was about the same for this case, although the impedance of the Styrofoam was different from that of the untreated hard walls of the plenum chamber. The computed plenum volumes were 9,676 $in.^3$ for the untreated (standard) case, 5,167 $in.^3$ for the case with the Styrofoam in place (reduced). The measured frequency of "buzz" is shown in Fig. 16 for the reduced volume compared to the standard volume case. As seen in Fig. 16, the shift in frequency is predicted closely by the following relation

$$f_2 = f_1 \sqrt{\frac{V_2}{V_1}} \tag{11}$$

This relation is indicative of Helmholtz-type response of the plenum chamber where the frequency is inversely proportional to the square root of the volume of a chamber excited through an opening that connects the chamber to the flow.

The results of the rod wall tests were encouraging in that the levels of ΔC_p for $M_\infty \leq 0.87$, approximately, were essentially the same as the solid wall background not requiring any noise suppressive measure. However, the appearance of the "buzz" tones at higher M_∞ revealed a potentially deleterious problem, possibly necessitating suppressive treatment for transonic tunnel applications. Low-frequency disturbances can be of great concern because of the potential to excite vibrational response in models.

4.4 PERFORATED WALLS WITH NORMAL HOLES

The two configurations of normal-hole perforated walls were tested with wire screen overlay as a noise suppressive measure. The "splitter

plate", Fig. 17a, was tested in the thick wall but was not effective in suppressing the noise. The wire screen overlay was pressed against the airstream surface and covered the entire wall sample as shown in Fig. 17b. Both configurations of standard walls, without suppressive measures, produced strong acoustic disturbances at high frequencies (whistling tones). The wire screen overlay, as will be seen, effectively suppressed the noise in both cases of thick wall (h/t = 1) and thin wall (h/t = 2.667).

The results of the thin-wall test, h/t = 2.667, are shown in Fig. 18 in the form of ΔC_p and S versus M_∞. For the untreated walls, there was a strong resonance peak in ΔC_p at $M_\infty = 0.65$ of five percent. The most predominant frequency at $M_\infty = 0.65$ was observed to be 3,150 Hz, approximately. There was also a double frequency harmonic of lesser amplitude. With wire screen overlay, the noise level was reduced nearly to that of the solid wall background.

The nondimensionalized frequencies (in the form of Strouhal number) are shown in Fig. 18b. The closed symbols in Fig. 18b represent frequencies of small remnant components not fully suppressed to the background by the screens. A harmonic array of nondimensionalized frequencies is apparent in Fig. 18b. The following empirical relationship

$$S = \frac{hf}{U_\infty} = 0.075 \frac{K_A}{M_\infty} \qquad K_A = 1, 2, 3, 4, \ldots \tag{12}$$

was found to give an adequate fit to the measured frequency data for $0.4 \leq M_\infty \leq 0.9$. Here, K_A is defined as an integer describing harmonic order or acoustic mode number for the complex periodic acoustic disturbances appearing in the test section with these untreated wall samples installed and h was the hole diameter. Harmonic orders $K_A = 2$ and $K_A = 4$ were observed to be predominant with mode number $K_A = 2$ occurring at 3,150 Hz at $M_\infty = 0.65$.

In the case of the untreated thick normal-hole walls, h/t = 1, ΔC_p was three percent at M_∞ = 0.2 and 2.6 percent at resonance near M_∞ = 0.6. Wire screen was equally as effective in suppressing complex periodic-type whistling noise that occurred from these wall samples as it was for the thin-wall samples. However, a higher level of ΔC_p was measured at M_∞ = 0.6 for this wall with "splitter plates" installed, ΔC_p being essentially unchanged at all other M_∞. The results for the thick-wall case are shown in Fig. 19 in the form of ΔC_p and S versus M_∞. Amplitudes of ΔC_p are shown in Fig. 19a. Nondimensionalized frequencies, S, for the thick normal-hole wall are seen in Fig. 19b to be in good agreement with the following relation

$$S = \frac{hf}{U_\infty} = \frac{1}{2\pi} \frac{K_A}{(1 + M_\infty)} \qquad K_A = 2, 3, 4, \ldots \tag{13}$$

Equation (13) was empirically derived in Ref. 9 for perforated walls having inclined holes and wall thickness ratio, h/t = 2, h = d/cos θ, and θ = 60 deg. For the h/t = 1 normal-hole wall, h being the hole diameter, modes K_A = 2, 4, 6, and 8 appeared with mode K_A = 4 being predominant (corresponding to 6,200 Hz at M_∞ = 0.6).

The wall differential pressure coefficients are shown in Fig. 20 for the thin-wall cases and in Fig. 21 for the thick-wall cases. The two noise suppressive measures tried in the thick wall made relatively larger changes in $C_{p\ wall}$ than existed between these two untreated configurations of the normal-hole wall. There is a distinct difference in the acoustic characteristics of these two untreated wall configurations, as evidenced by different behavior of S with M_∞ in Eqs. (12 and 13), although there was little difference in $C_{p\ wall}$. The difference in noise generation characteristics is possibly related to subtle differences in the nature of the shear layer over each hole for varied h/t.

4.5 PERFORATED WALLS WITH INCLINED HOLES

The tones produced by the perforated walls having 60-deg inclined holes are high-frequency whistling tones occurring in a harmonic family and previously described in Ref. 9 as being edgetones. The density patterns associated with the occurrence of the edgetones were clearly visible using schlieren photography when a particular harmonic became strongly predominant. Such a schlieren view of the sound field from untreated Tunnel 16T wall samples at $M_\infty = 0.79$ is shown in Fig. 22. Use of the "splitter plate" in these walls suppressed the inclined, steep-fronted waves from view as shown in Fig. 22. With the "splitter plates" installed, only small remnants of the tones were scarcely perceptible above the broadband background noise during spectral analysis of the microphone signal.

An enlarged view of the 40- by 40-mesh wire screen over a hole in a Tunnel 16T wall sample is shown in Fig. 23. (This is the same screen that was used on the perforated walls with normal holes and other perforated walls with inclined holes having smaller hole diameter.) The screen solidity in this and all other cases was 60 percent or, conversely, the percent open area for the hole was 40 percent. No attempt was made in this investigation to optimize screen mesh size to hole size because good results were obtained for all hole sizes tried with this screen. The wire screen gave effective suppression of edgetones in all cases of inclined-hole walls investigated (holes ranging in diameter from 0.125 in. to 0.75 in.) as it did in both cases of normal-hole perforated walls.

Tunnel 16T Wall Samples

The reductions in ΔC_p achieved with the "splitter plate" and wire screen overlay in Tunnel 16T wall samples are shown in Fig. 24, which gives for comparison the data with the respective noise suppression measure and the data for the untreated wall samples. Although the

"splitter plate" was able to produce a reduction in ΔC_p by nearly a factor of five at high Mach numbers, the suppression was not as complete as that by the wire screen, the "splitter plate" giving a ΔC_p level a factor of two greater than the solid wall background, the wire screen closely approaching the solid wall background.

Predominant frequencies in nondimensional form from the untreated Tunnel 16T wall samples are shown in Fig. 25. The component observed to reach maximum amplitude in these spectra was the $K_A = 4$ mode ($S = 0.350$ at $M_\infty = 0.82$). Shown for reference in Fig. 25 are the $h/t = 1$ normal-hole wall measured values of S for $K_A = 4$. Note the consistency in the data with the value for S given by Eq. (13).

The wall differential pressure coefficient, $C_{p\ wall}$, for the Tunnel 16T wall samples - untreated (standard), with the "splitter plates", and with the wire screen overlay, is shown in Fig. 26. The significance of these $C_{p\ wall}$ data lies in the fact that these noise suppression measures alter the wall crossflow characteristics and the use of either method in a wind tunnel would require a tunnel calibration. (The usual practice in ventilated wall tunnels is to use plenum chamber pressure as the static source for setting Mach number, requiring precise knowledge of the relationship between the pressure in the plenum chamber to that of the free stream in the test section.)

Tunnel 1T Wall Samples

The degree of noise reduction achieved in the Tunnel 1T wall samples with "splitter plates" and with wire screen overlay is shown in Fig. 27. Again, the wire screen overlay was more effective than the "splitter plate", achieving essentially complete suppression to the solid wall background level while the "splitter plate" was only a factor of about 1.3 higher at its maximum.

Nondimensionalized frequencies are shown in Fig. 28 for the untreated Tunnel 1T wall samples. These data, being in conformance with Eq. (13), indicate that the same mechanism of noise generation is active in these walls as in the Tunnel 16T wall samples, except the K_A = 1, 2, 3, and 4 modes were detected. The fundamental mode, K_A = 1, was predominant in these spectra with a frequency of 4,400 Hz at M_∞ = 0.4. A schlieren view of the density pattern associated with the sound field emitted by the Tunnel 1T wall samples is shown in Fig. 29.

The Tunnel 1T wall samples were closest to the proper scale for the hole size boundary-layer thickness in actual tunnels having inclined holes. (See Ref. 11 for the significance of hole size in these walls.) For this reason, these samples were selected for an experimental investigation of the effectiveness of the "splitter plate" modification at varied δ^*/d. At M_∞ = 0.5 near the tunnel midsection, δ^*/d was about 0.5 for the Tunnel 1T walls with the normally installed 24-in.-long test section. With the 24-in.-long extension channel installed ahead of the test section, the boundary-layer thickness was approximately doubled, giving $\delta^*/d \cong 1.0$. If a mean δ^*/d for inclined holes is taken to be 0.75 from Ref. 11, these two cases gave slightly lower and slightly higher δ^* than the correct scale. The results for both δ^*/d values are shown in Fig. 30 in the form of ΔC_p versus M_∞ and are seen to have been essentially the same with the edgetones effectively suppressed, ΔC_p being 0.63 percent maximum at M_∞ = 0.8.

Tunnel 4T Wall Samples

The Tunnel 4T wall samples were tested at porosity, τ, of six and four percent. These two values of porosity were chosen because five- or six-percent porosity is used in practice at subsonic Mach numbers in Tunnel 4T. The "splitter plate" was tested at τ = six and four percent, but the wire screen overlay was tested at only six percent.

The results of these noise measurements made on the Tunnel 4T wall samples are presented in Fig. 31 in the form of ΔC_p versus M_∞. The "splitter plate" was slightly more effective at τ = six percent than at τ = four percent. The wire screen was again more effective than the "splitter plate", these results being about the same as in the other perforated walls having inclined holes.

These variable-porosity walls generally had more of the harmonic tones present than the fixed-porosity walls as seen in Fig. 32 with frequencies likewise in conformance with Eq. (13). Mode Nos. K_A = 2, 4, and 6 were observed to be predominant, largest amplitudes occurring at K_A = 2, with mode Nos. K_A = 3 and 8 appearing intermittently. In general, the variable-porosity wall samples had a less stationary sound field over any timespan of measurements, jumping from one harmonic to another at any particular M_∞ more frequently than the fixed-porosity walls. At M_∞ = 0.8, for example, mode No. K_A = 2 was observed to be predominant at a frequency of 1,850 Hz. A shadowgraph view taken at M_∞ = 0.8 is shown in Fig. 33. The shadowgraph in lieu of schlieren enhances the apparent intensity of waves inclined in one direction - white waves - while suppressing those inclined in the other direction - black waves - and gives more details of the turbulence in the boundary layer close to the wall sample.

Finally, one additional experiment yielded information of academic interest about the propensity for sound production from inclined-hole perforated walls. Tones had been observed from holes inclined 60 deg and holes normal to the airstream surface. This experiment was to turn one set of samples in the opposite direction such that the holes were inclined against the flow. The experiment was done with Tunnel 4T wall samples at τ = six percent. The results are shown in Fig. 34 in the form of ΔC_p versus M_∞. No tones were produced. The level of ΔC_p was slightly above the solid wall case, about the same as the cases with wire screen overlay.

Wall differential pressure coefficients are shown in Fig. 35 for these Tunnel 4T wall sample cases. The trends in $C_{p\ wall}$ were shifts toward the negative with the "splitter plate". Surprisingly, the case for the holes inclined against the flow gave $C_{p\ wall}$ not very much different from the natural inclination case of the standard untreated wall.

4.6 LONGITUDINAL BAFFLED SLOTS

The longitudinal baffled slots emit noise at high discrete frequencies of similar amplitudes in the ART test section to the perforated walls. These whistling tones remained nearly constant in frequency, as did the thin normal-hole wall tones, instead of changing frequency with M_∞ as did the other perforated walls.

Association of the tones with the slot baffles was a conclusion of the tests performed in the full-scale 11-ft tunnel at NASA/Ames Research Center (Ref. 7) where tape covering the airstream surfaces of these slots effectively eliminated the tones. The tape essentially converted the test section to a solid wall configuration, and the tones disappeared from the noise spectra. The final step in the identification of the baffled-slot as the source of these tones was in their appearance during slot sample tests in the ART.

It is theorized that a set of standing waves is produced in the baffled slots, the frequencies having dependence upon the slot depth dimension. The measured frequencies and a suggested waveform pattern for harmonic production are shown in Fig. 36. The frequency levels are approximated by the simple half-wave organ pipe formula

$$f = \frac{K_A}{2} \frac{c_\infty}{\ell_{eff}} \qquad K_A = 1, 2, 3, \ldots \tag{14}$$

The characteristic dimension ℓ_{eff} was taken to be the baffle depth with end corrections. The actual baffle depth was 2.25 in. Measurements to substantiate or refute the suggested acoustic mechanism (standing waves) were not made.

The fundamental frequency of nominally 2,700 Hz is adequately predicted by Eq. (14) with an assumed ℓ_{eff} = 2.375 in. and K_A = 1. The local speed of sound may actually differ slightly from the assumed free-stream speed of sound, c_∞, changing the trends in frequency with M_∞. However, c_∞ was used to approximate the sound speed in Eq. (14). Plenum suction was applied for $M_\infty \geq 0.8$. A change in ℓ_{eff} to 2.25 in. for the case of plenum suction improved the agreement in Fig. 36a with measured frequencies for $M_\infty \geq 0.8$. Three harmonic multiple tones appeared in the spectra, the fundamental K_A = 1 being much larger than K_A = 2 and 3 and thus predominant.

Having had success in suppressing perforated wall noise using wire screen overlay, screen of the same fine mesh was applied to the air-stream surface of the baffled slot as shown in Fig. 37. The screen was bonded to the wall using epoxy resin. The region of the bond on either side of the slot was then finish ground. The data acquired in this experiment with screen are shown in Fig. 38, ΔC_p versus M_∞. While some noise reduction was realized from screen alone, the degree of suppression was not satisfactory. Following the premise that disruption of the assumed organ pipe standing waves could suppress the tones, steel wool was then packed loosely into each baffle. The steel wool was held in place by a second screen on the back side of the slot. The result was an effective elimination of the tones, again approximating the solid wall level as shown in Fig. 38.

Although it had been demonstrated that the baffled-slot tones could be suppressed, the particular steel wool configuration produced a significant change in wall crossflow characteristics. The wall

differential pressure coefficient is shown in Fig. 39 for the standard untreated slot, slot with screen, and the slot with steel wool held by screens. The level of $C_{p\ wall} = 0.28$ at $M_\infty = 0.85$ is extremely high, requiring a much reduced plenum chamber pressure to establish the flow for the wire screen/steel wool combination.

5.0 CONCLUDING REMARKS

Data have been presented from a set of experiments to disclose acoustic parameters associated with various ventilated wall configurations for transonic wind tunnel test sections. These data were acquired on a comparative basis whereby predominant noise generation mechanisms could be isolated and the effectiveness of particular noise suppressive measures assessed. Three types of noise suppressive measures were investigated - the splitter plate, which has application to perforated walls, and wire screen overlay, which was investigated in both perforated walls and baffled-slotted walls, and a wire screen/steel wool configuration, which was investigated in the baffled-slotted walls.

A particular longitudinal tapered-slotted wall configuration was found to produce very low levels of noise. Longitudinal rodded walls also produced low levels of noise up to Mach numbers where plenum suction was required. With the rod walls installed, for $M_\infty \geq 0.92$ approximately, a low-frequency "buzz" disturbance occurred which was believed to be related to response of the plenum chamber to the flow between the rods.

Both the "splitter plate" and the wire screen overlay were demonstrated to provide effective suppression of the edgetone mode which occurs in perforated walls having 60-deg inclined holes. The wire screen gave better noise reduction than did the "splitter plate" in both fixed- and variable-porosity holes inclined 60 deg. The wire screen was

also effective in suppressing the noise emitted by perforated walls having normal holes and two widely differing hole size/plate thickness ratios. The splitter plate was not effective in the thick normal-hole walls.

Wire screen alone was not effective in suppressing a suspected organ pipe (standing wave) mode occurring in longitudinal baffled slots. Wire screen plus steel wool stuffing in the baffles produced a reduction in noise level comparable to the perforated walls with wire screen overlay.

It was demonstrated in this investigation that all four basic conceptual configurations of transonic wind tunnel ventilated walls in current use, i.e., open longitudinal slots, baffled longitudinal slots, perforated walls with normal holes, and perforated walls with inclined holes, can be made to operate at noise levels approaching the solid wall background level for subsonic Mach numbers. In the ART, the solid wall background level being approximately 0.47 percent of the free-stream dynamic pressure for $M_\infty \leq 0.87$, in all cases with the exception of the "buzz" with the rod walls, noise levels not exceeding 0.75 percent of the dynamic pressure were shown possible.

Wall differential pressure coefficients are presented also for the various configurations of wall samples to show relative changes in test section-to plenum chamber pressure for geometrical differences and applications of noise suppressive measures. The wall characteristic is an important consideration in any transonic tunnel for tunnel calibration and the interference imposed on test models.

The present research did not include optimization for the needs of any particular wind tunnel. Optimization studies including wall boundary-layer evaluations would be beneficial before modifying a particular transonic tunnel with noise suppression measures. This research has

served to point out that the high-amplitude acoustic disturbances predominant in many present-day ventilated-wall tunnels need not be tolerated but can be effectively suppressed by the application of appropriate noise suppressive measures.

Considerations for the choice of suppression measures must also include long-term durability for continuous use, ease of installation and maintenance, and possible changes in work procedures inside a wind tunnel test section. These considerations may play a significant role in optimizations.

REFERENCES

1. Goethert, B. H. Transonic Wind Tunnel Testing, AGARDograph No. 49, Pergamon Press, 1961.

2. Cox, R. N. and Freestone, M. M. "Design of Ventilated Walls with Special Emphasis on the Aspect of Noise Generation." Fluid Motion Problems in Wind Tunnel Design, AGARD Report No. 602, No. 6, November 1972.

3. McCanless, G. F. "Additional Corrections of 4% Saturn V Protuberance Test Data." Chrysler Corp. TR HSM-R1-71, January 1971.

4. Dods, J. B. and Hanly, R. D. "Evaluation of Transonic and Supersonic Wind Tunnel Background Noise and Effects on Surface Pressure Fluctuation Measurements." AIAA Paper No. 72-1004, Presented at the AIAA 7th Aerodynamic Testing Conference, Palo Alto, California, September 1972.

5. Credle, O. P. "Perforated Wall Noise in the AEDC-PWT 16-Ft and 4-Ft Transonic Tunnels." AEDC-TR-71-216 (AD888561L), October 1971.

6. Karabinus, R. J. and Sanders, B. W. "Measurements of Fluctuating Pressures in 8- by 6-Foot Supersonic Wind Tunnel for Mach Number Range of 0.56 to 2.07." NASA TM X-2009, May 1970.

7. Dougherty, N. S., Jr. and Steinle, F. W., Jr. "Transition Reynolds Number Comparisons in Several Major Transonic Tunnels." AIAA Paper No. 74-627, Presented at the AIAA 8th Aerodynamic Testing Conference, Bethesda, Maryland, July 8-10, 1974.

8. Mabey, D. B. "Flow Unsteadiness and Model Vibration in Wind Tunnels at Subsonic and Transonic Speeds." RAE, Bedford, England, CP No. 1155, October 1970.

9. Dougherty, N. S., Jr., Anderson, C. F., and Parker, R. L., Jr. "An Experimental Investigation of Techniques to Suppress Edgetones from Perforated Wind Tunnel Walls." AEDC-TR-75-88 (ADA013728), August 1975; also AIAA Paper No. 76-50, Presented at the AIAA 14th Aerospace Sciences Meeting, Washington, D. C., January 26-28, 1976.

10. Pindzola, M. and Chew, W. L. "A Summary of Perforated Wall Wind Tunnel Studies at the Arnold Engineering Development Center." AEDC-TR-60-9 (AD241573), August 1960.

11. Lukasiewicz, J. "Effects of Boundary Layer and Geometry on Characteristics of Perforated Walls for Transonic Wind Tunnels." Aerospace Engineering, Vol. 20, No. 4, April 1961.

12. Schutzenhofer, L. A. and Howard, P. W. "Suppression of Background Noise in a Transonic Wind Tunnel Test Section." Fall 1974 Research Technology Review, NASA/Marshall Space Flight Center, Huntsville, Alabama, October 1974, also AIAA Journal, Vol. 13, No. 11, November 1975.

13. Vaucheret, X. "Fluctuations Acoustiques Engendrees Par Les Parois Permeables D'Une Soufflerie Transsonique." Presented at the AGARD Meeting on Techniques of Construction of Wind Tunnel Test Sections, Paper No. 25, London, England, October 6-8, 1975.

14. Binion, T. W. and Anderson, C. F. "An Experimental Investigation of the Acoustic and Wall Interference Properties of Rod and Perforated Wind Tunnel Walls in Two-Dimensional Flow." AEDC-TR-74-41 (AD922394L), September 1974.

15. Jacocks, J. L. "Determination of Optimum Operating Parameters for the AEDC PWT 4-ft Transonic Tunnel with Variable Porosity Test Section Walls." AEDC-TR-69-164 (AD857045), August 1969.

16. Varner, M. O. "Noise Generation in Transonic Wind Tunnels." AIAA Paper No. 74-633, Presented at the AIAA 8th Aerodynamic Testing Conference, Bethesda, Maryland, July 8-10, 1974, also AEDC-TR-74-126 (ADA007688), April 1975.

17. Benek, J. A. "Effects of Acoustic and Vortical Disturbances on the Turbulent Boundary Layer." AEDC-TR-77-73.

18. Lilley, G. M. "Wall Pressure Fluctuations Under Turbulent Boundary Layers at Subsonic and Supersonic Speeds." AGARD Report No. 454, April 1963.

19. Willmarth, W. W. "Pressure Fluctuations Beneath Turbulent Boundary Layers." Annual Review of Fluid Mechanics, Vol. 7, 1975, Annual Reviews, Inc., Palo Alto, California.

20. Lowson, M. V. "Prediction of Boundary Layer Pressure Fluctuations." AFFDL-TR-67-167 (AD832715), April 1968.

21. Gilliam, F. T. "An Experimental Investigation of the Acoustic and Wave Attenuation Characteristics of a Rod Wall Wind Tunnel in Transonic Flow." AFIT GAE/AE/74D-13, December 1974, also AIAA Paper No. 76-215, Presented at the AIAA 14th Aerospace Sciences Meeting, Washington, D. C., January 26-28, 1976.

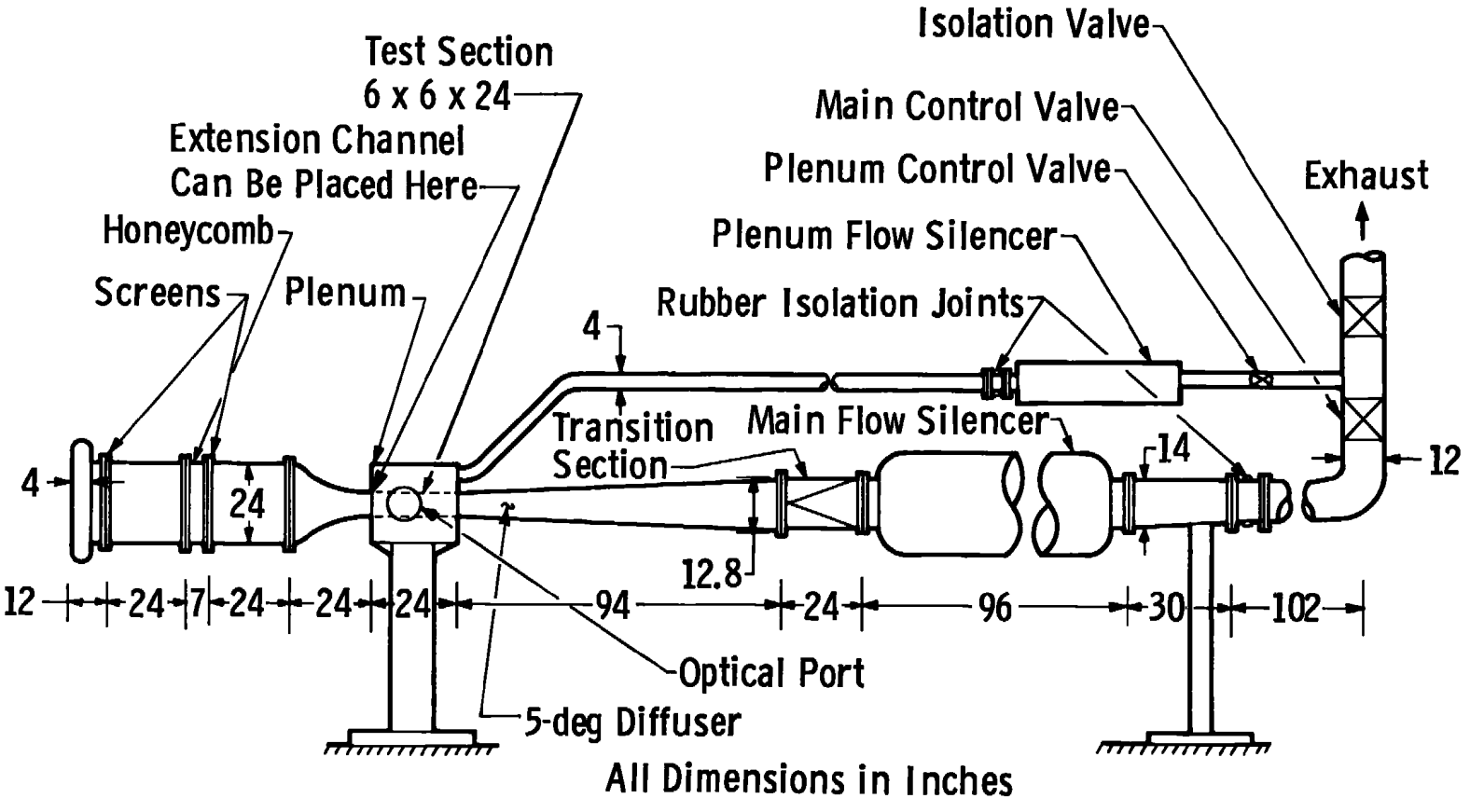

a. Overall layout

Figure 1. Acoustic research tunnel.

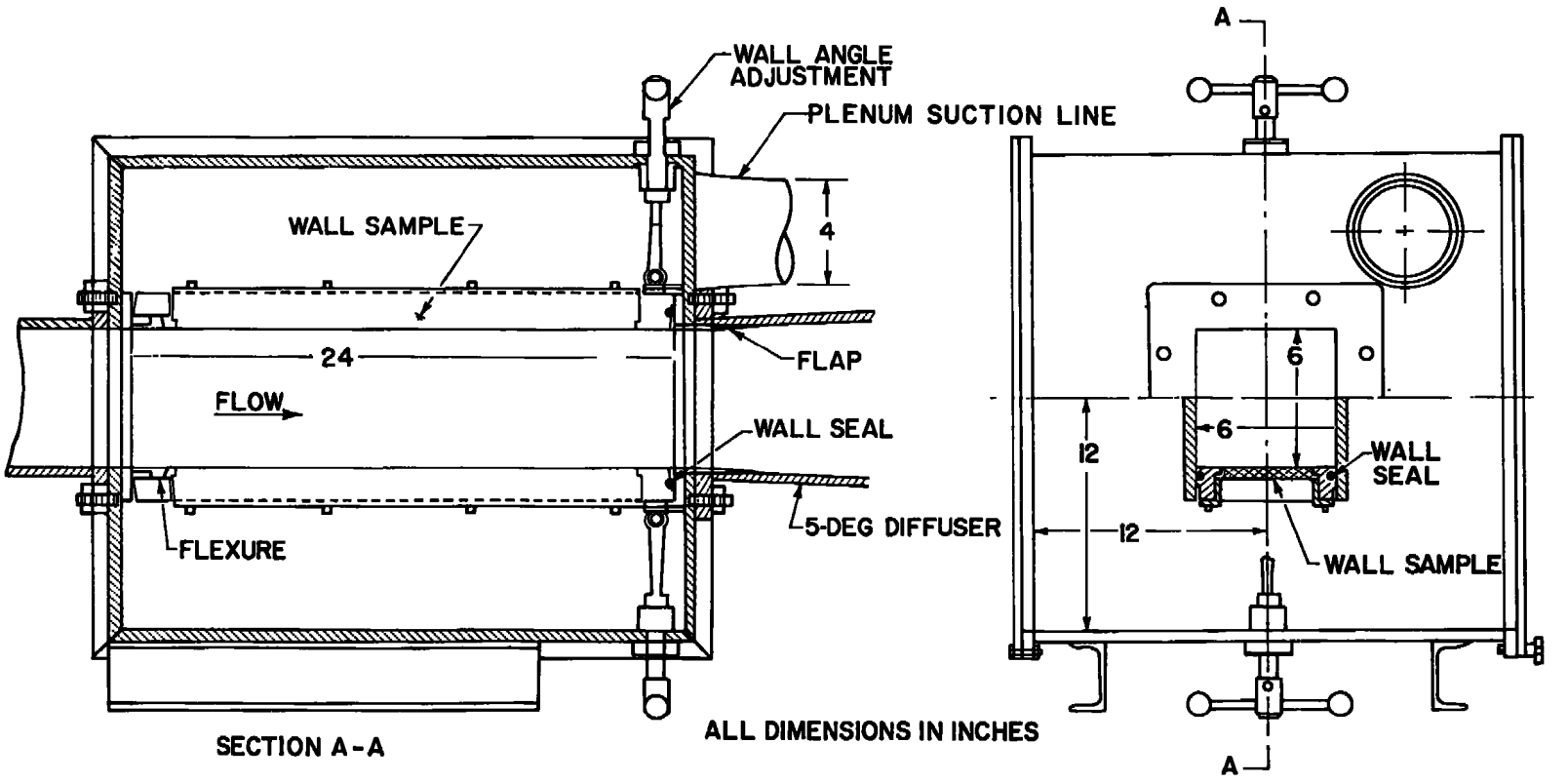

b. Test section and plenum details

Figure 1. Concluded.

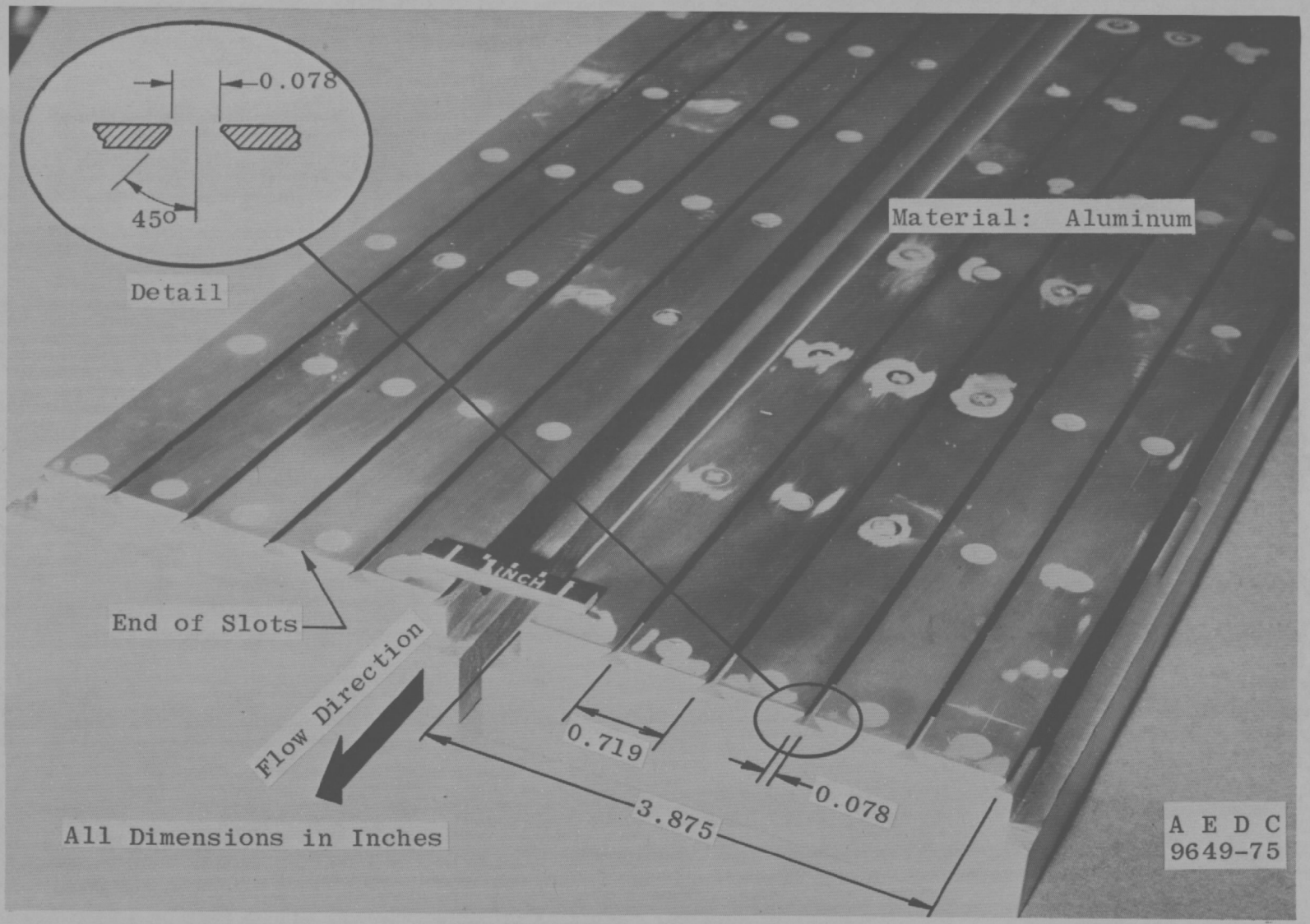

Figure 2. Longitudinal tapered slots.

a. Transition region details

Figure 3. Longitudinal rod wall.

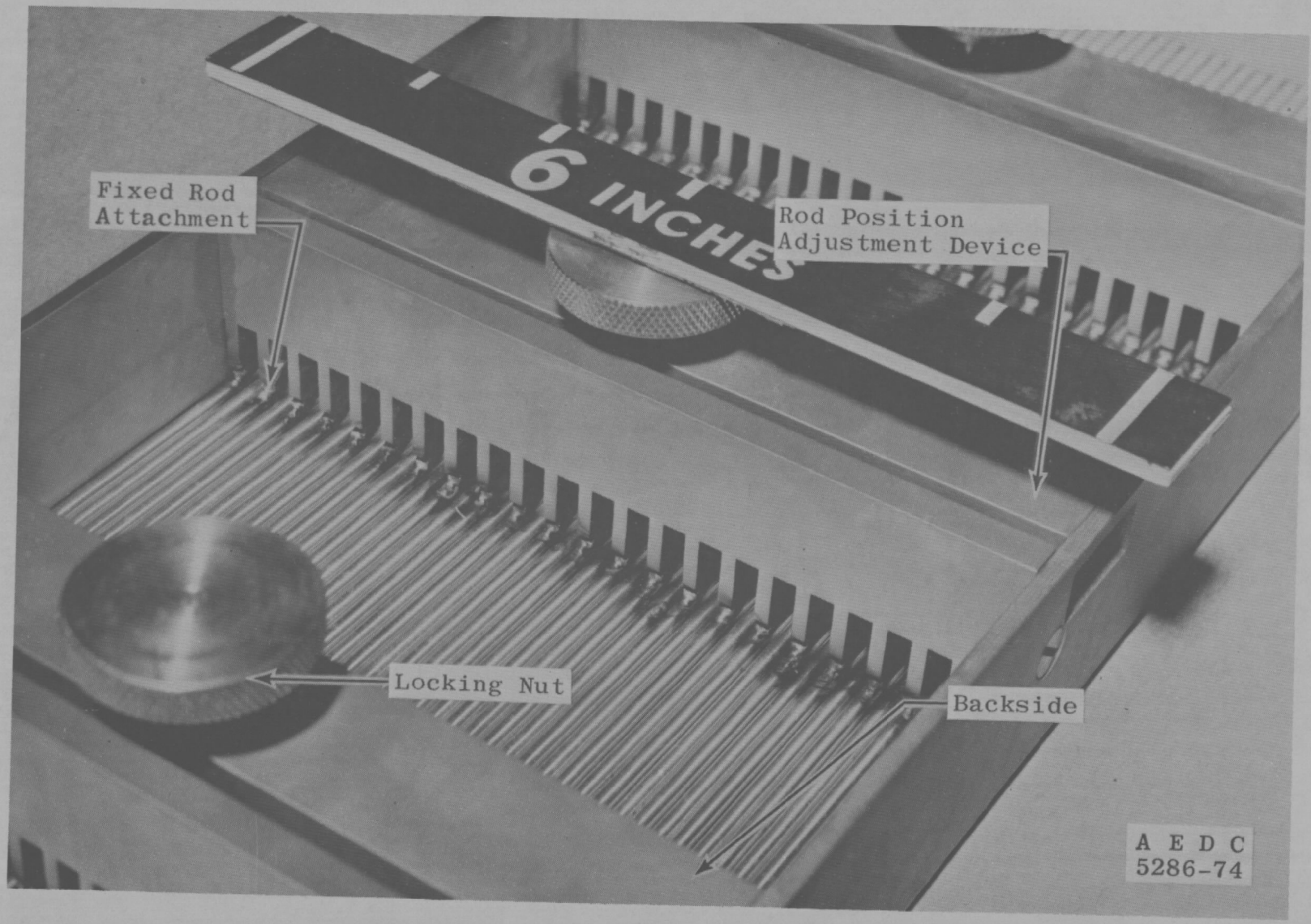

b. Rod positioner details
Figure 3. Concluded.

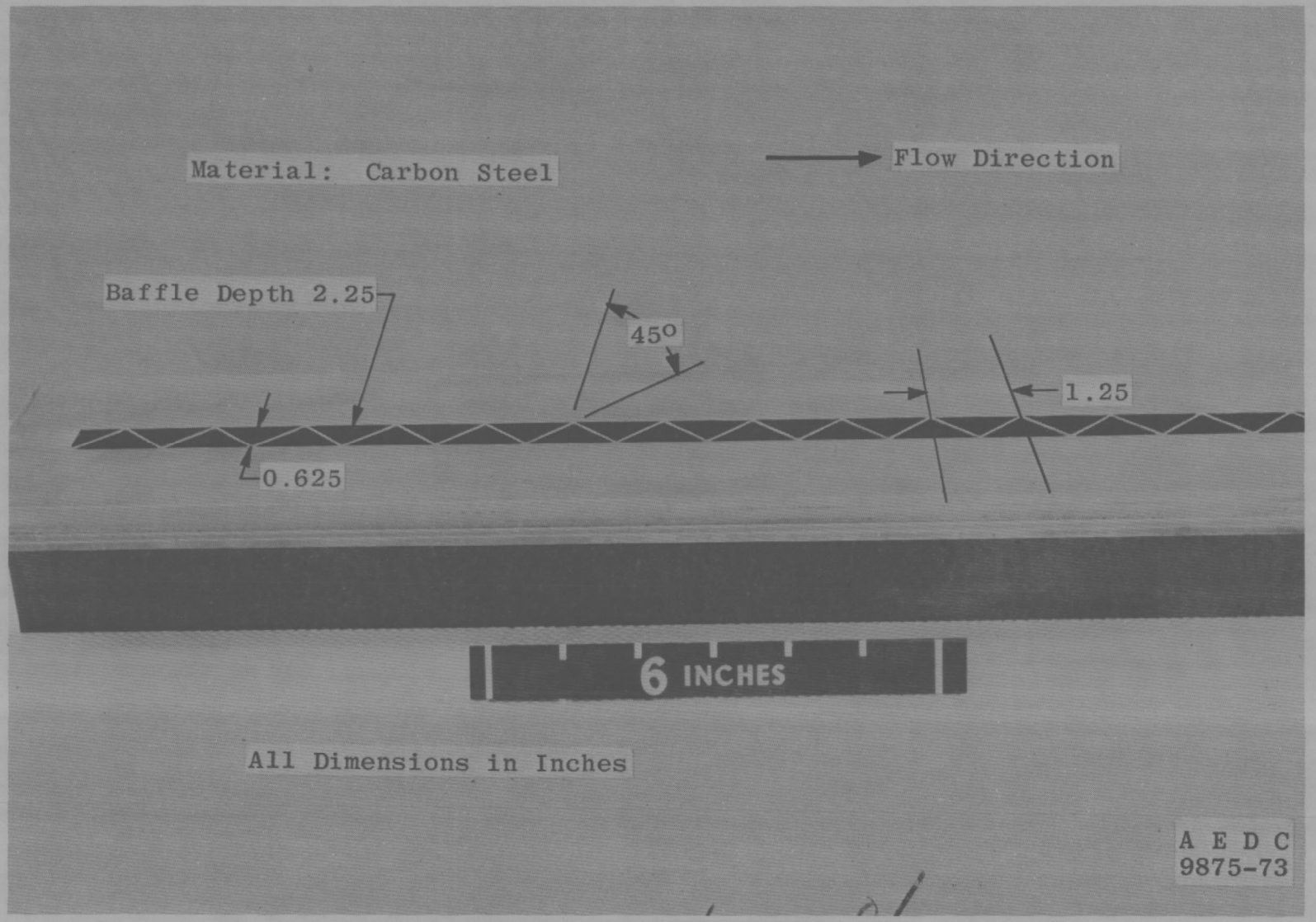

Figure 4. Longitudinal baffled slot.

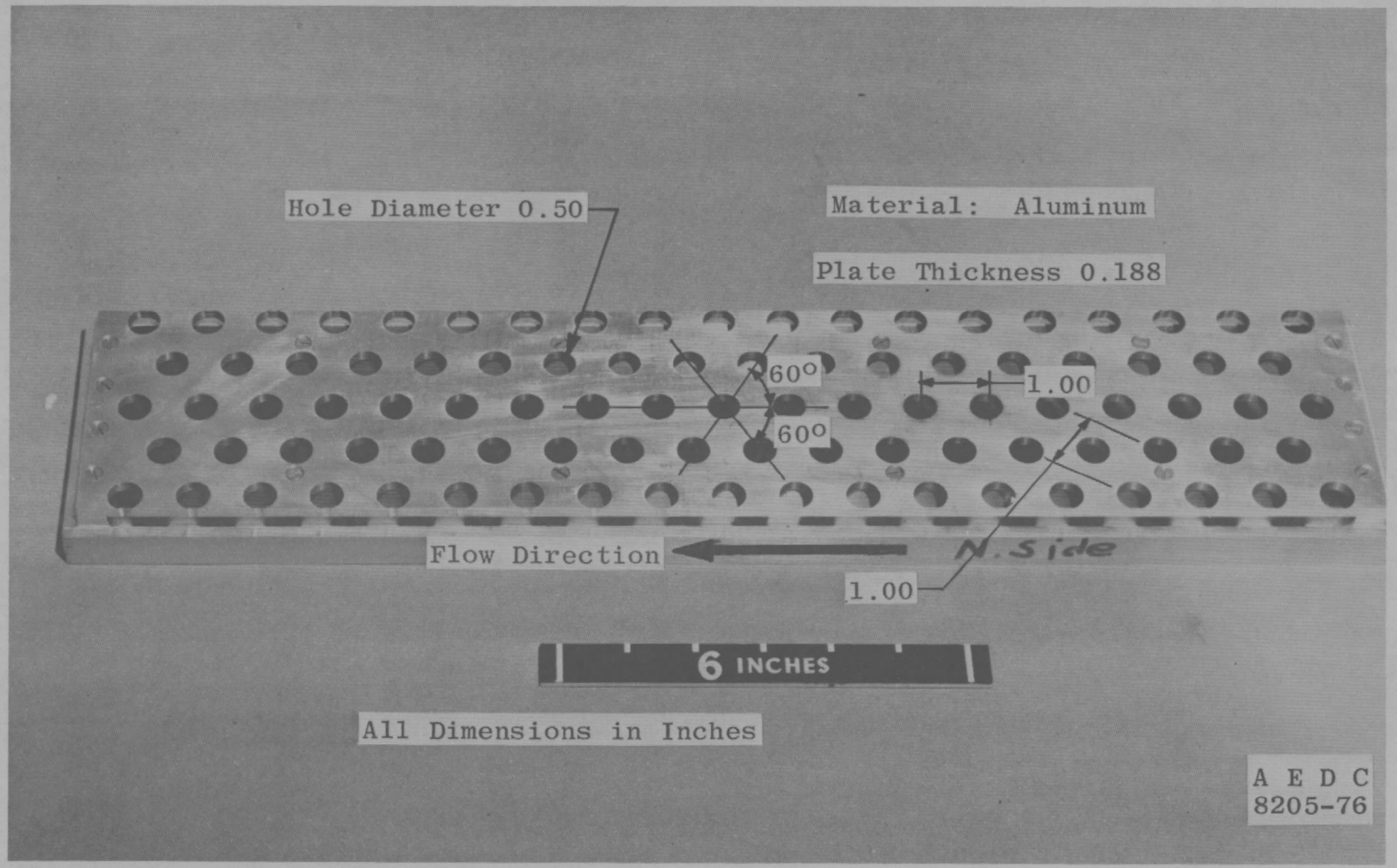

a. Thin wall

Figure 5. Perforated walls with normal holes.

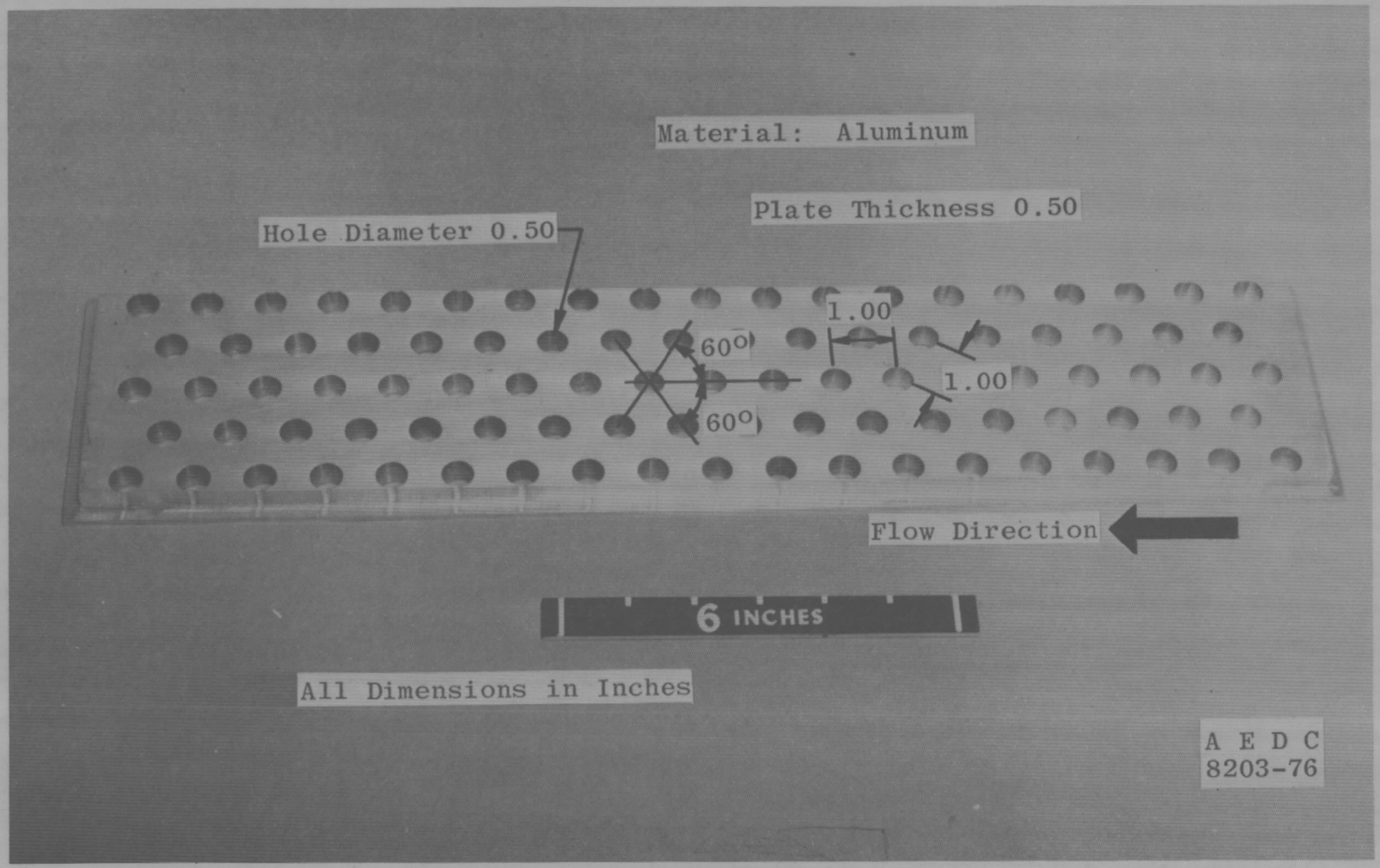

b. Thick wall

Figure 5. Concluded.

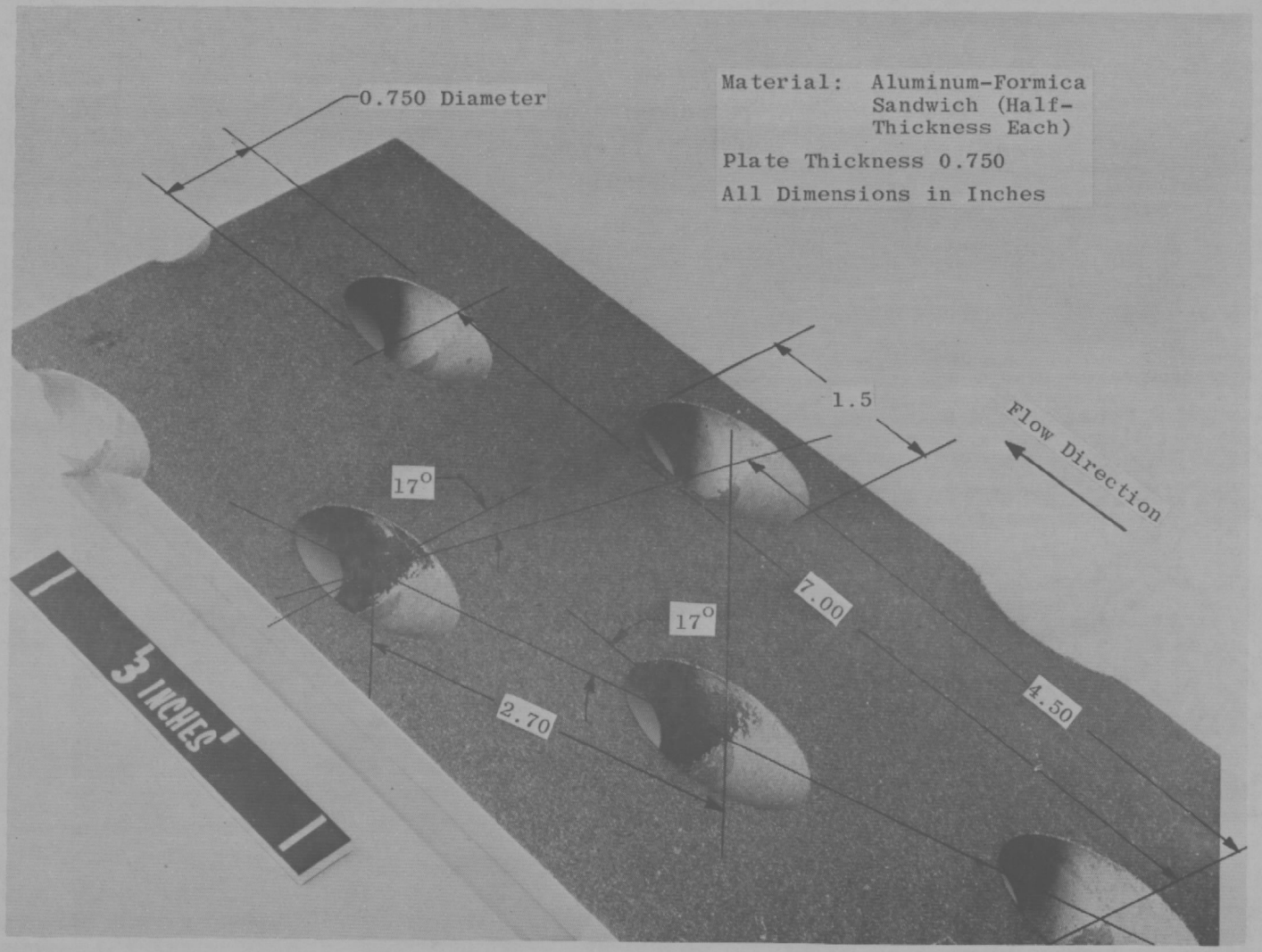

a. Tunnel 16T wall sample

Figure 6. Perforated walls with inclined holes.

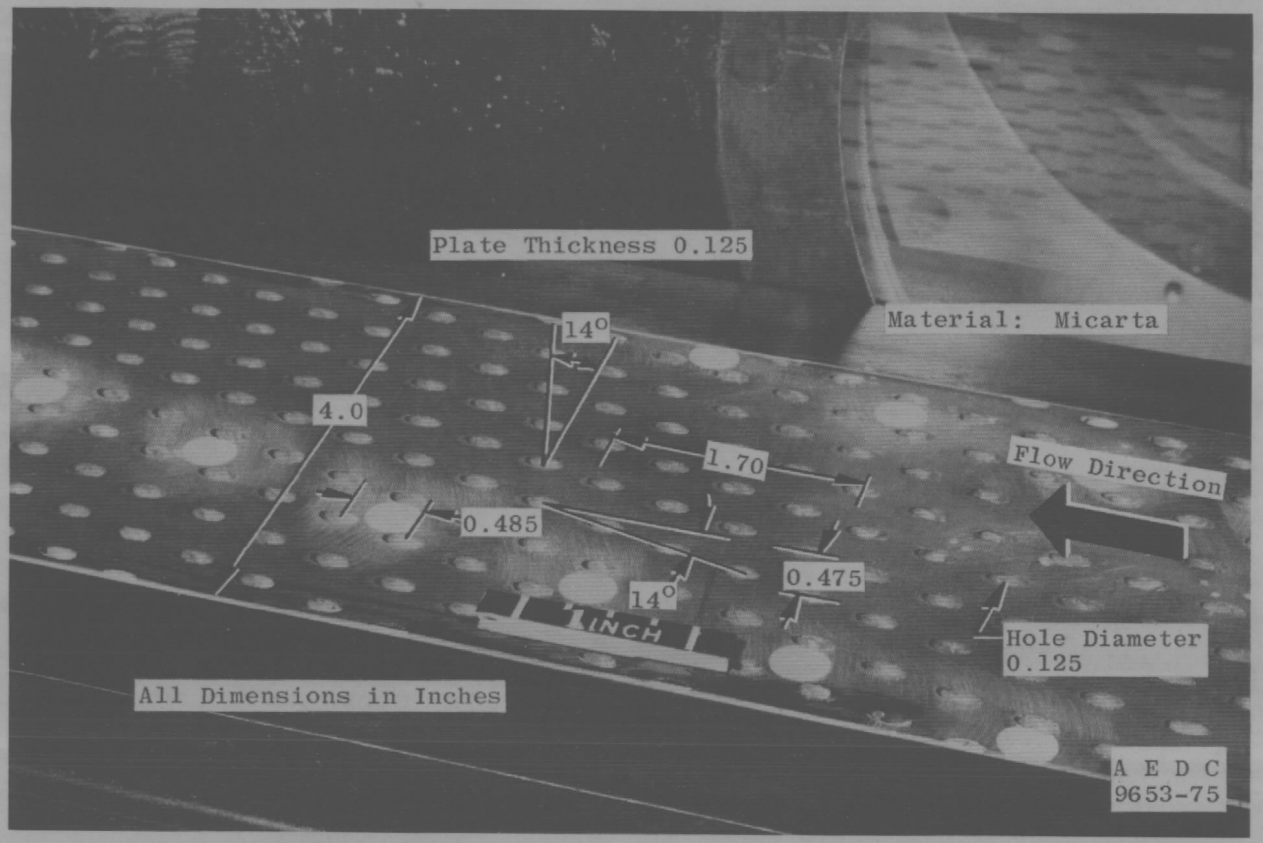

b. Tunnel 1T wall sample
Figure 6. Continued.

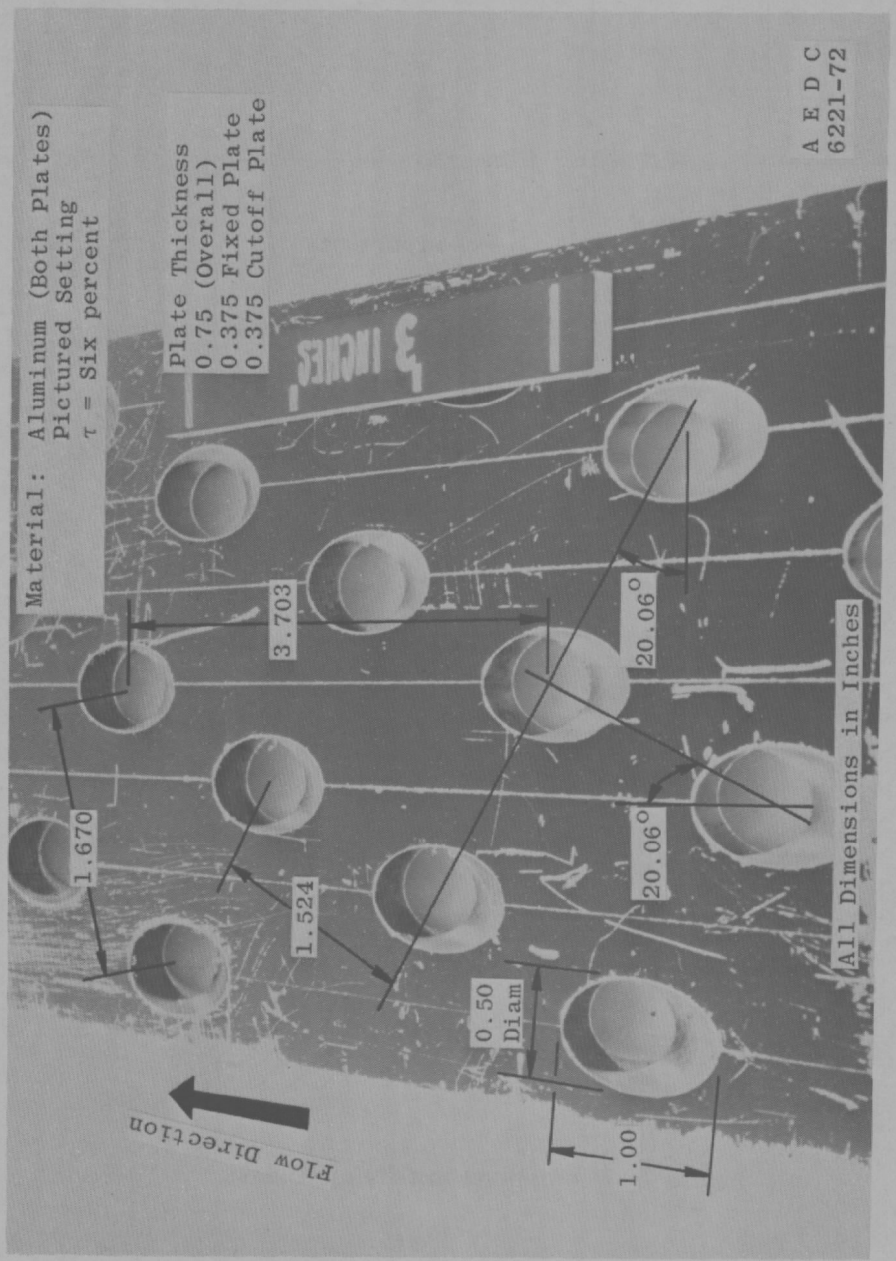

c. Tunnel 4T wall sample
Figure 6. Concluded.

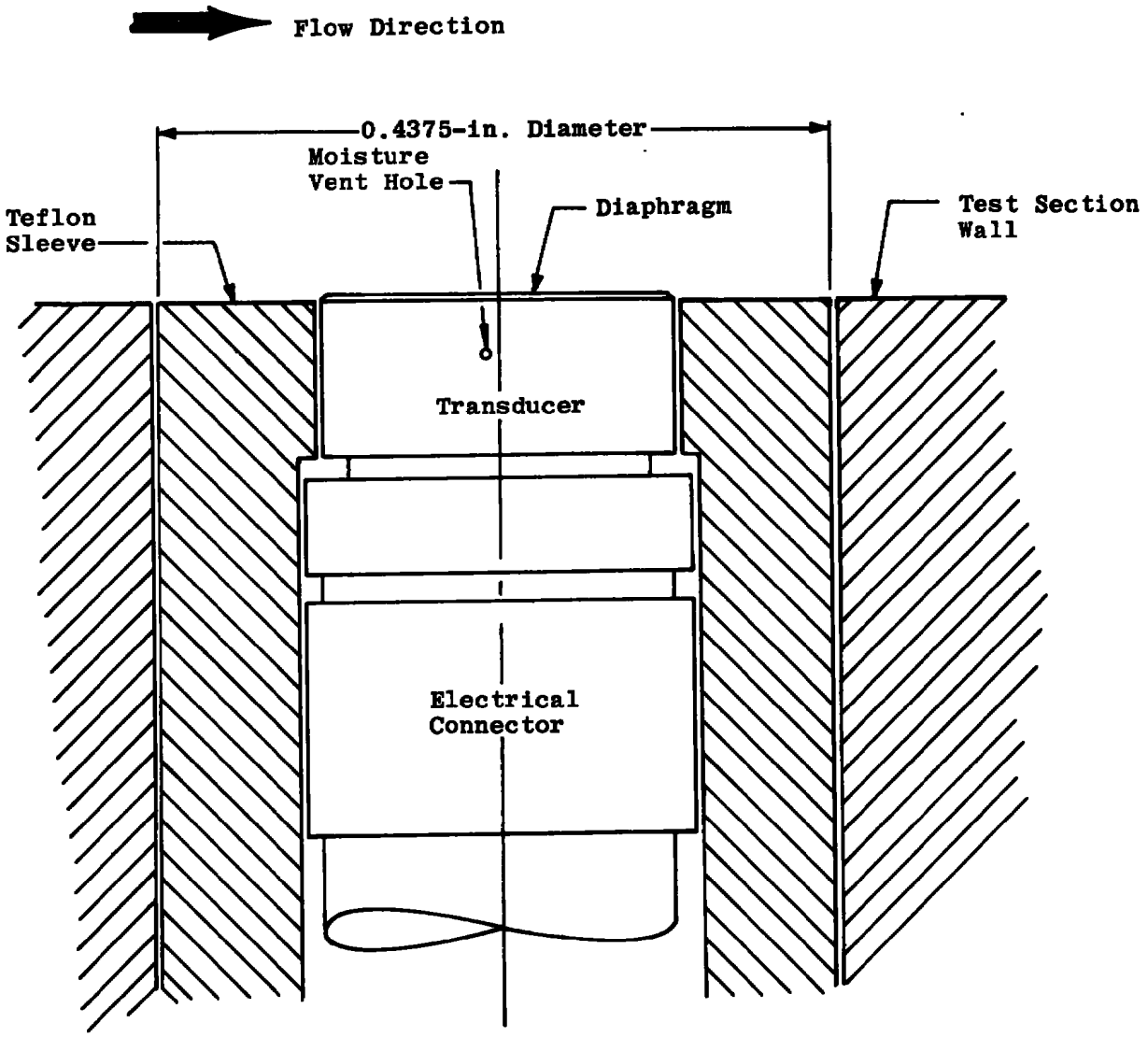

Figure 7. Microphone installation details.

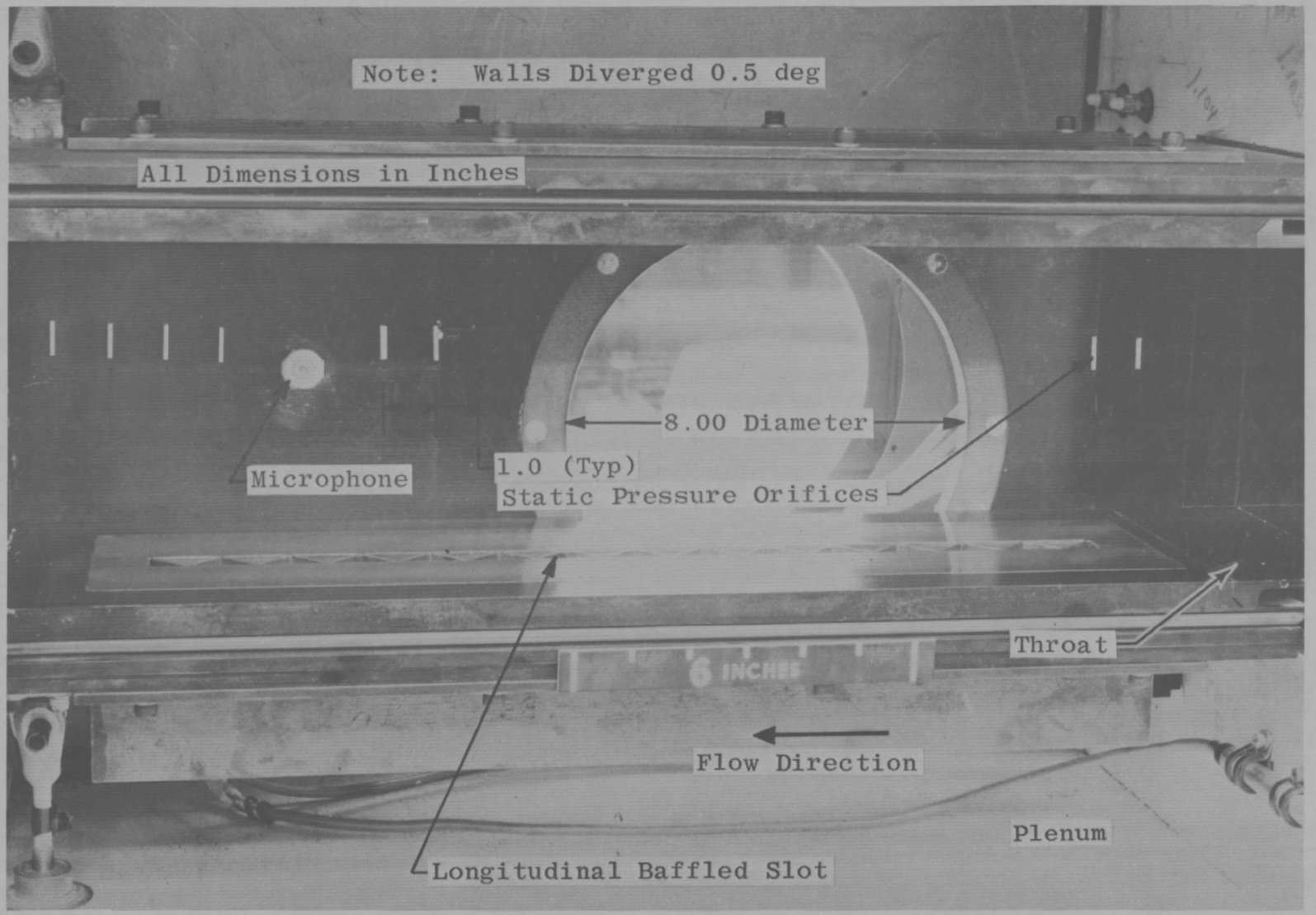

Figure 8. Test section arrangement.

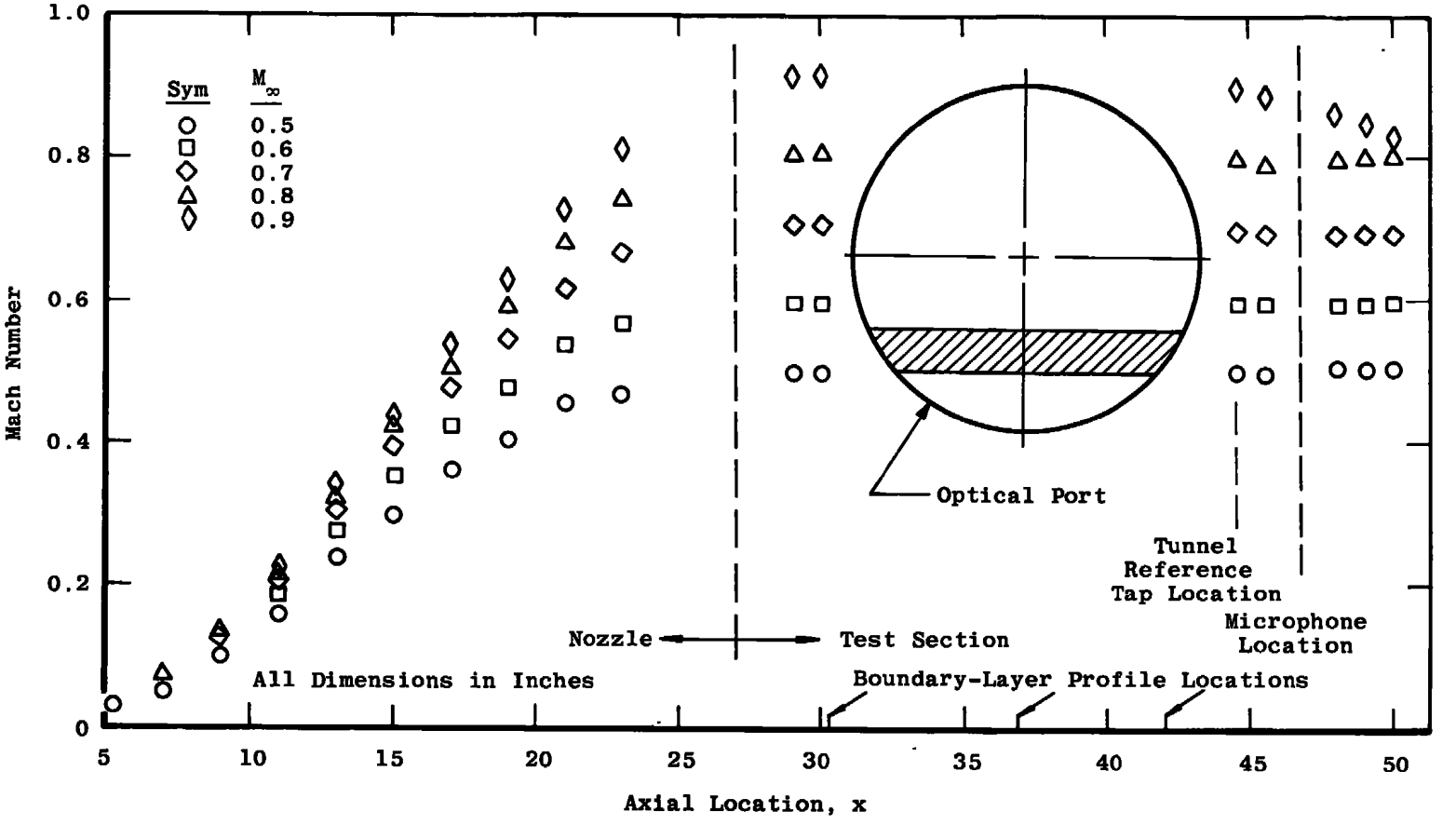

a. Mach number history-nozzle/test section

Figure 9. Tunnel flow quality data.

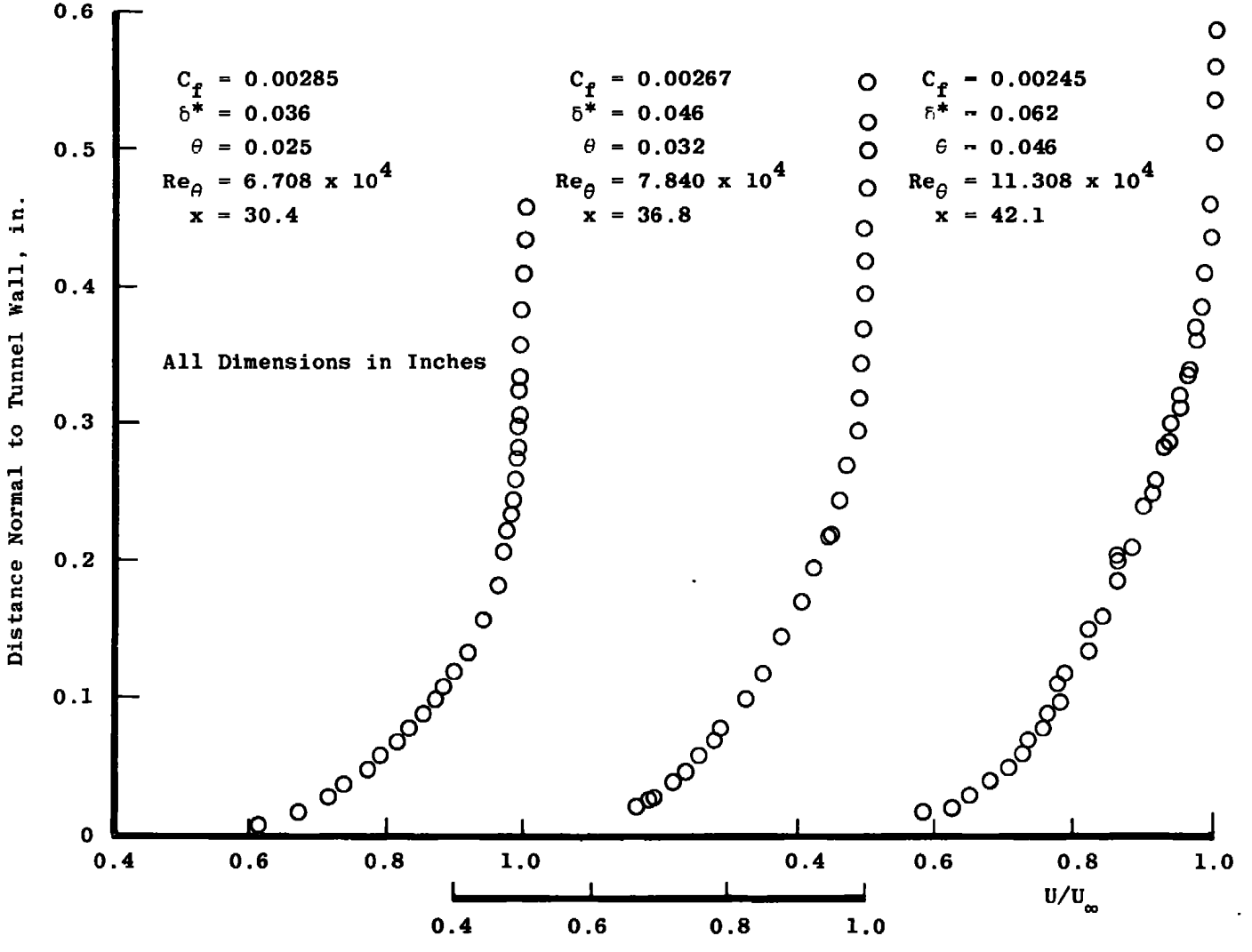

b. Wall boundary-layer development
Figure 9. Continued.

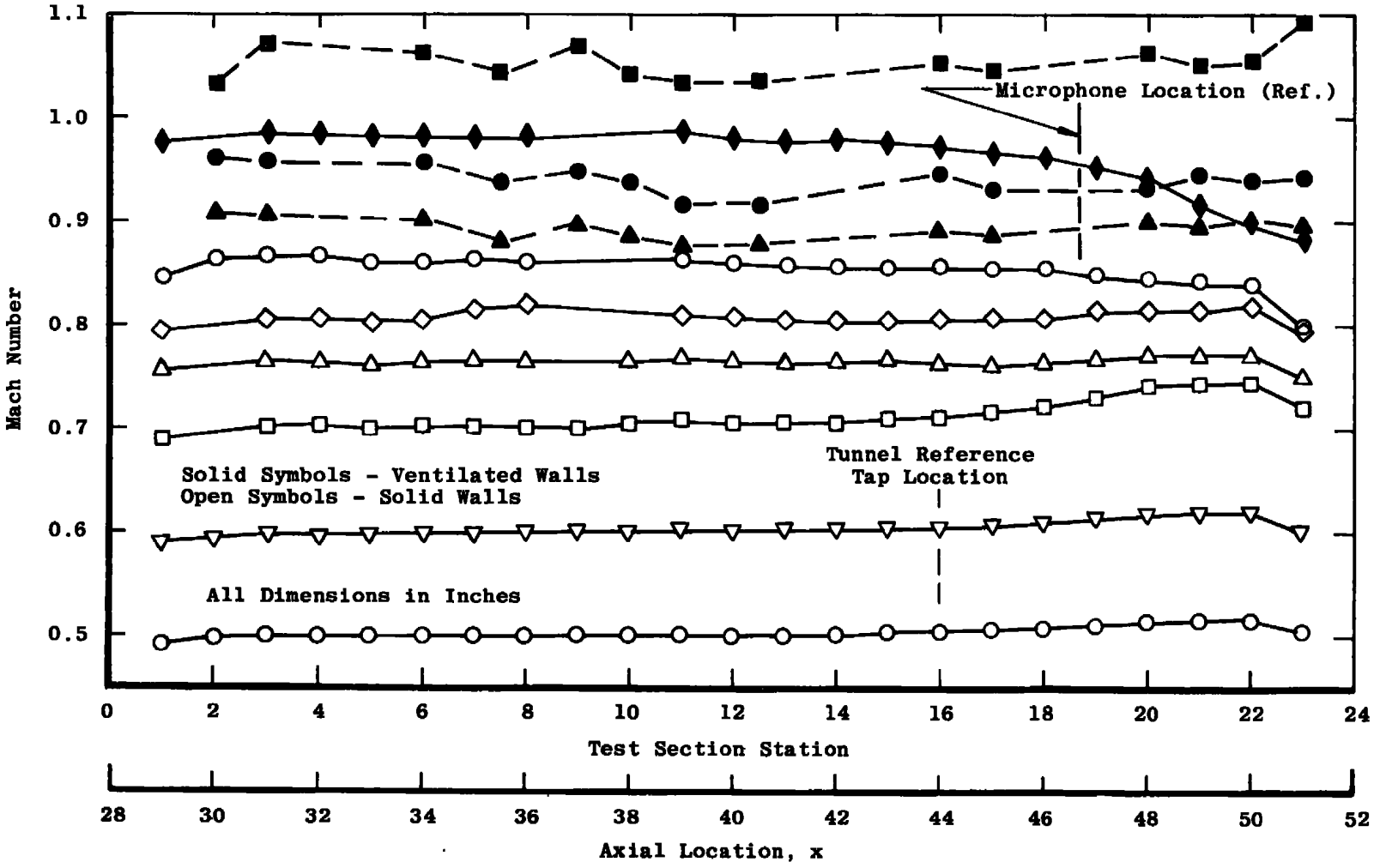

c. Axial Mach number distribution through test section

Figure 9. Concluded.

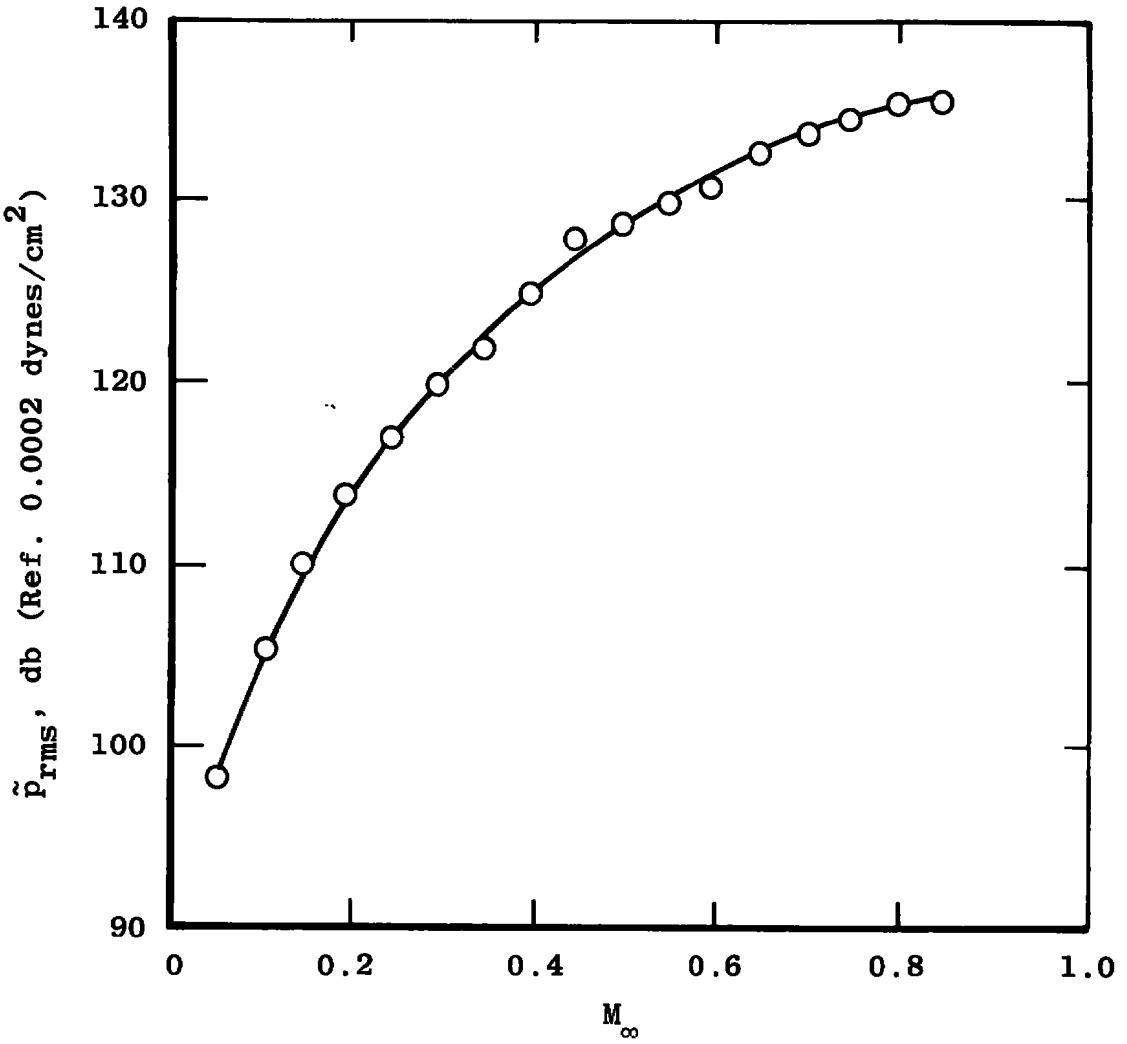

a. Amplitudes

Figure 10. Solid wall background noise.

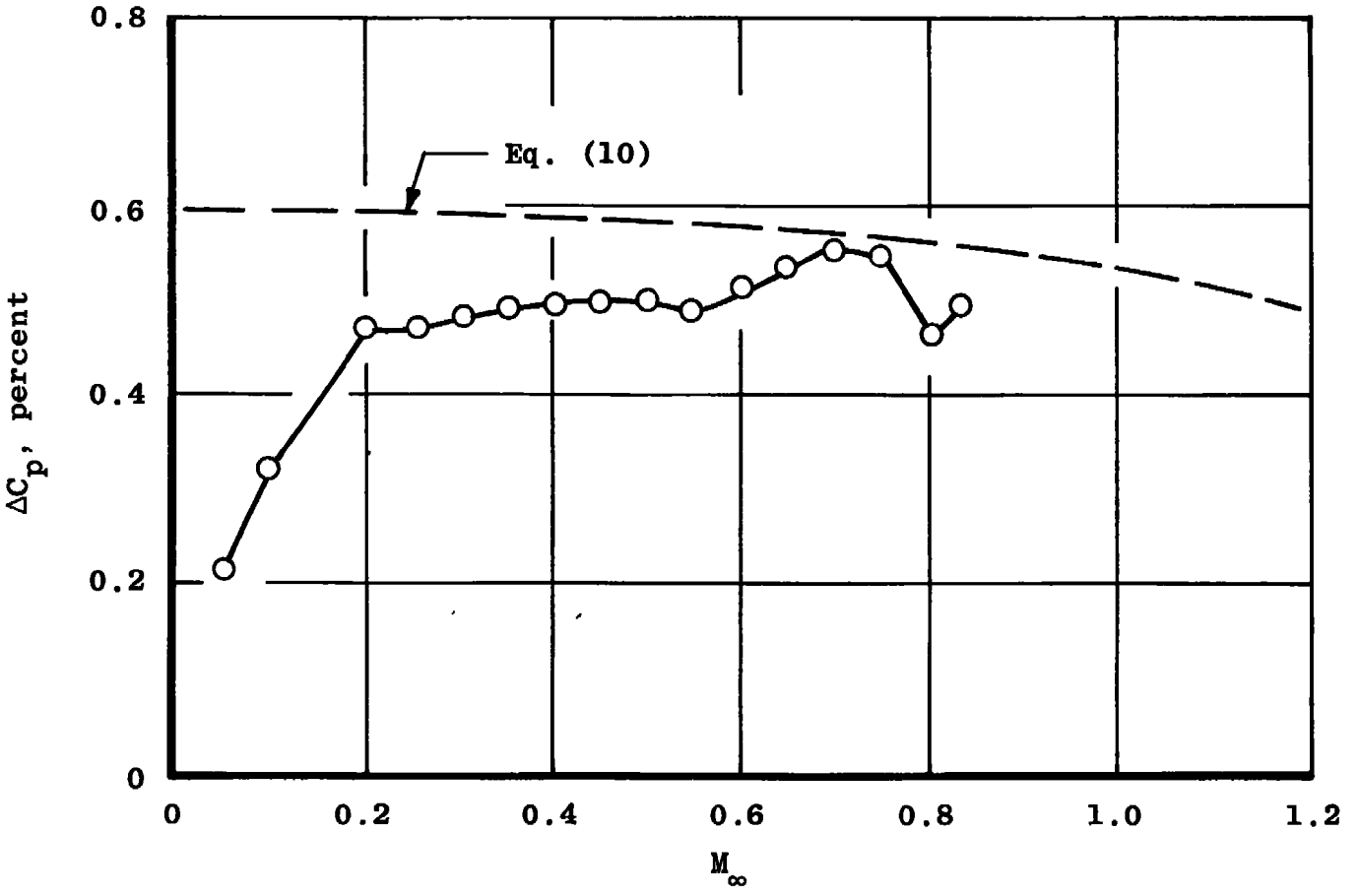

b. Normalized amplitudes
Figure 10. Concluded.

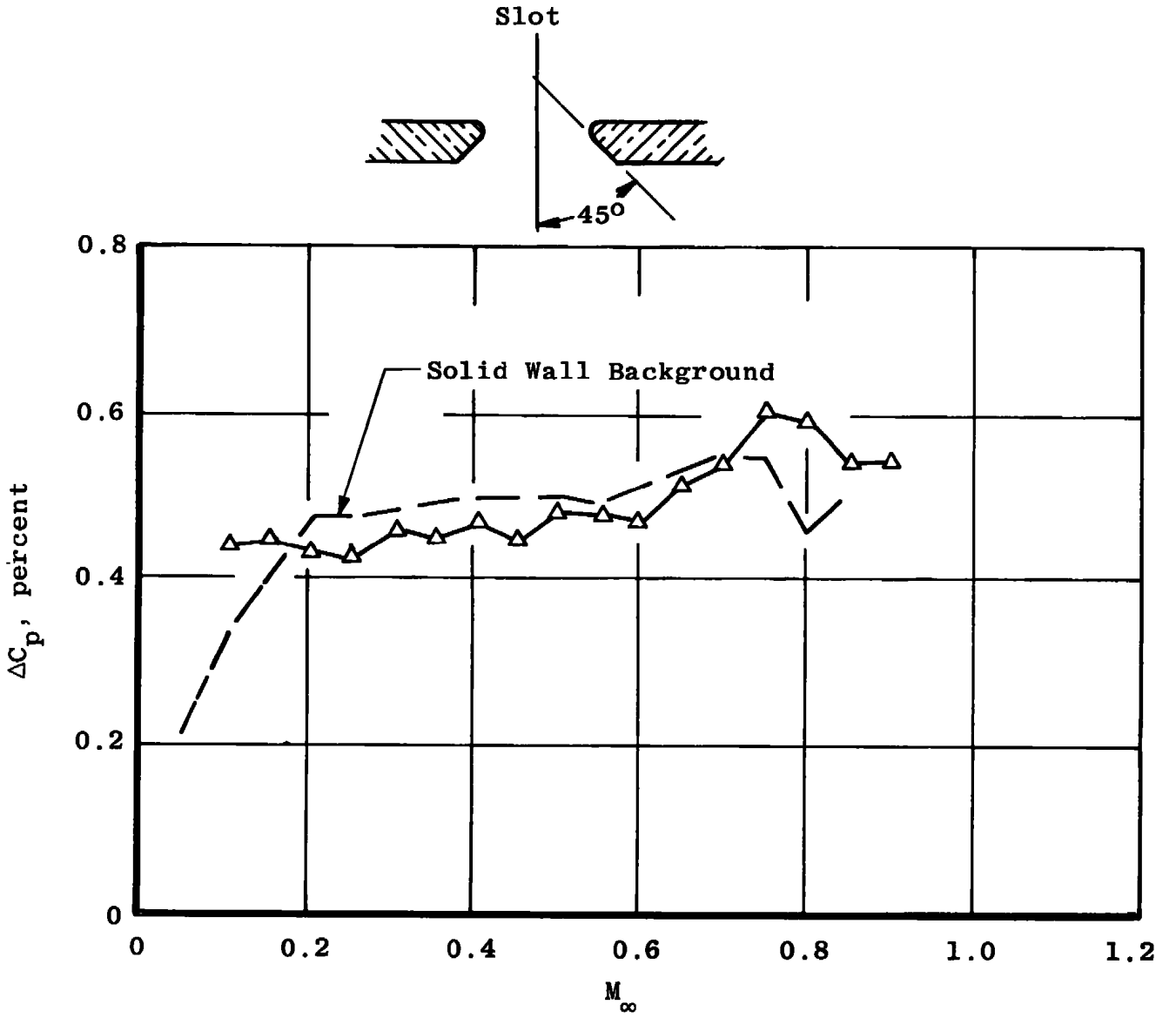

Figure 11. Longitudinal tapered slot noise.

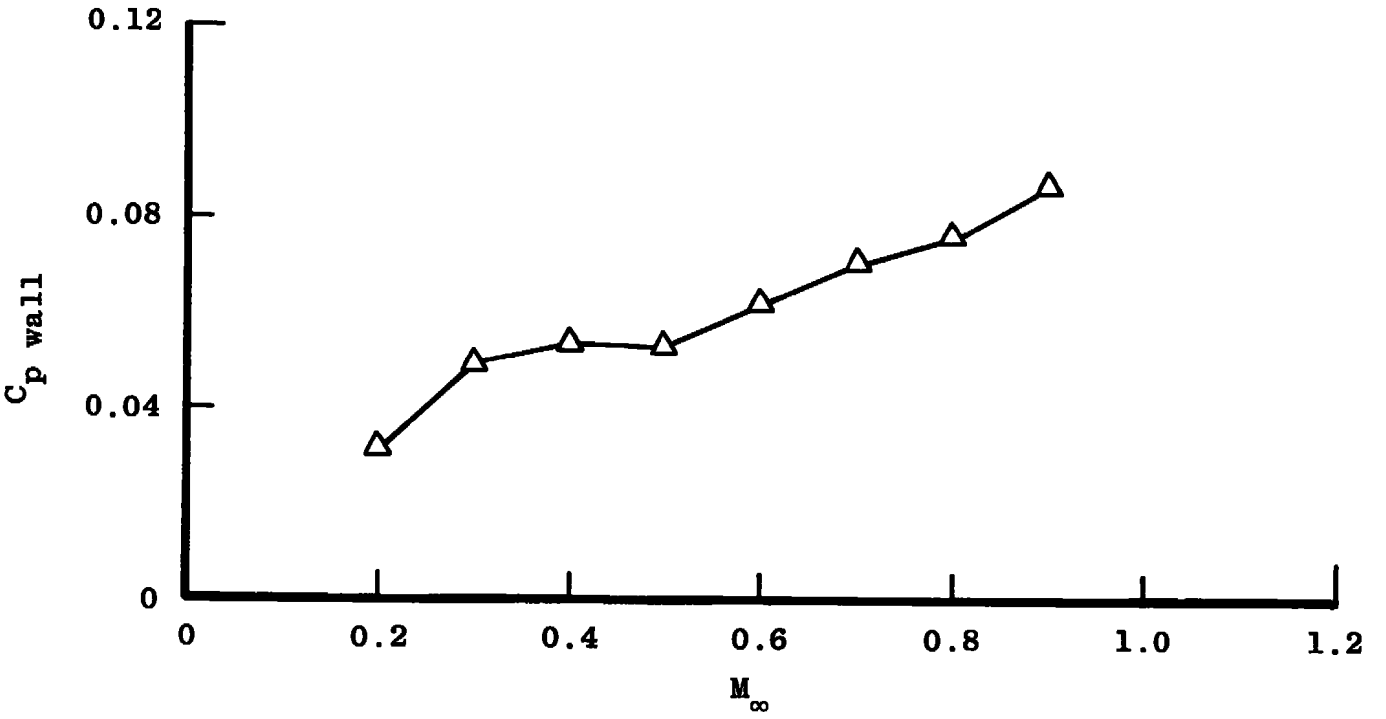

Figure 12. Slotted-wall differential pressure.

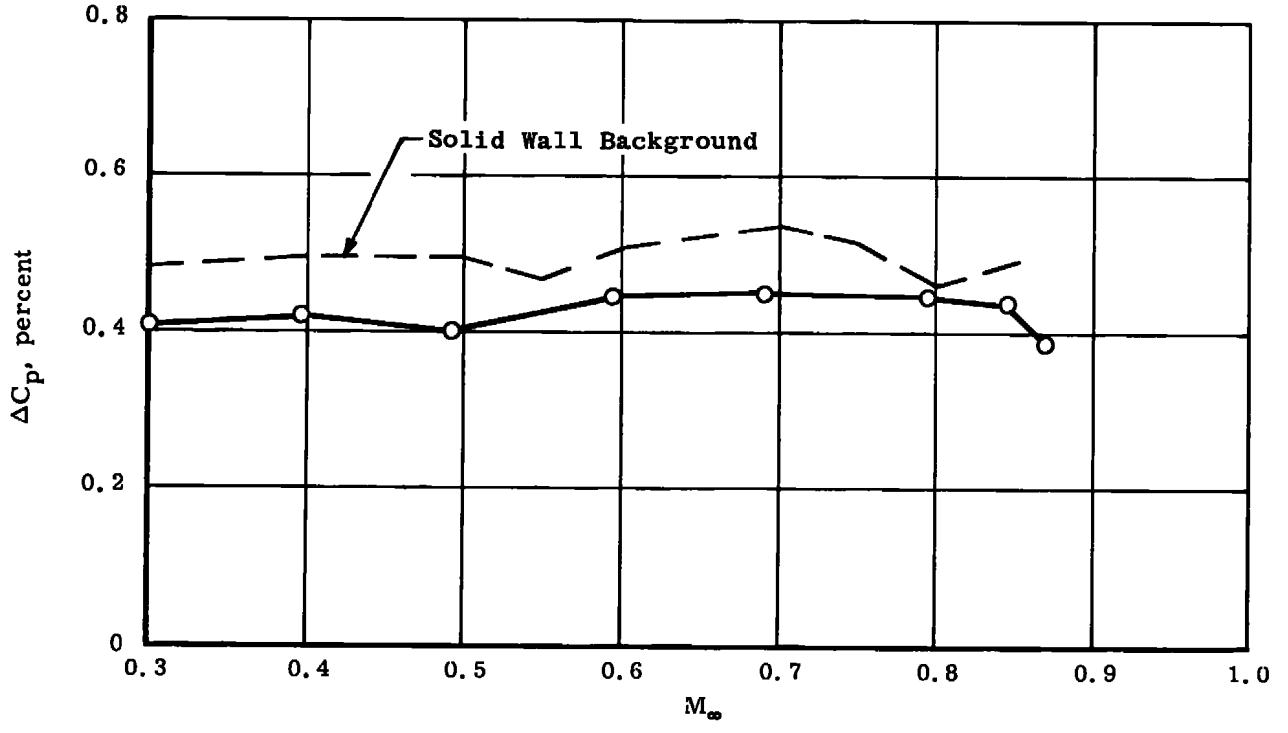

a. Porosity, τ = zero

Figure 13. Longitudinal rod wall noise levels.

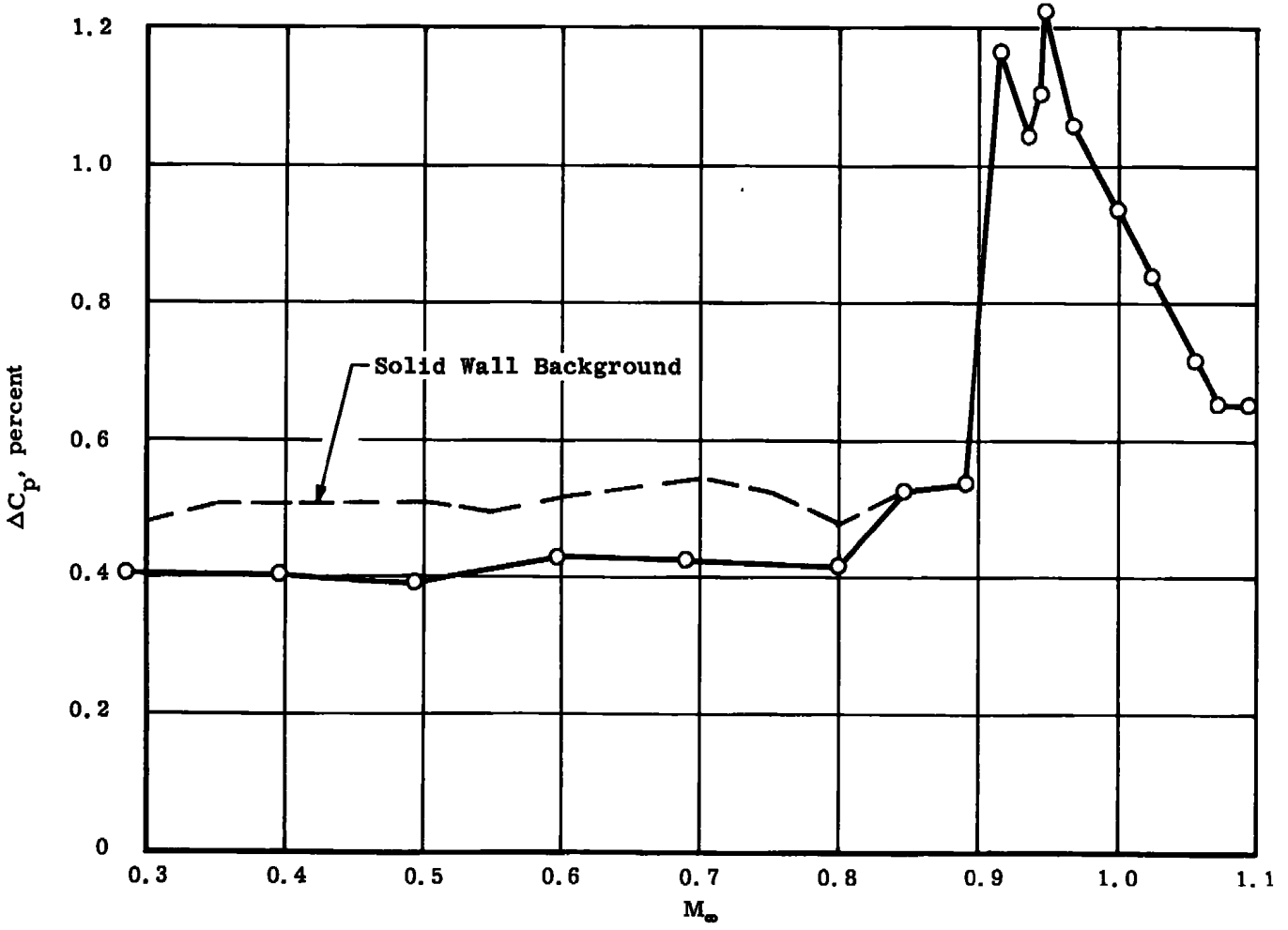

b. Porosity, τ = one percent
Figure 13. Continued.

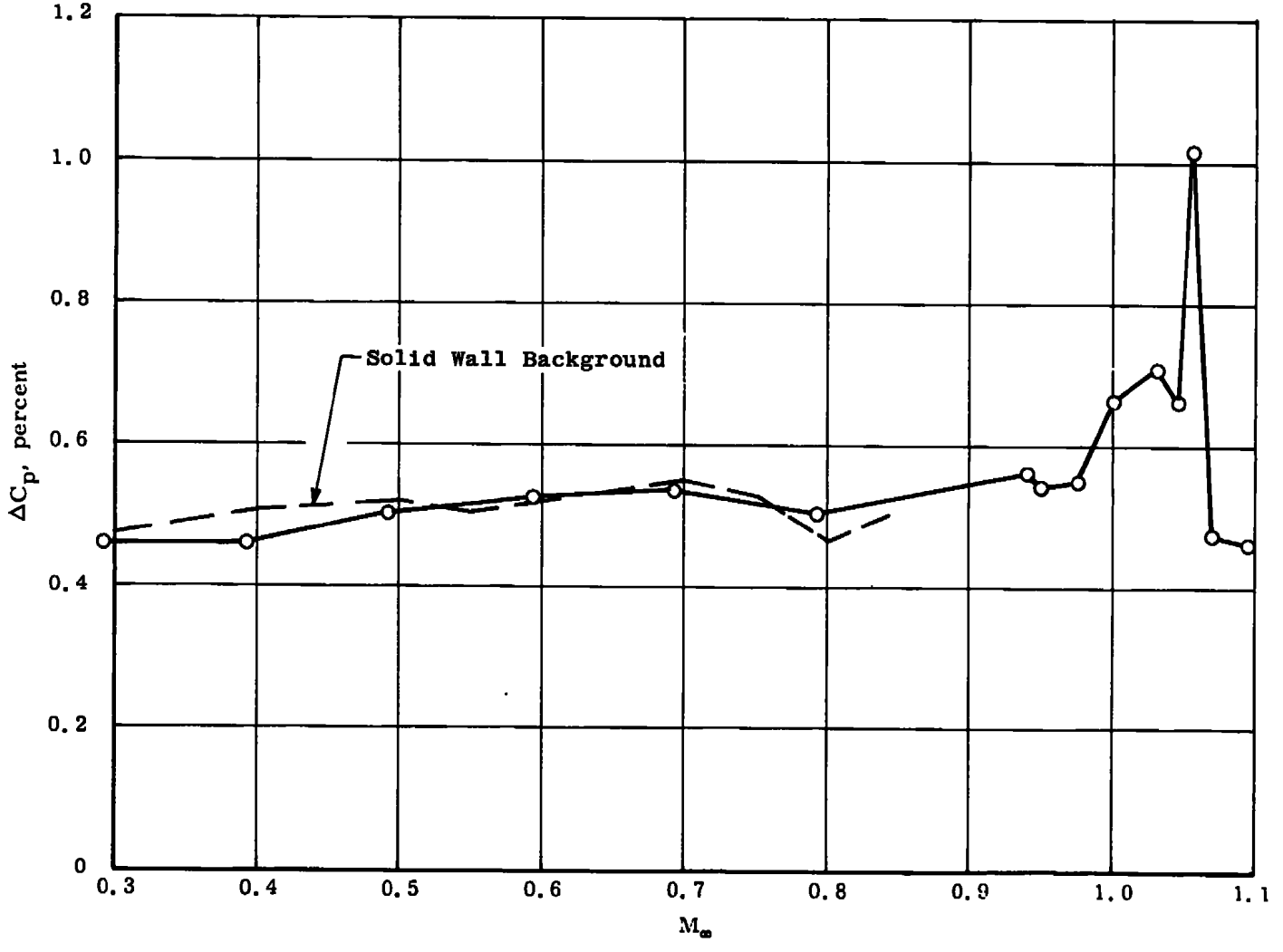

c. Porosity, τ = two percent
Figure 13. Continued.

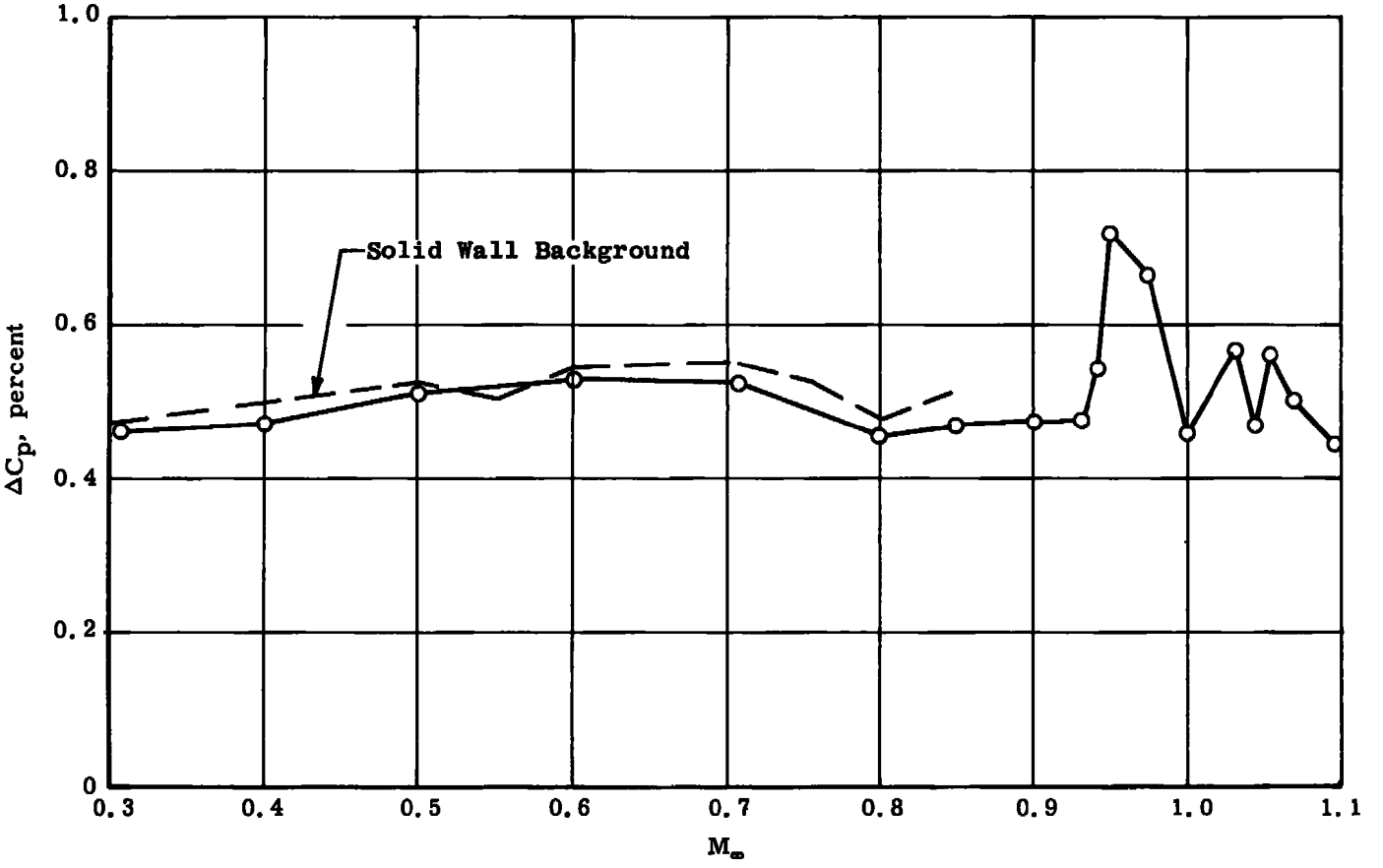

d. Porosity, τ = four percent
Figure 13. Continued.

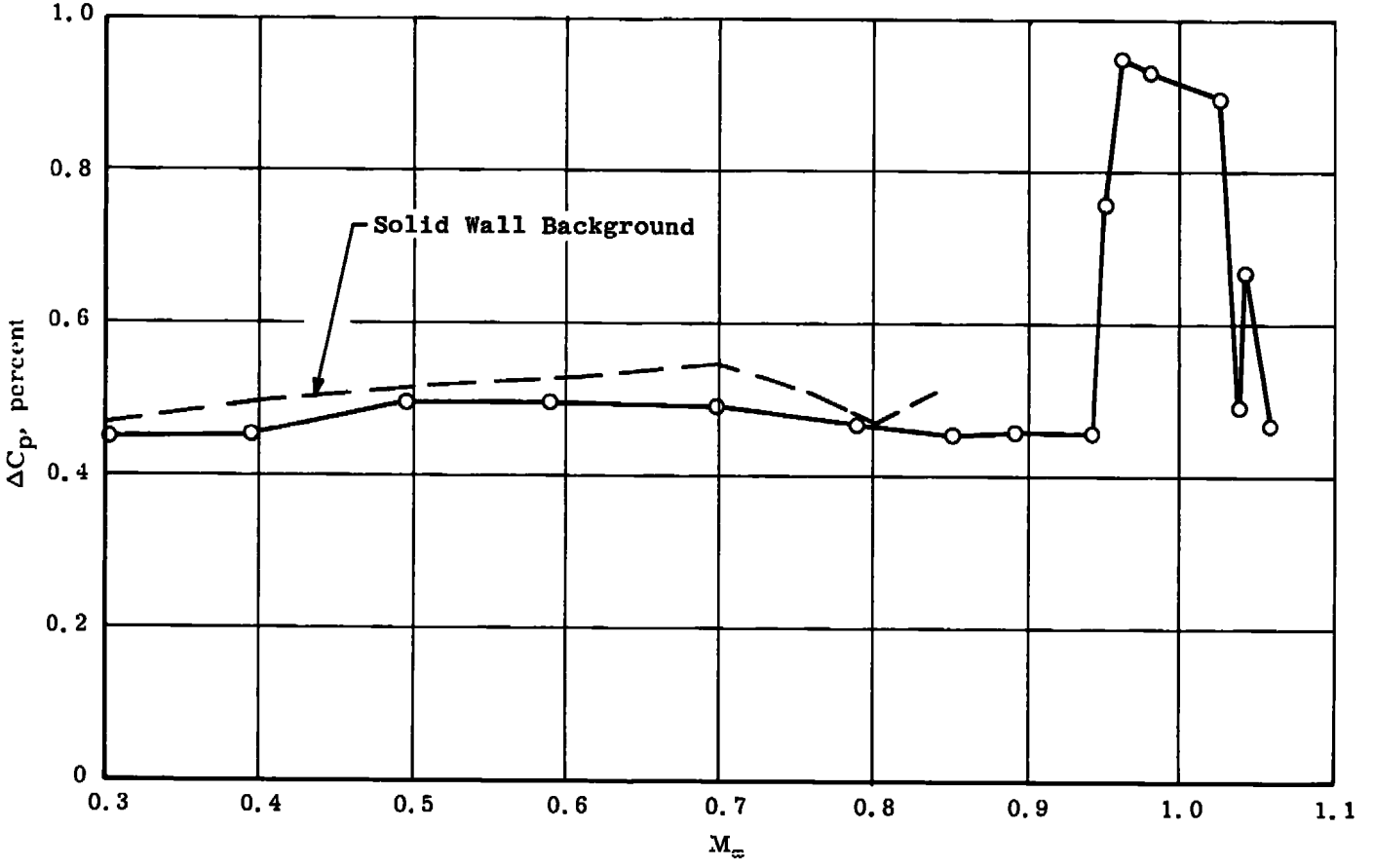

e. Porosity, τ = six percent
Figure 13. Continued.

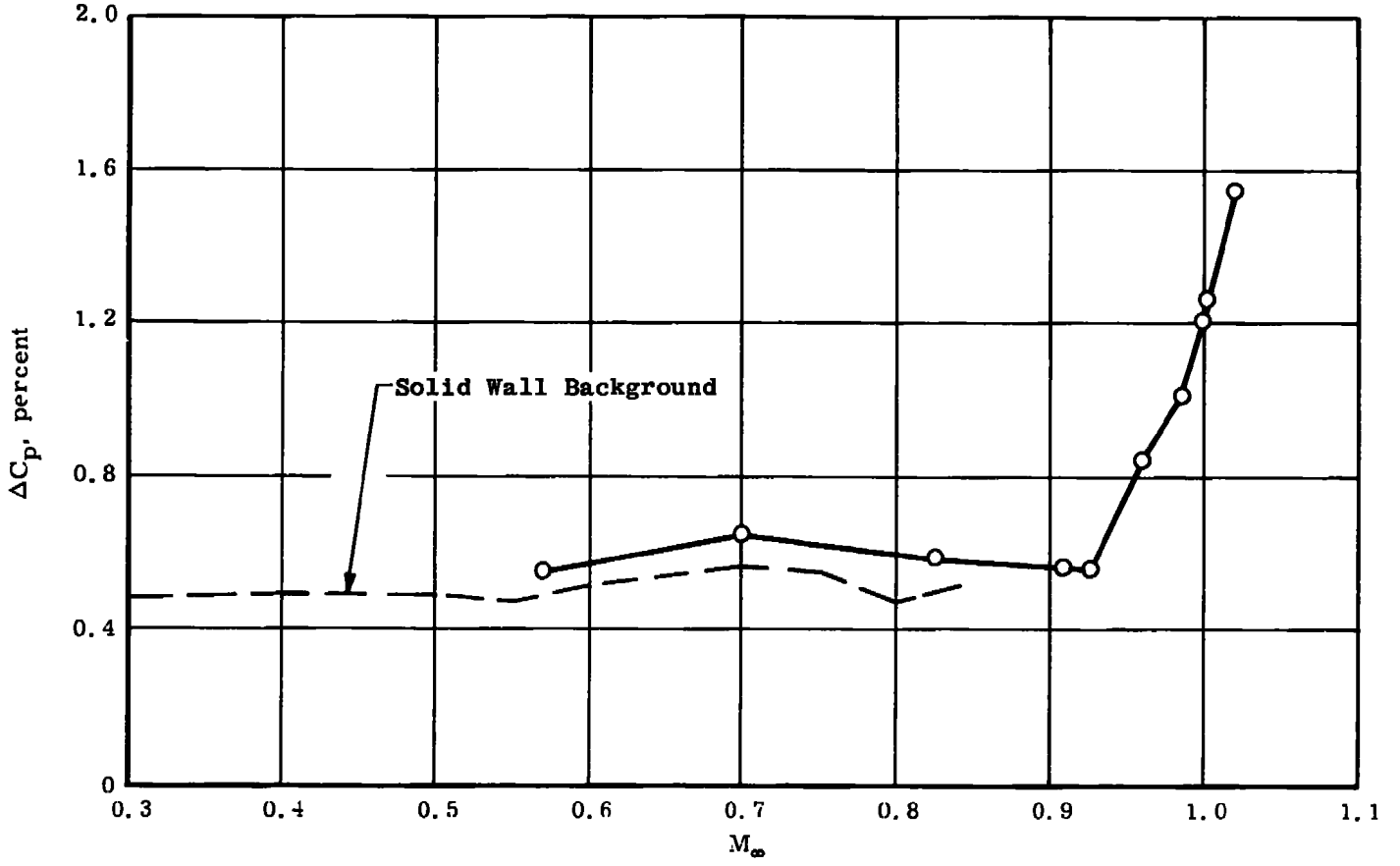

f. Porosity, τ = ten percent
Figure 13. Concluded.

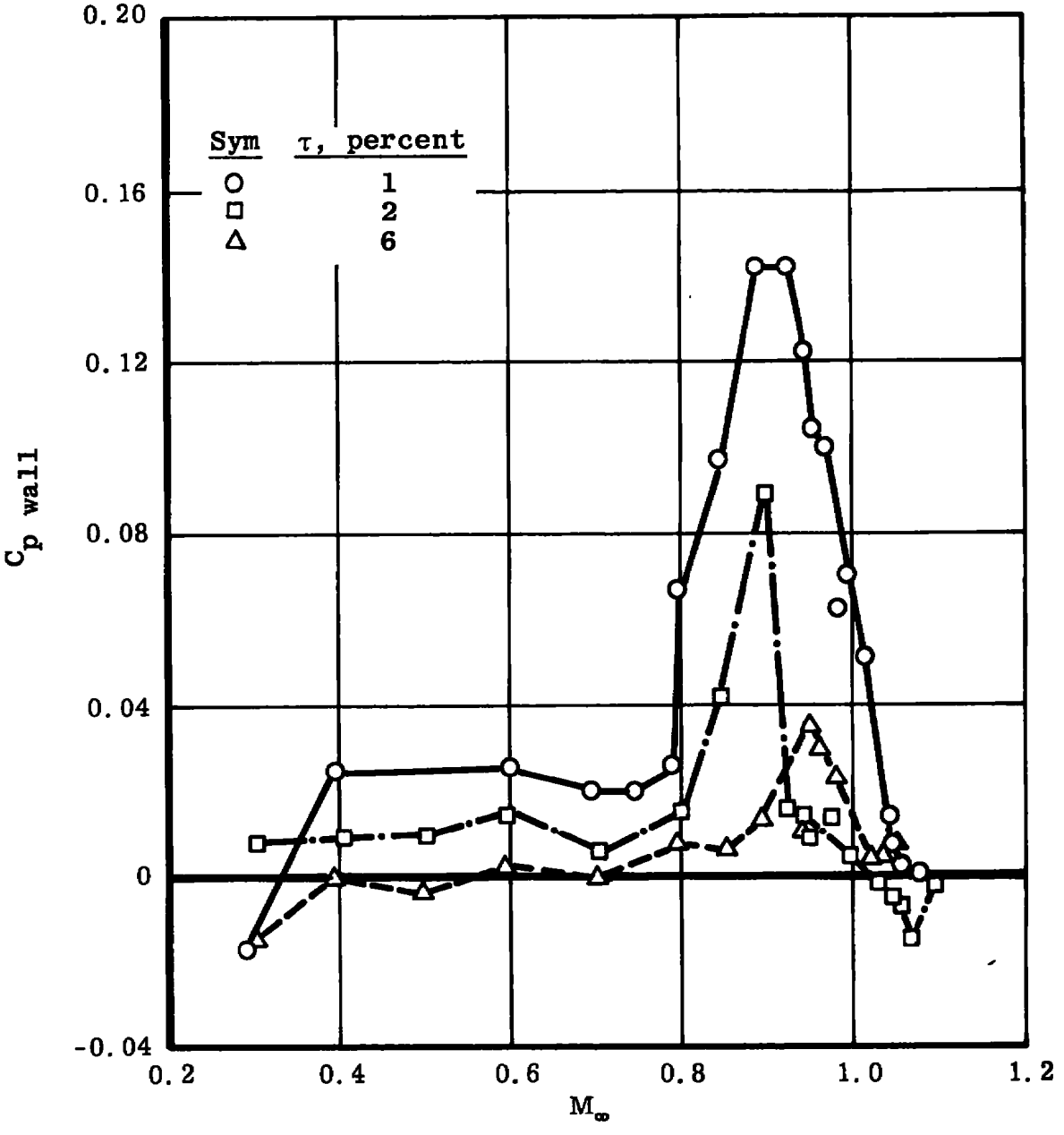

Figure 14. Rod wall differential pressure.

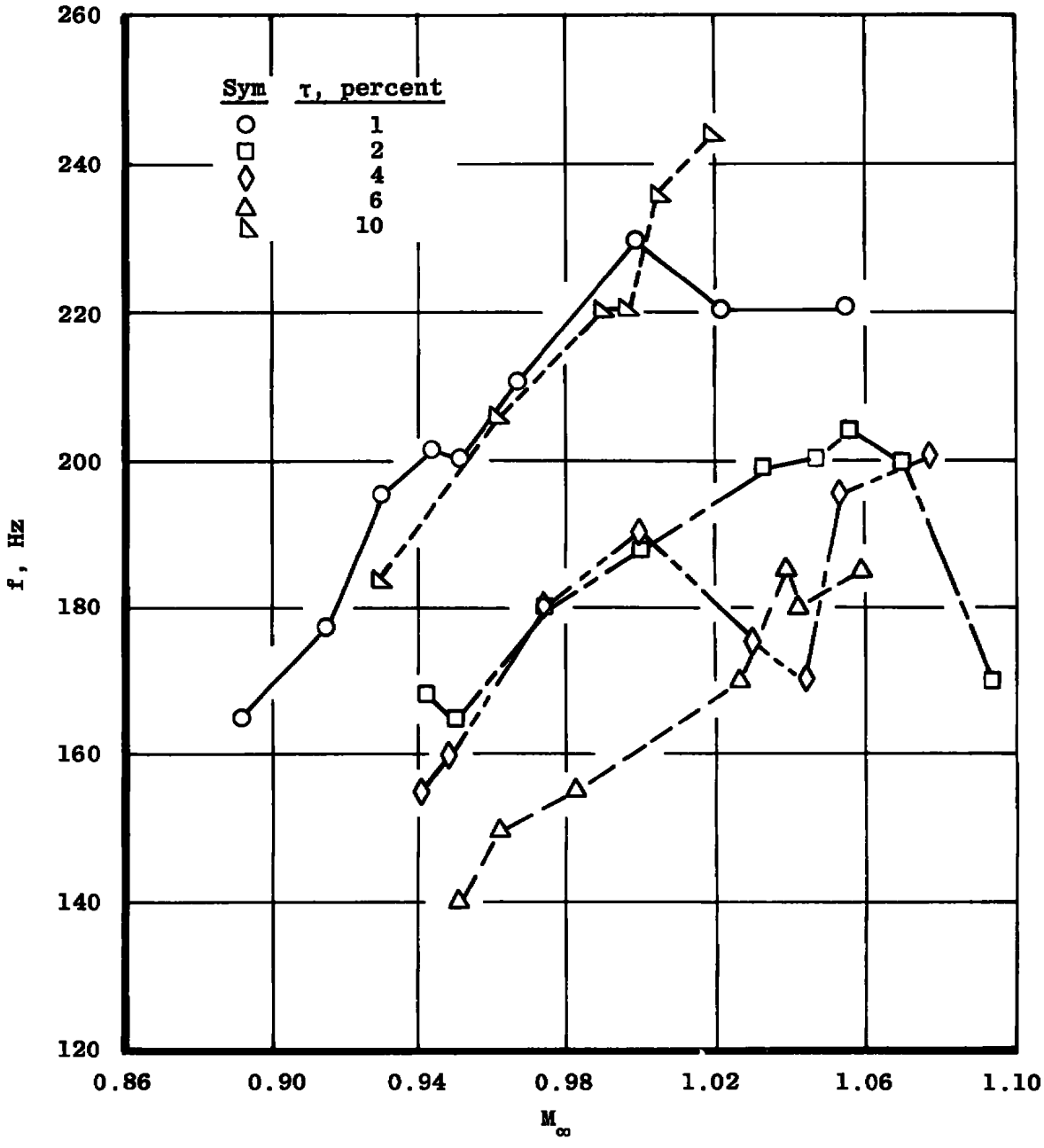

Figure 15. "Buzz" frequencies.

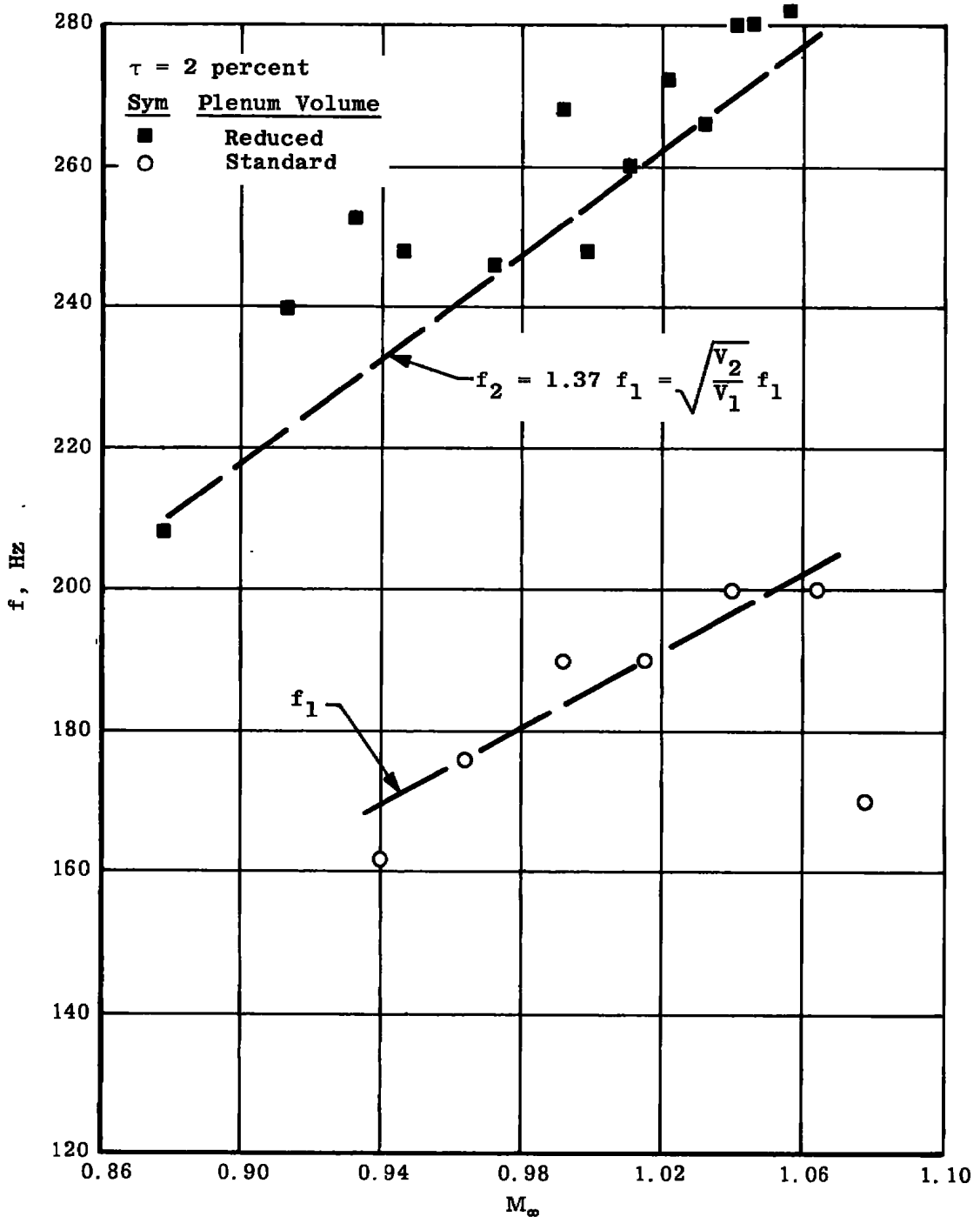

Figure 16. Effect of plenum volume "Buzz" frequency.

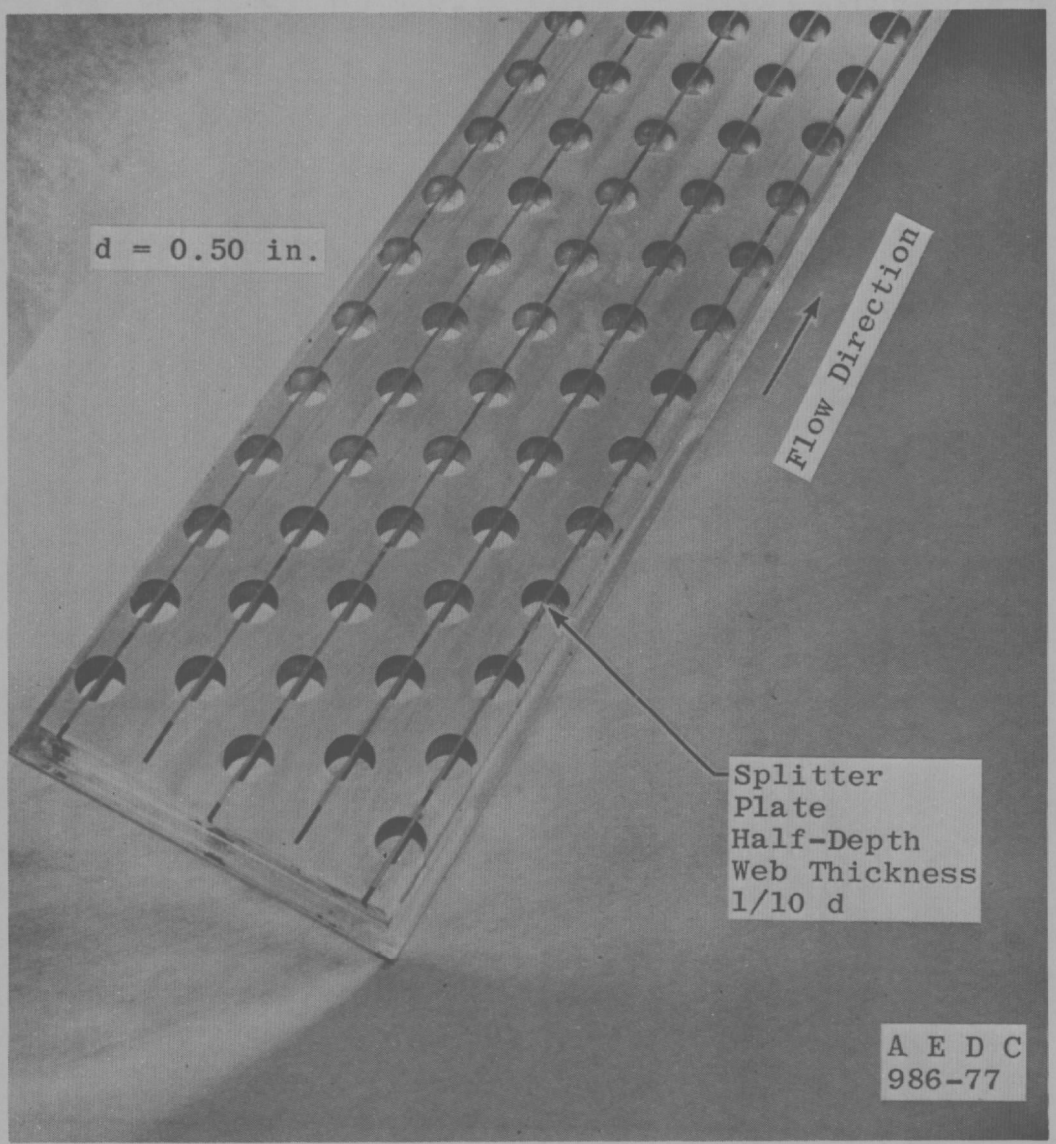

a. Splitter plate in thick normal-hole walls

Figure 17. Noise suppression measures for perforated walls.

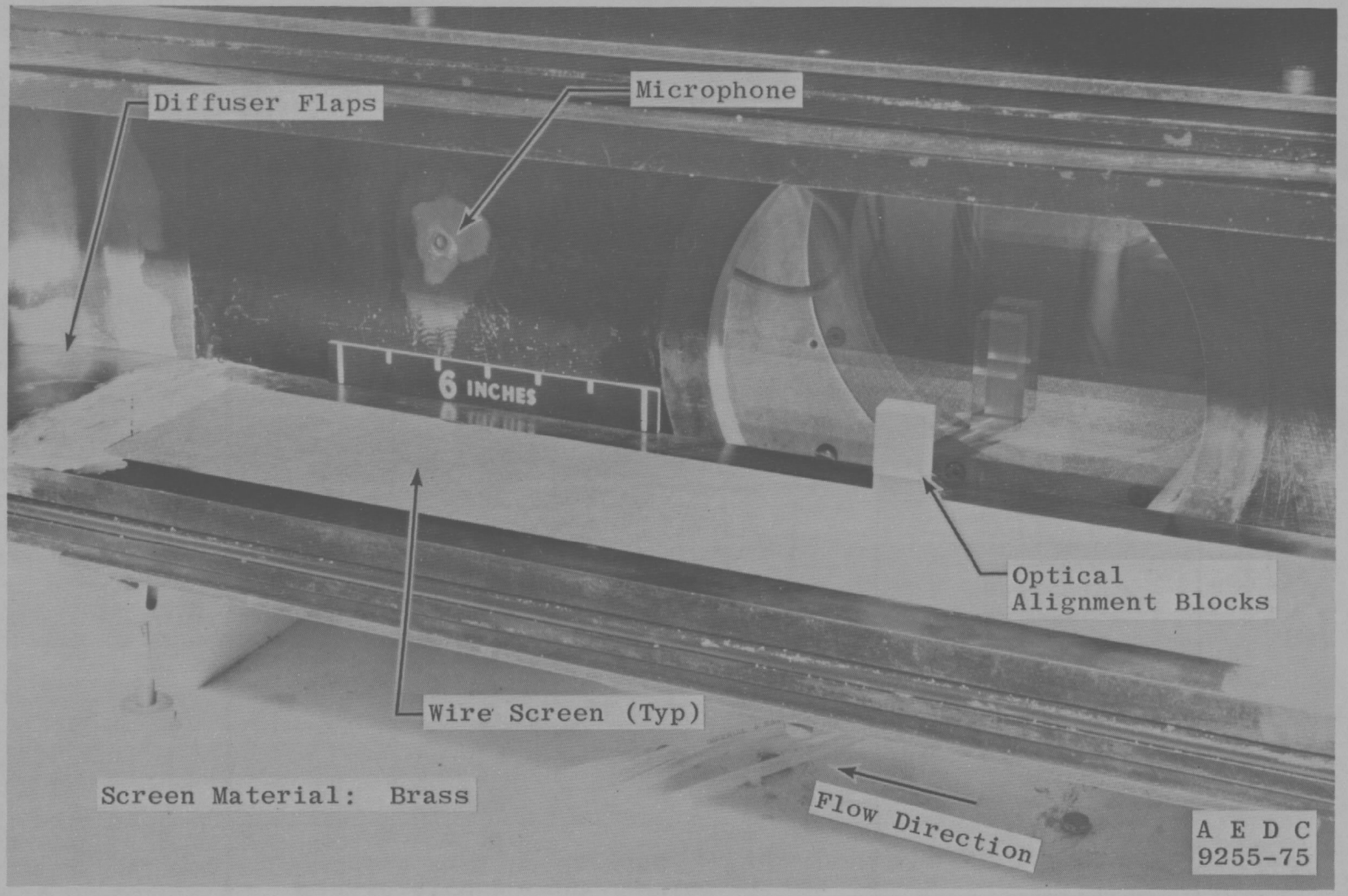

b. Wire screen installation
Figure 17. Concluded.

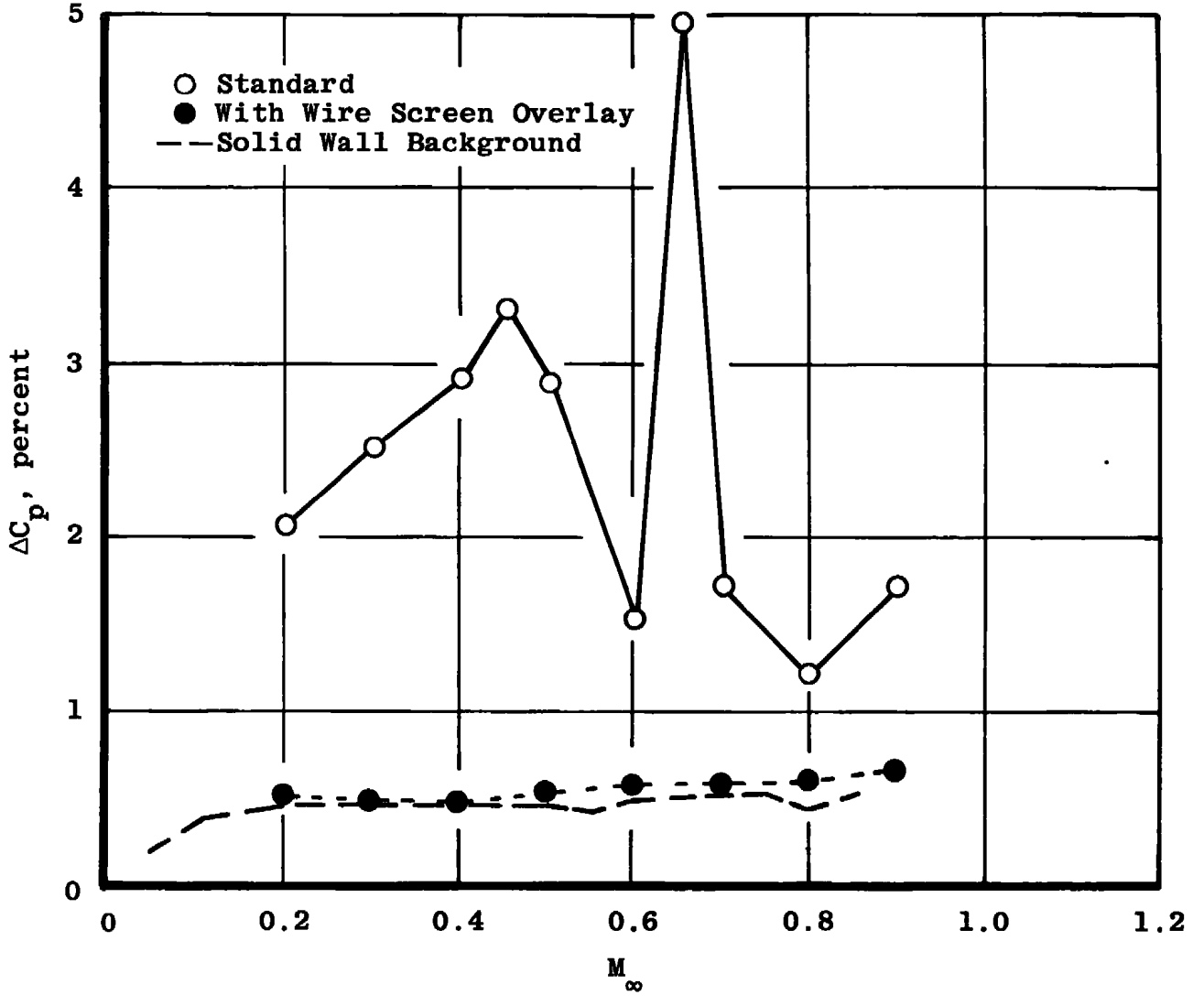

a. Amplitude levels

Figure 18. Noise data from thin perforated walls with normal holes.

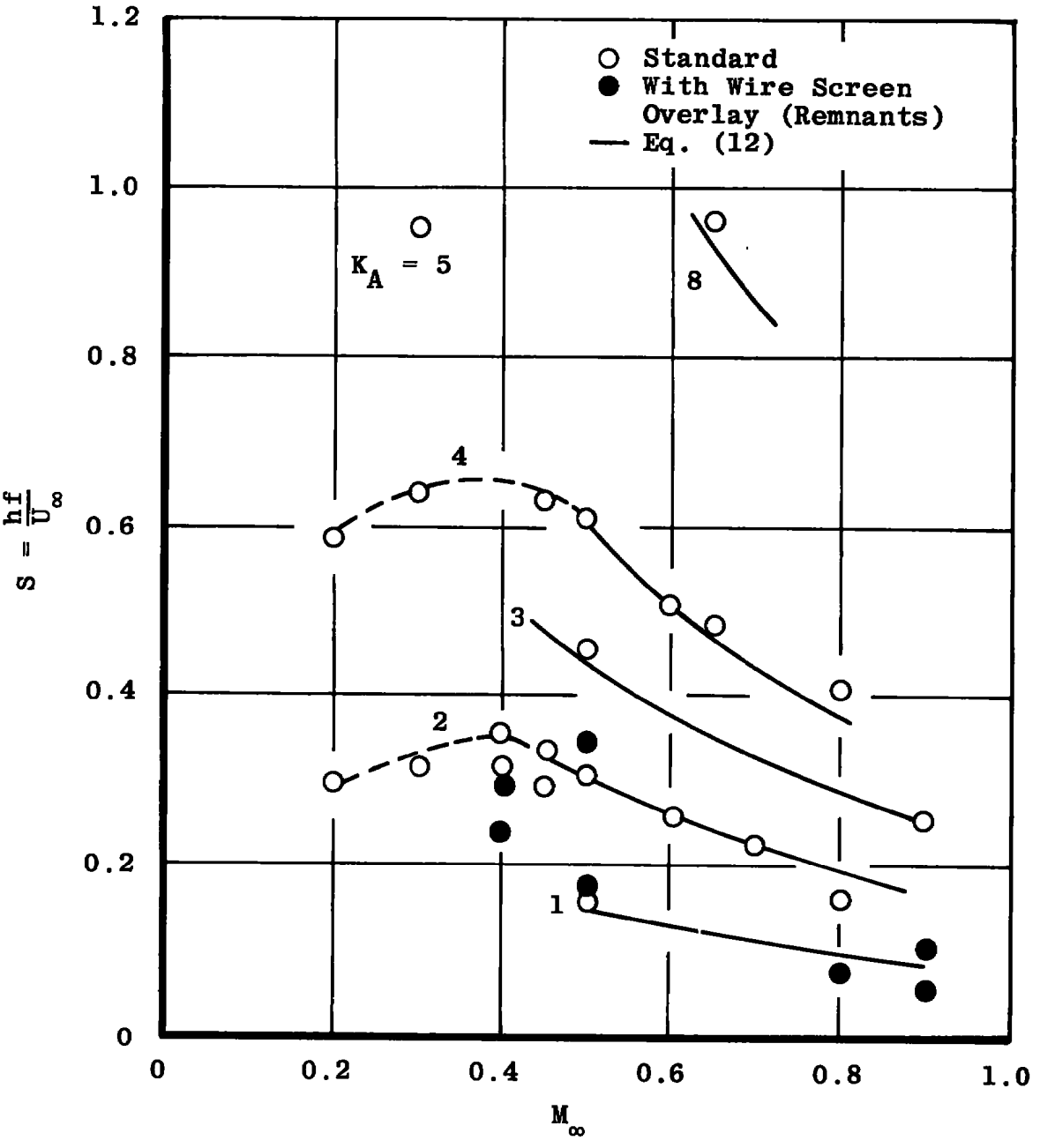

b. Predominant frequencies
Figure 18. Concluded.

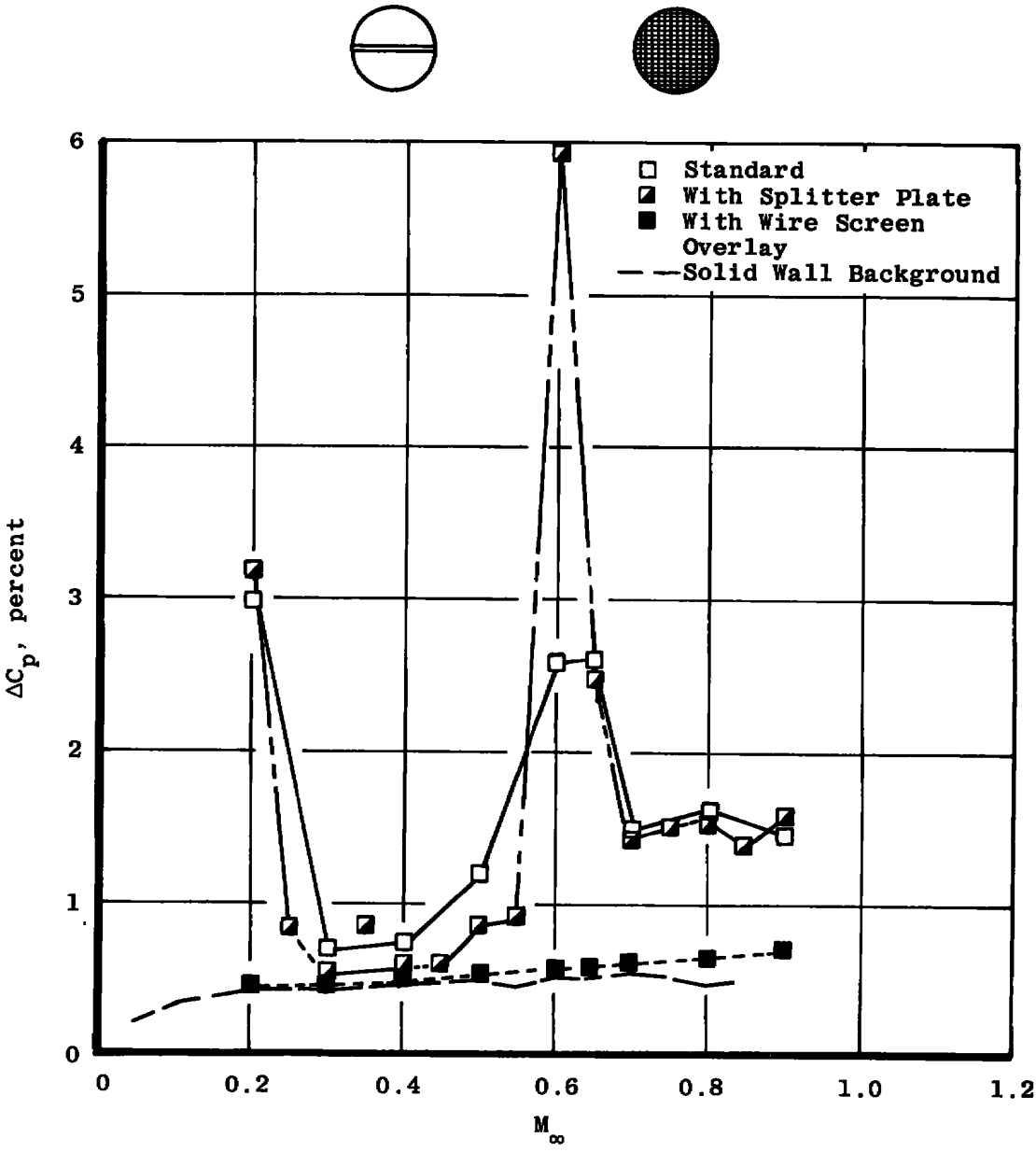

a. Amplitude levels

Figure 19. Noise data from thick perforated walls with normal holes.

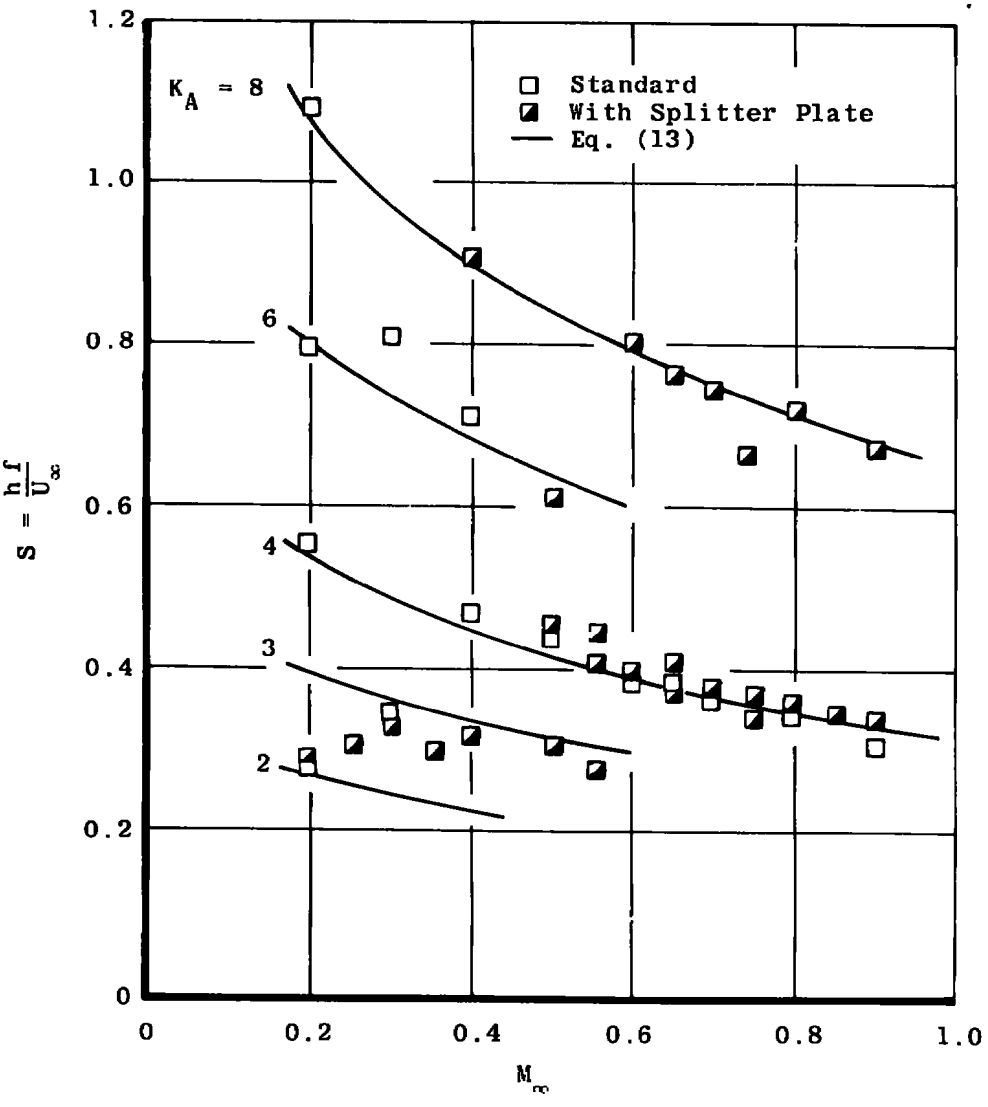

b. Predominant frequencies
Figure 19. Concluded.

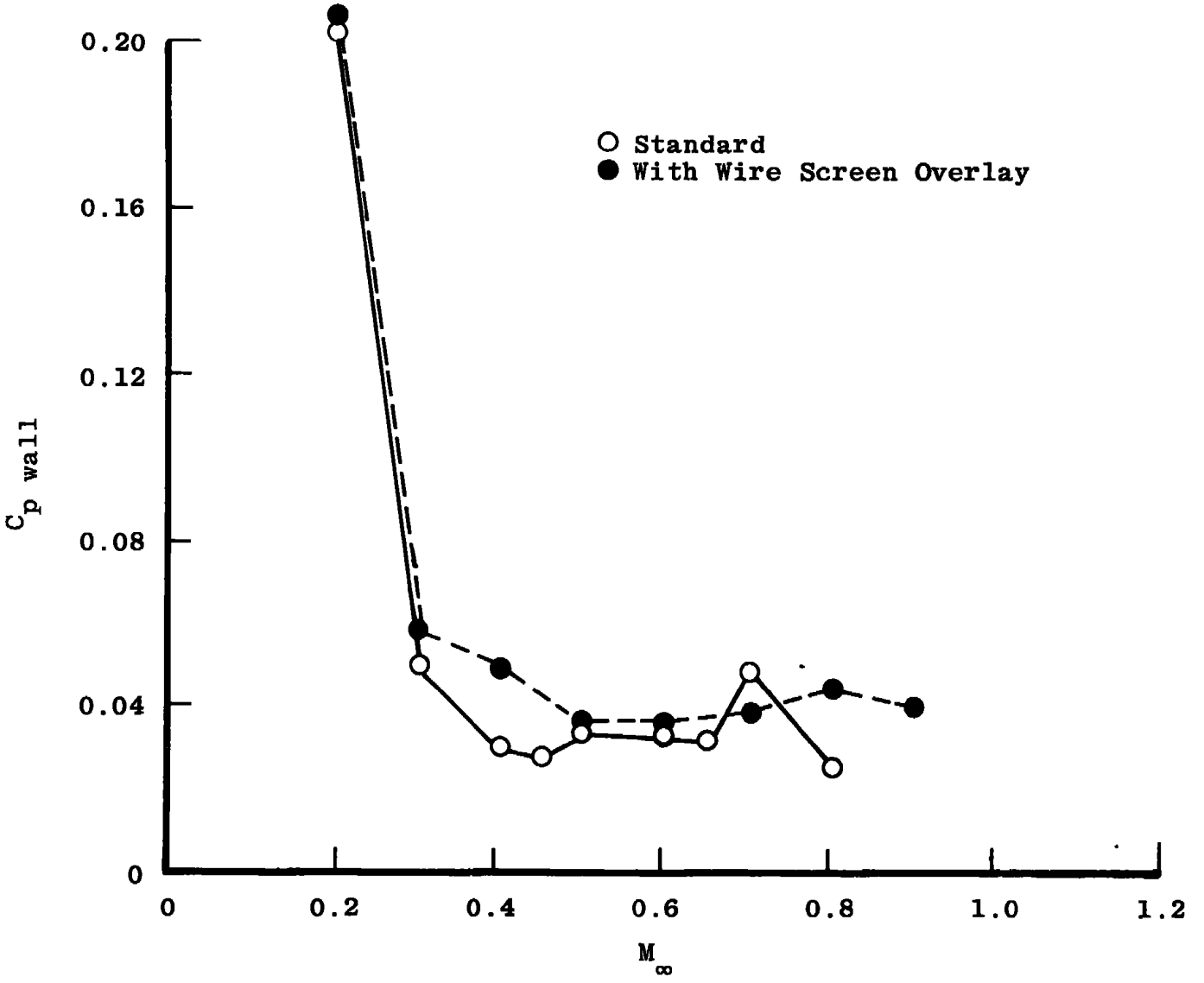

Figure 20. Differential pressure across thin normal-hole walls.

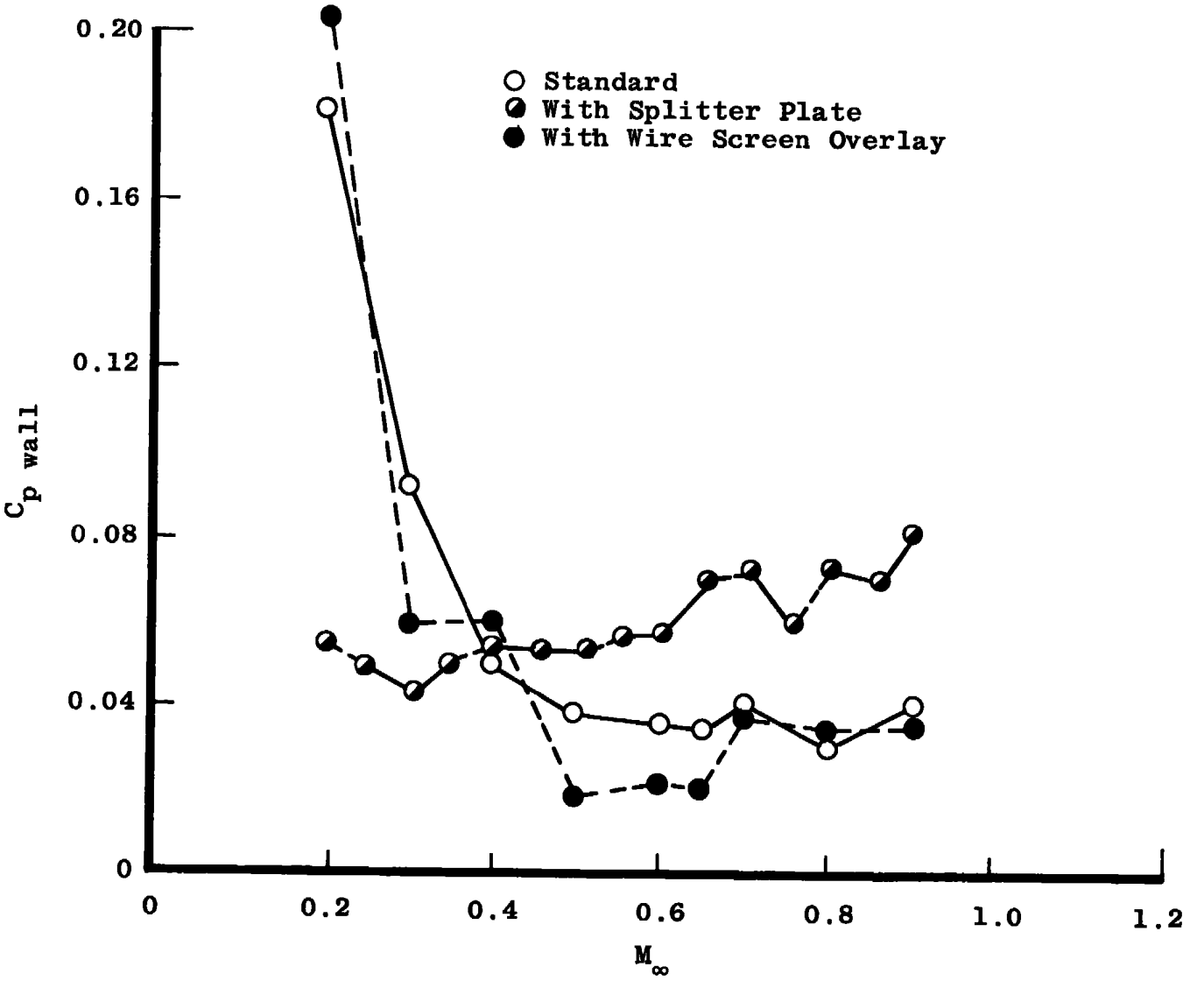

Figure 21. Differential pressure across thick normal-hole walls.

Figure 22. Schlieren data illustrating noise suppression from splitter plates.

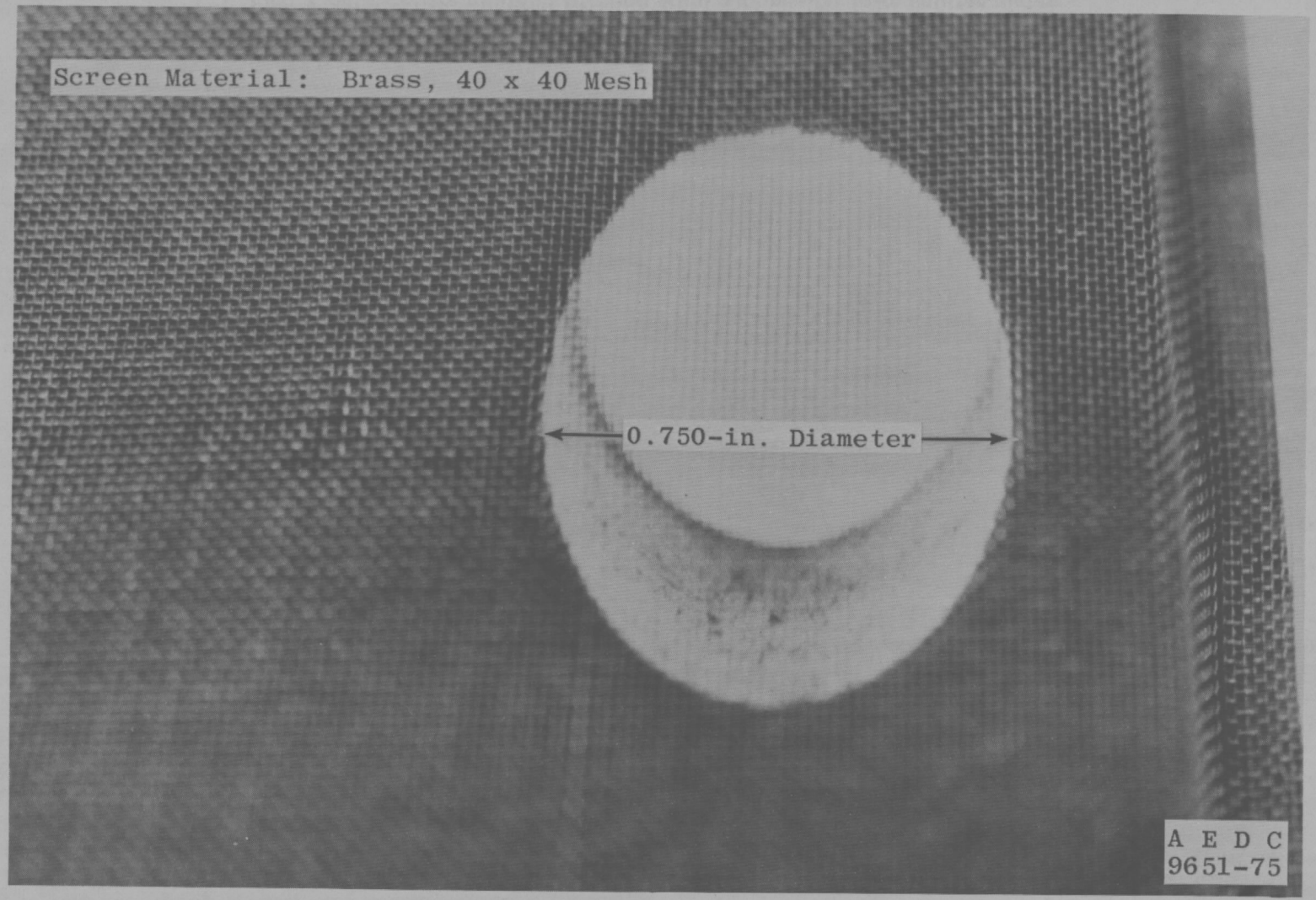

Figure 23. Wire screen overlay on Tunnel 16T wall sample.

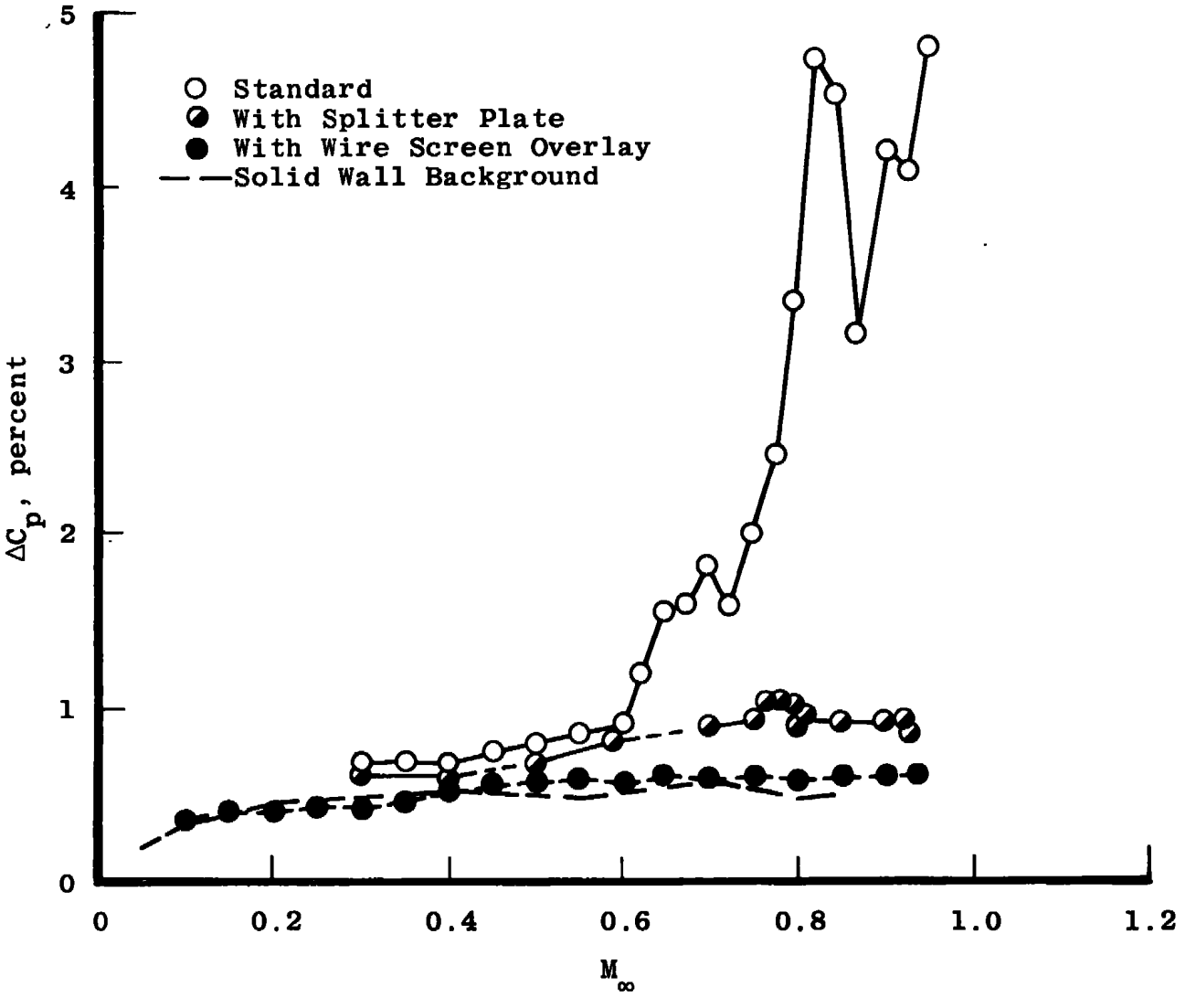

Figure 24. Amplitudes of noise from Tunnel 16T wall samples.

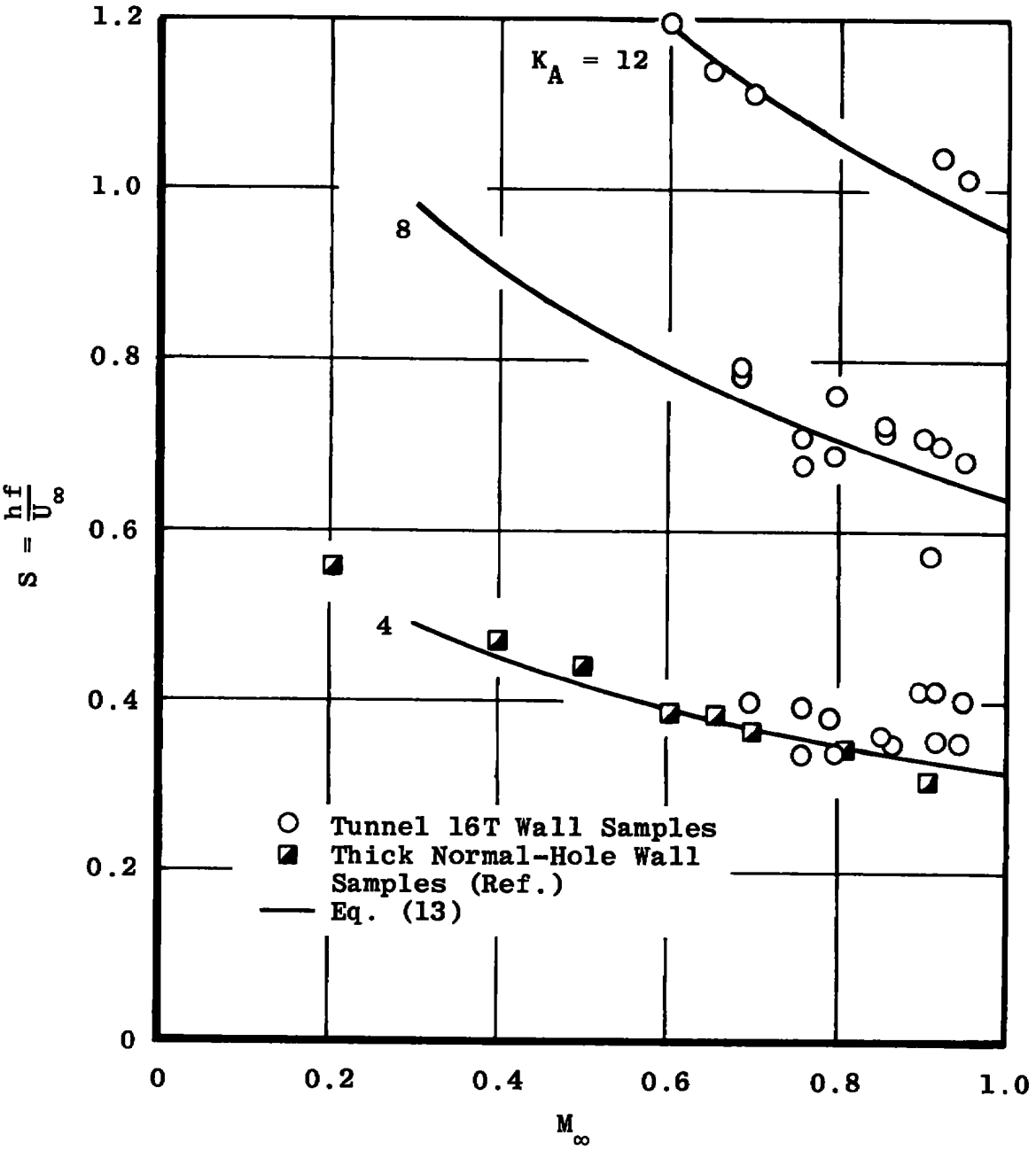

Figure 25. Predominant frequencies from Tunnel 16T wall samples.

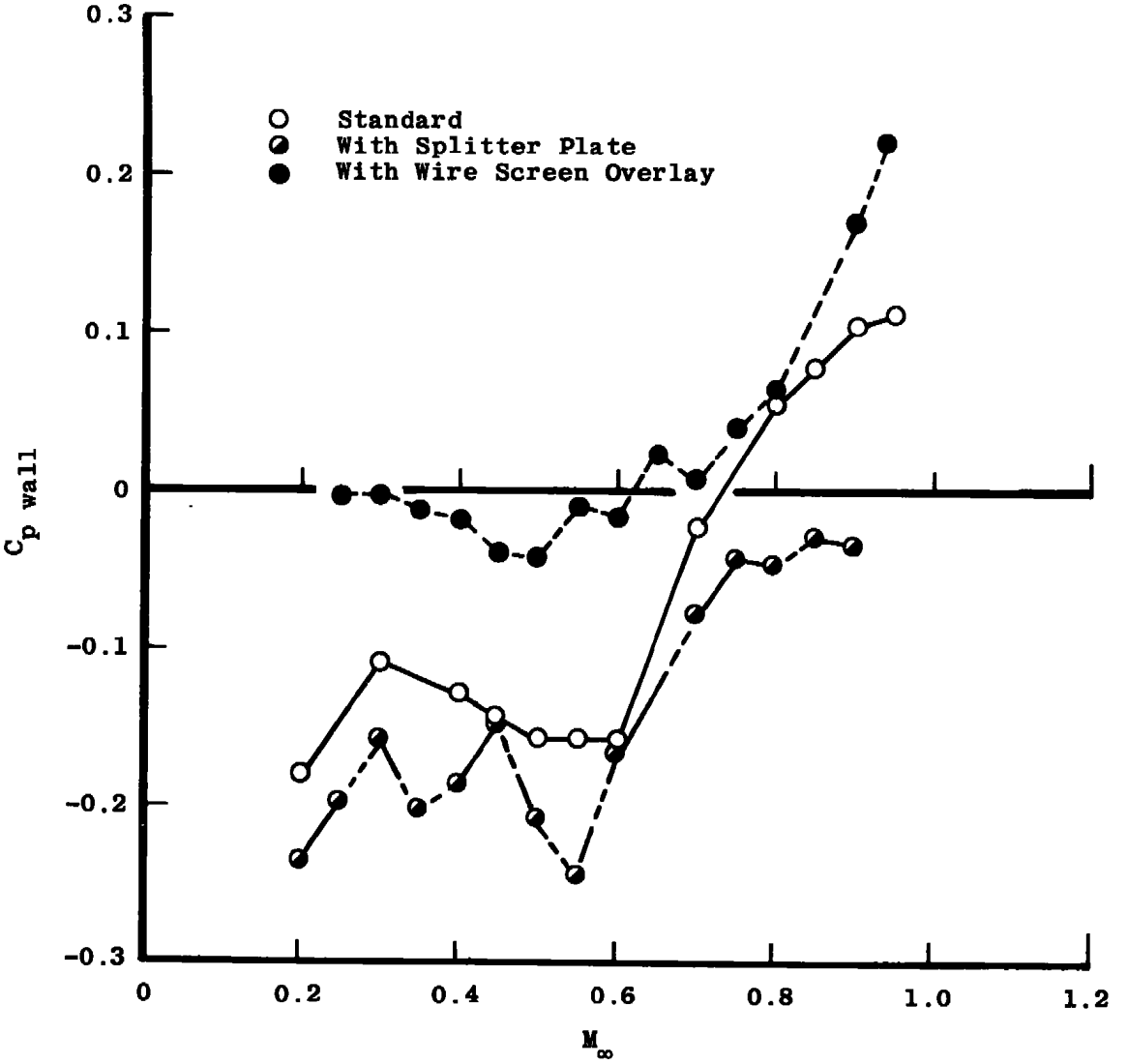

Figure 26. Differential pressure across Tunnel 16T wall samples.

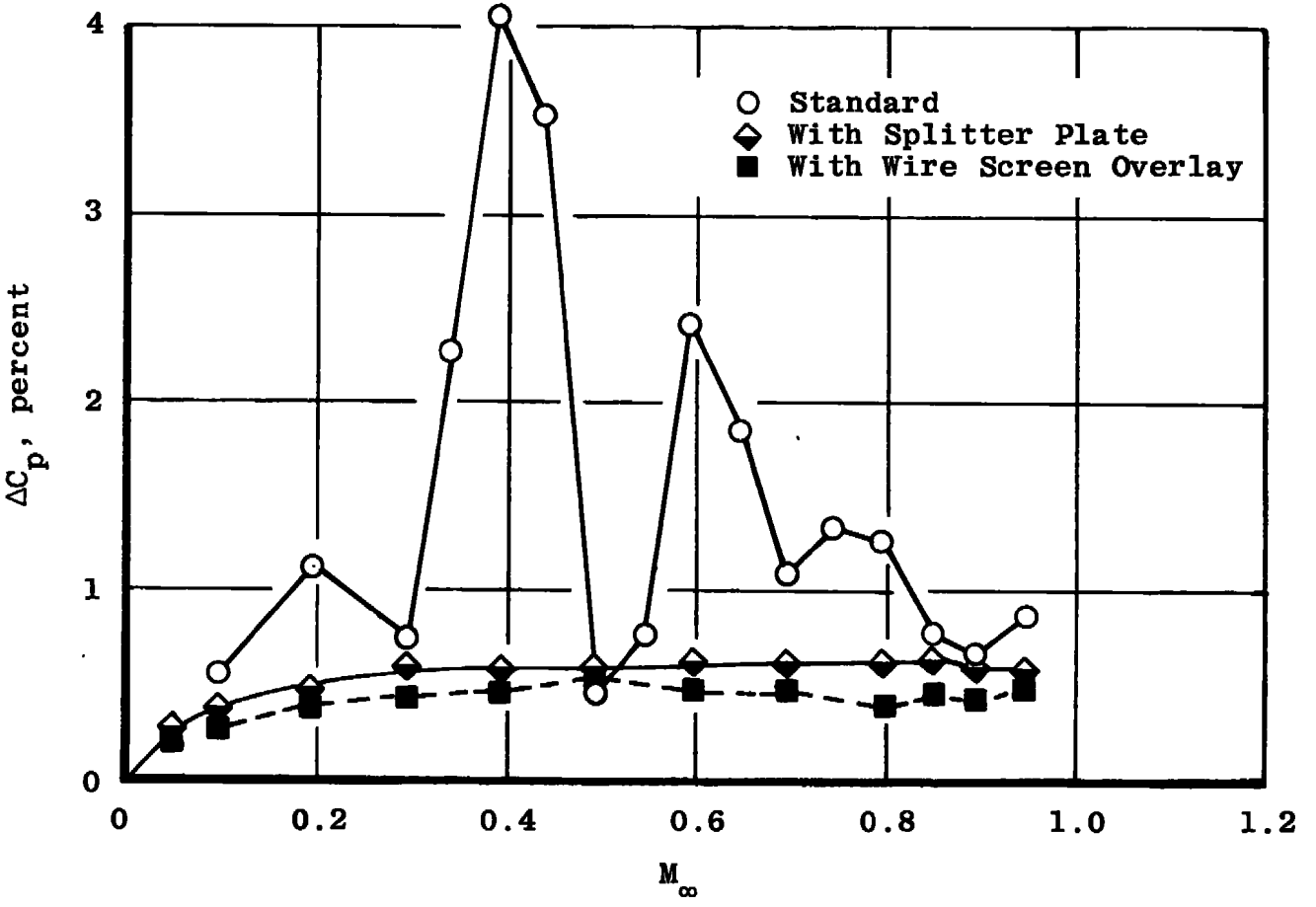

Figure 27. Amplitude of noise from Tunnel 1T wall samples.

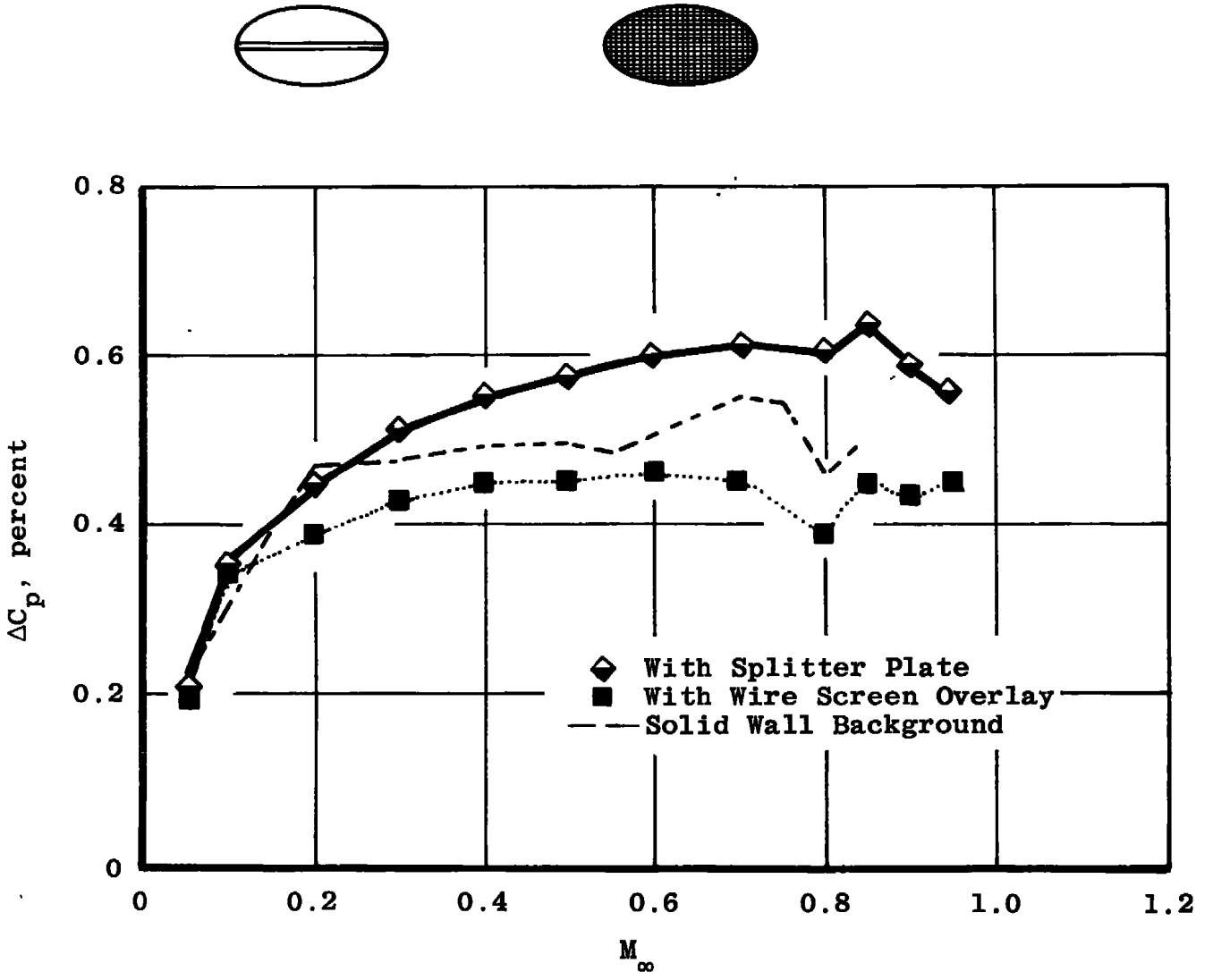

Figure 27. Concluded.

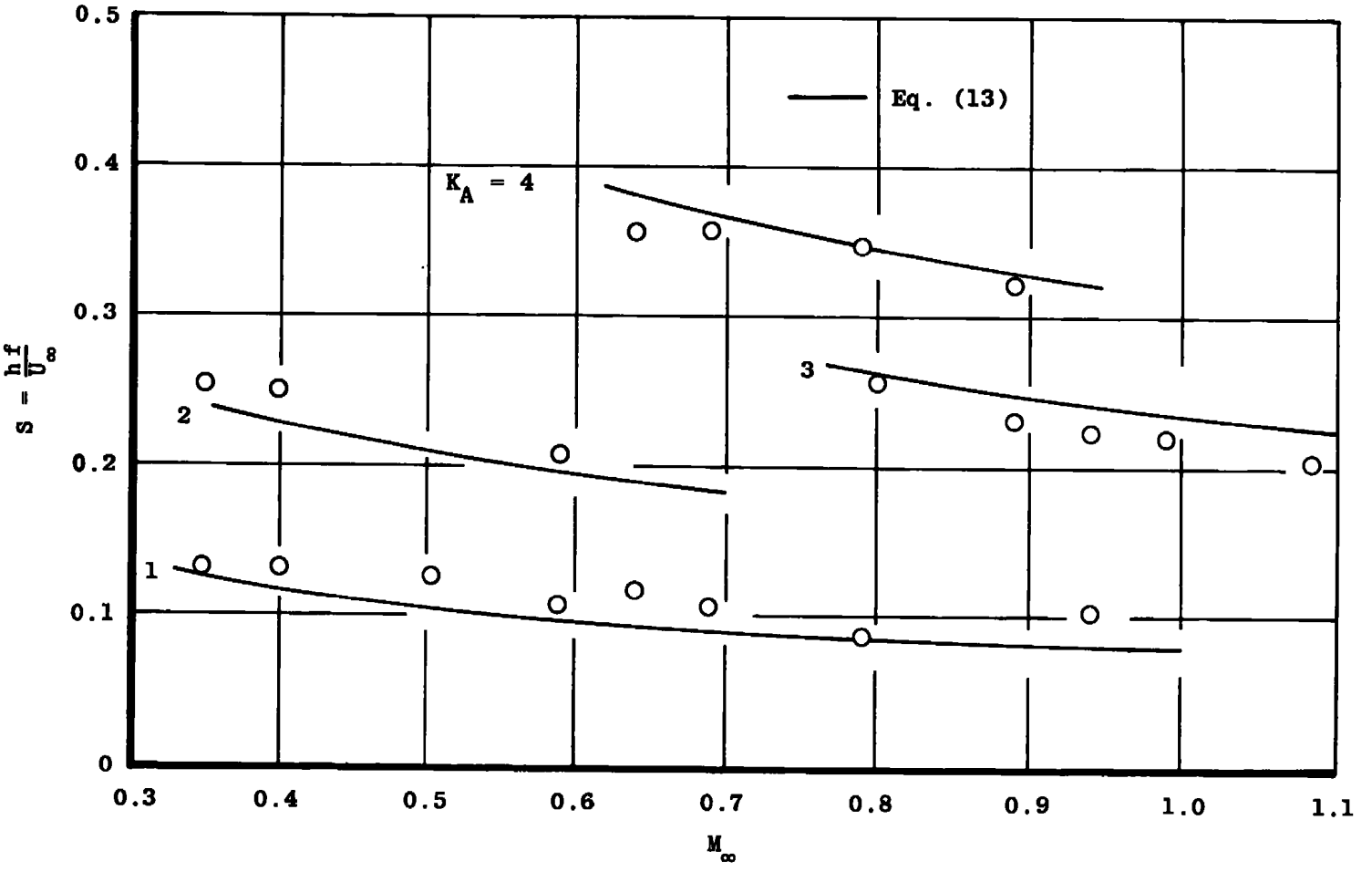

Figure 28. Predominant frequencies from Tunnel 1T wall samples.

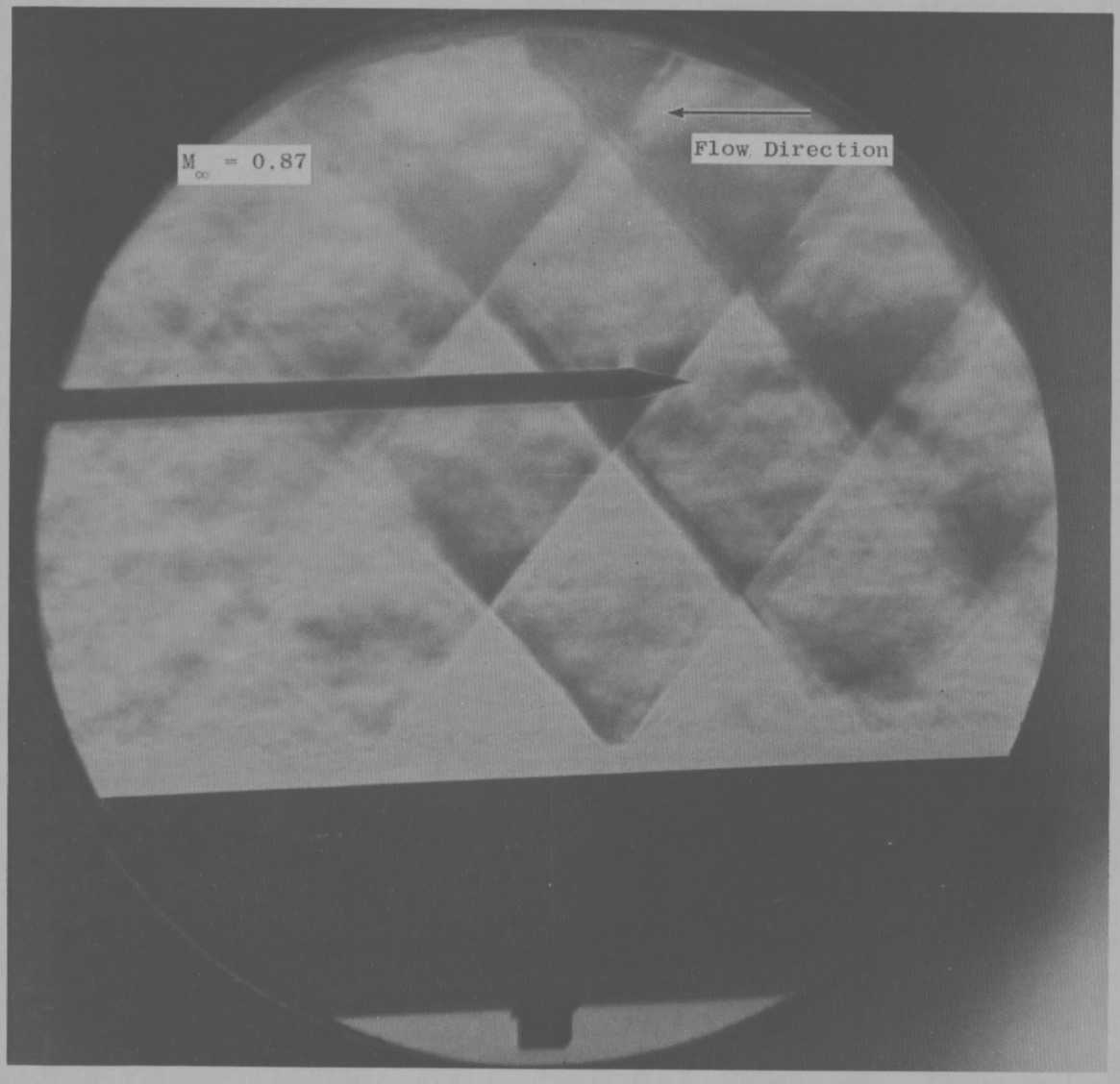

Figure 29. Schlieren view of sound field from Tunnel 1T wall samples.

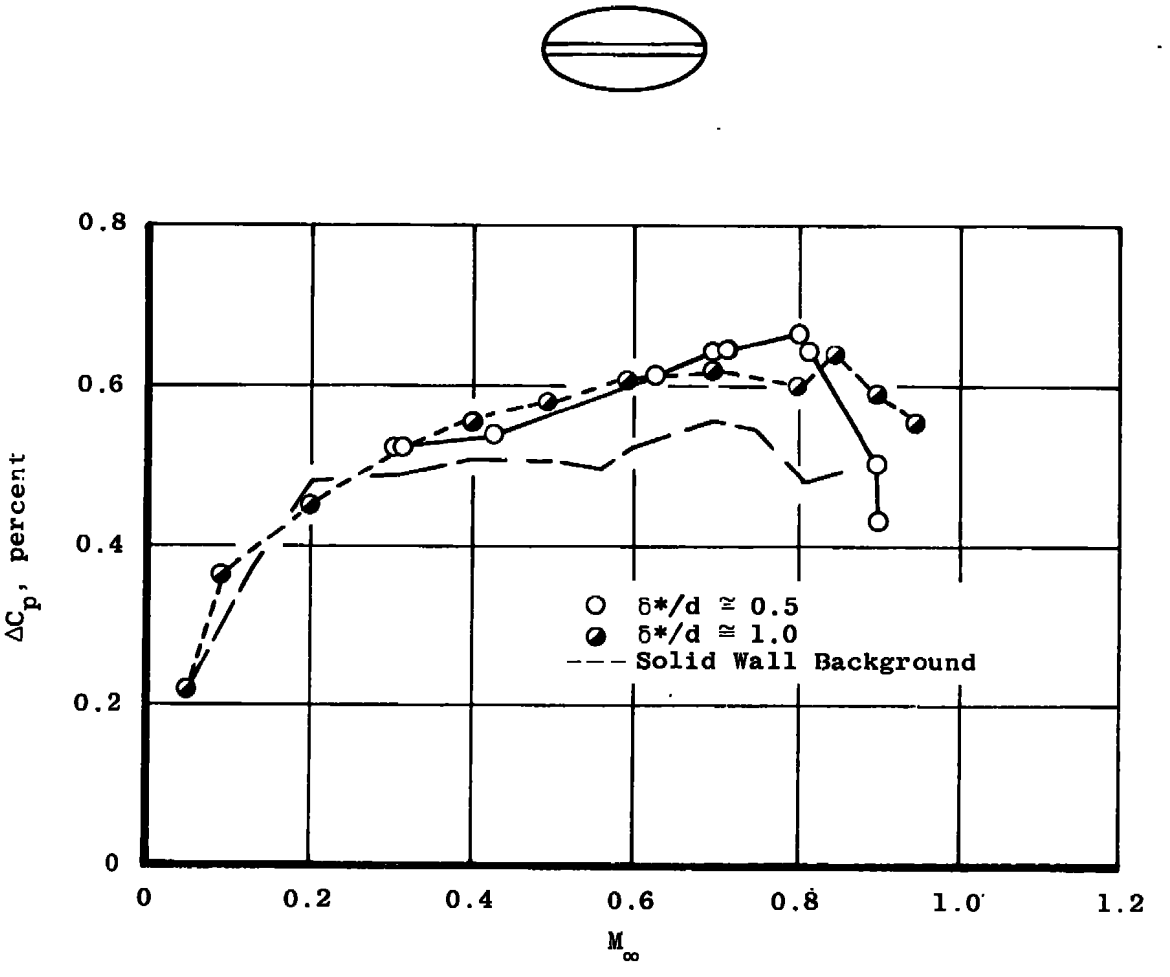

Figure 30. Splitter plate effectiveness in Tunnel 1T wall samples with varied boundary-layer thickness.

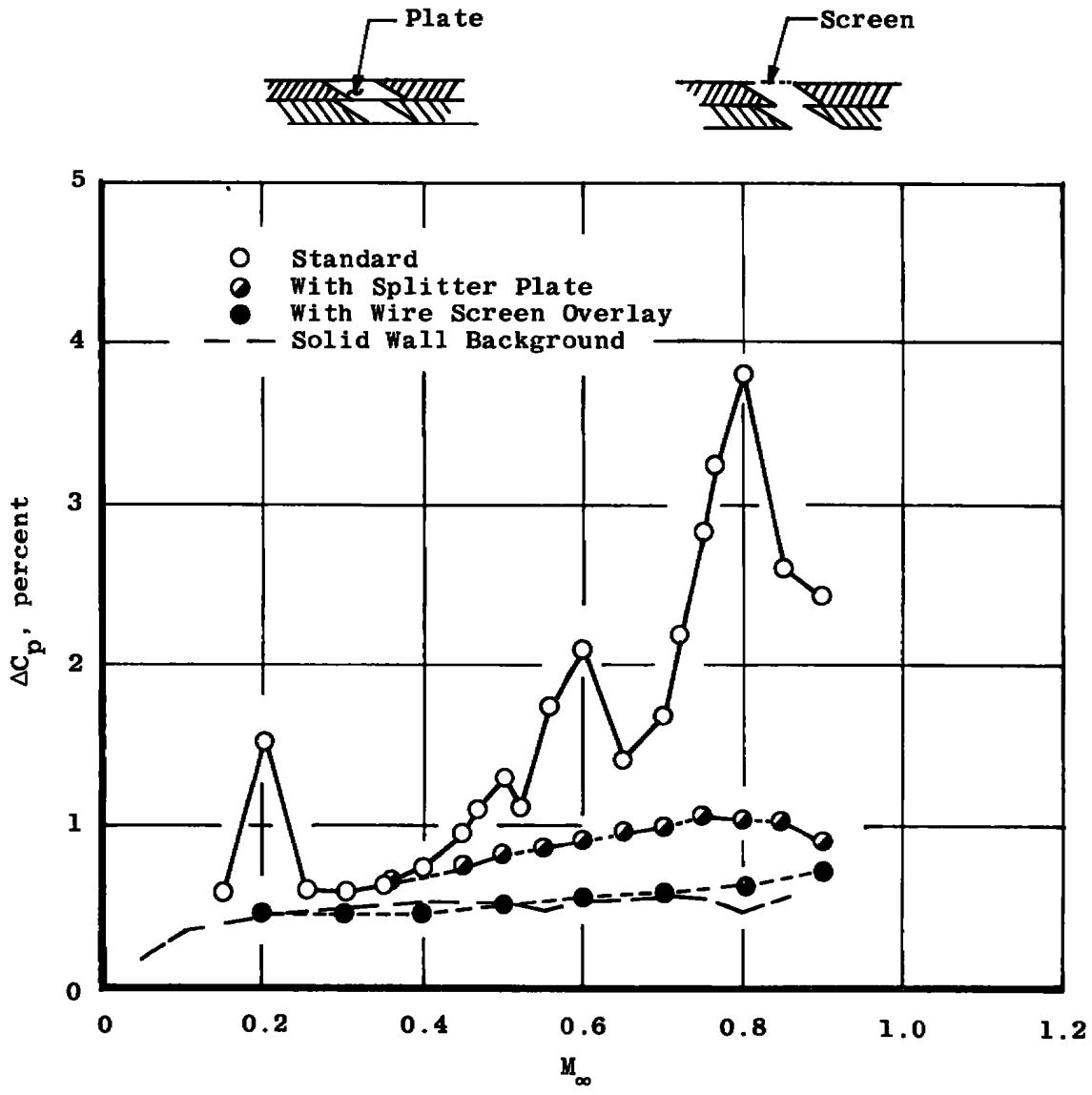

a. Porosity, τ = six percent

Figure 31. Noise data from Tunnel 4T variable-porosity wall samples.

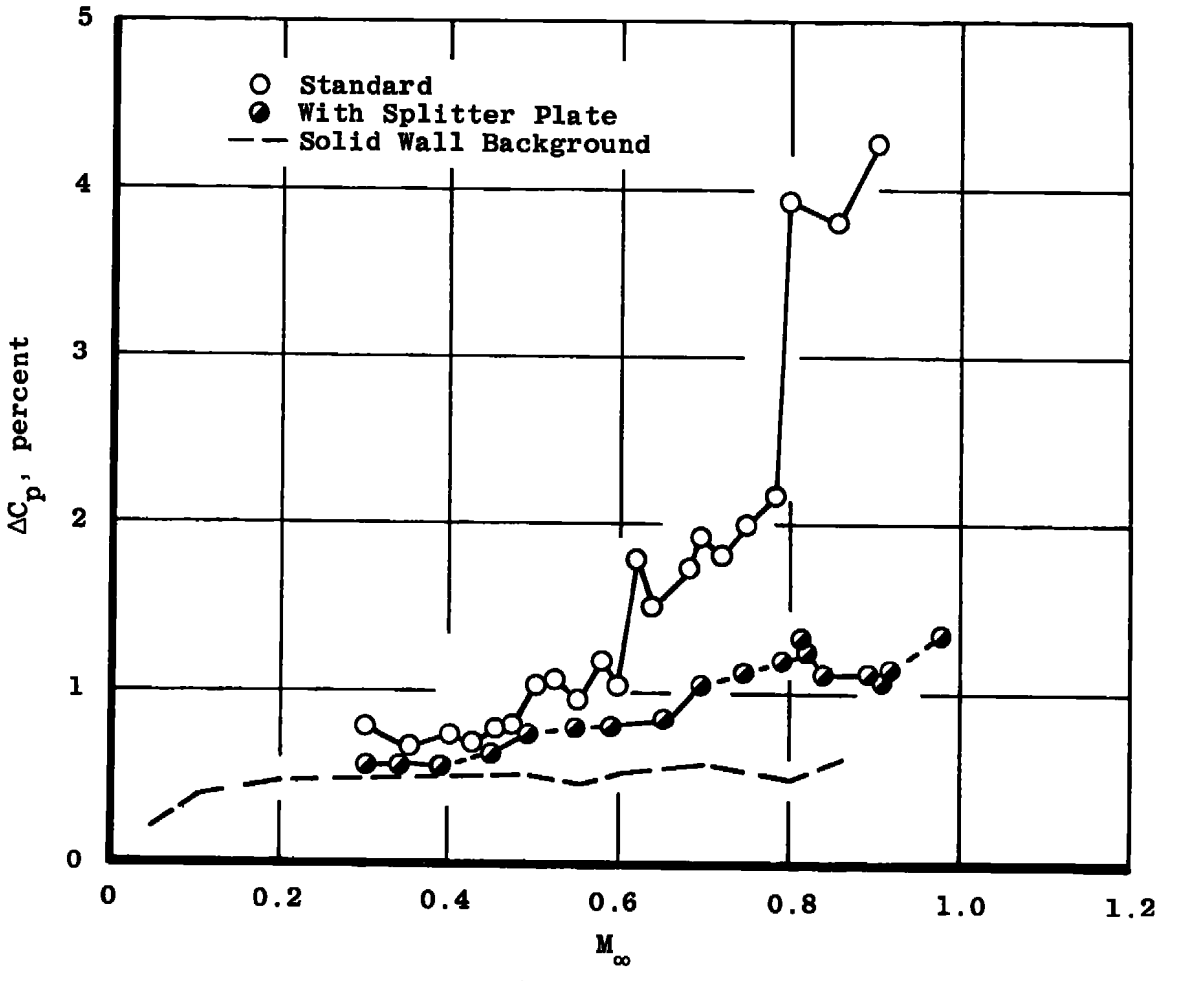

b. Porosity, τ = four percent
Figure 31. Concluded.

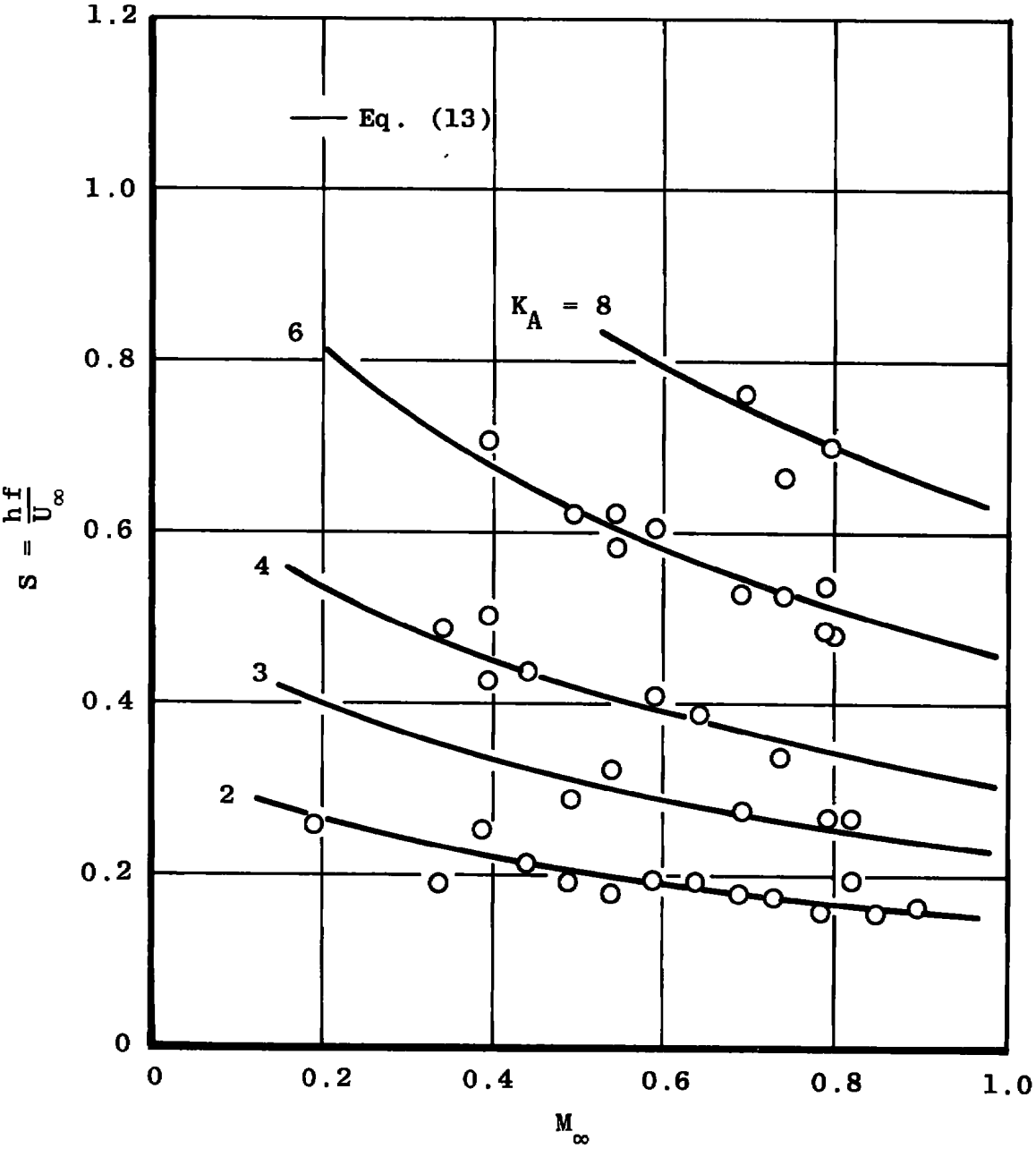

Figure 32. Predominant frequencies from Tunnel 4T wall samples.

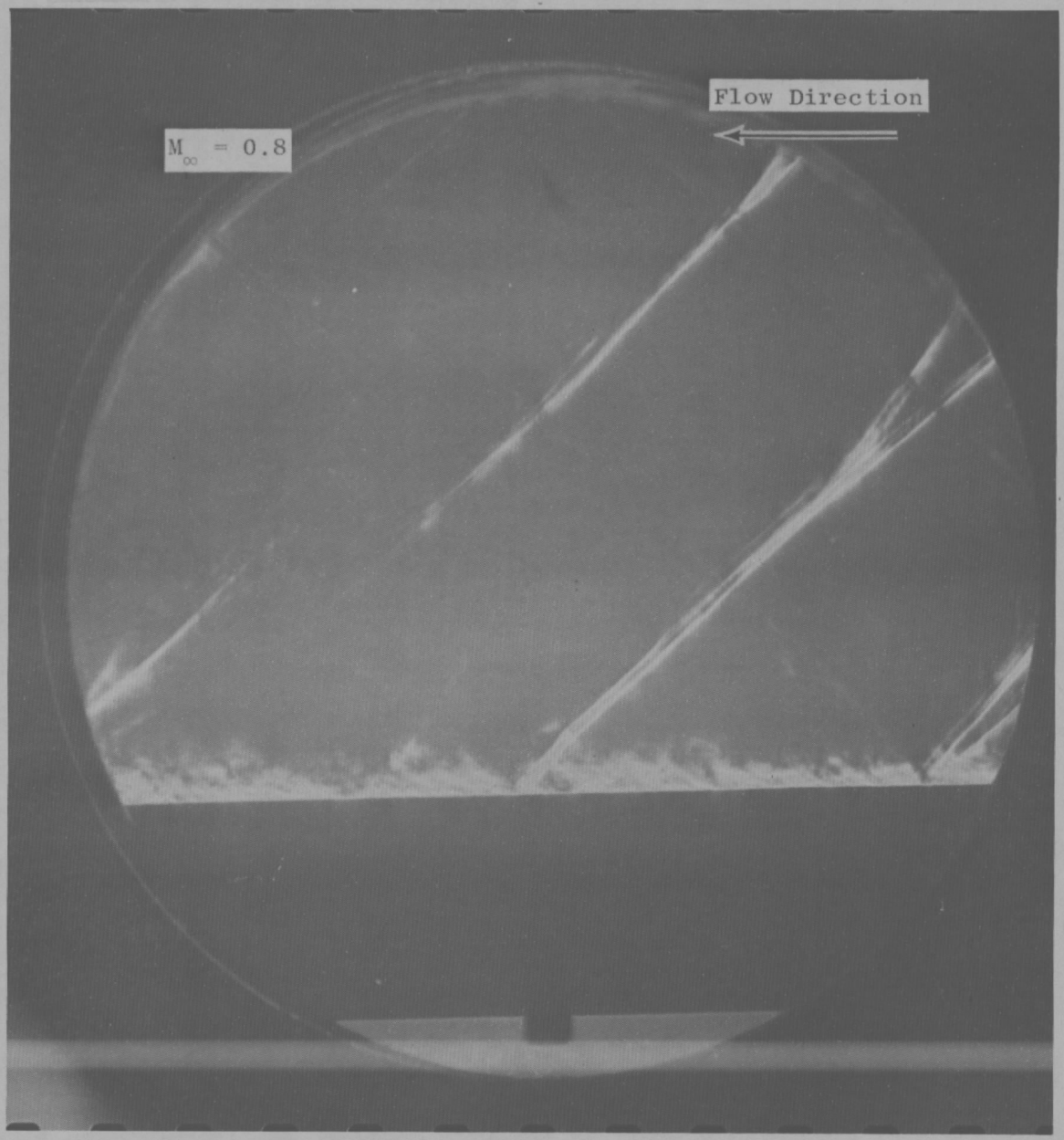

Figure 33. Shadowgraph view of sound field from Tunnel 4T wall samples.

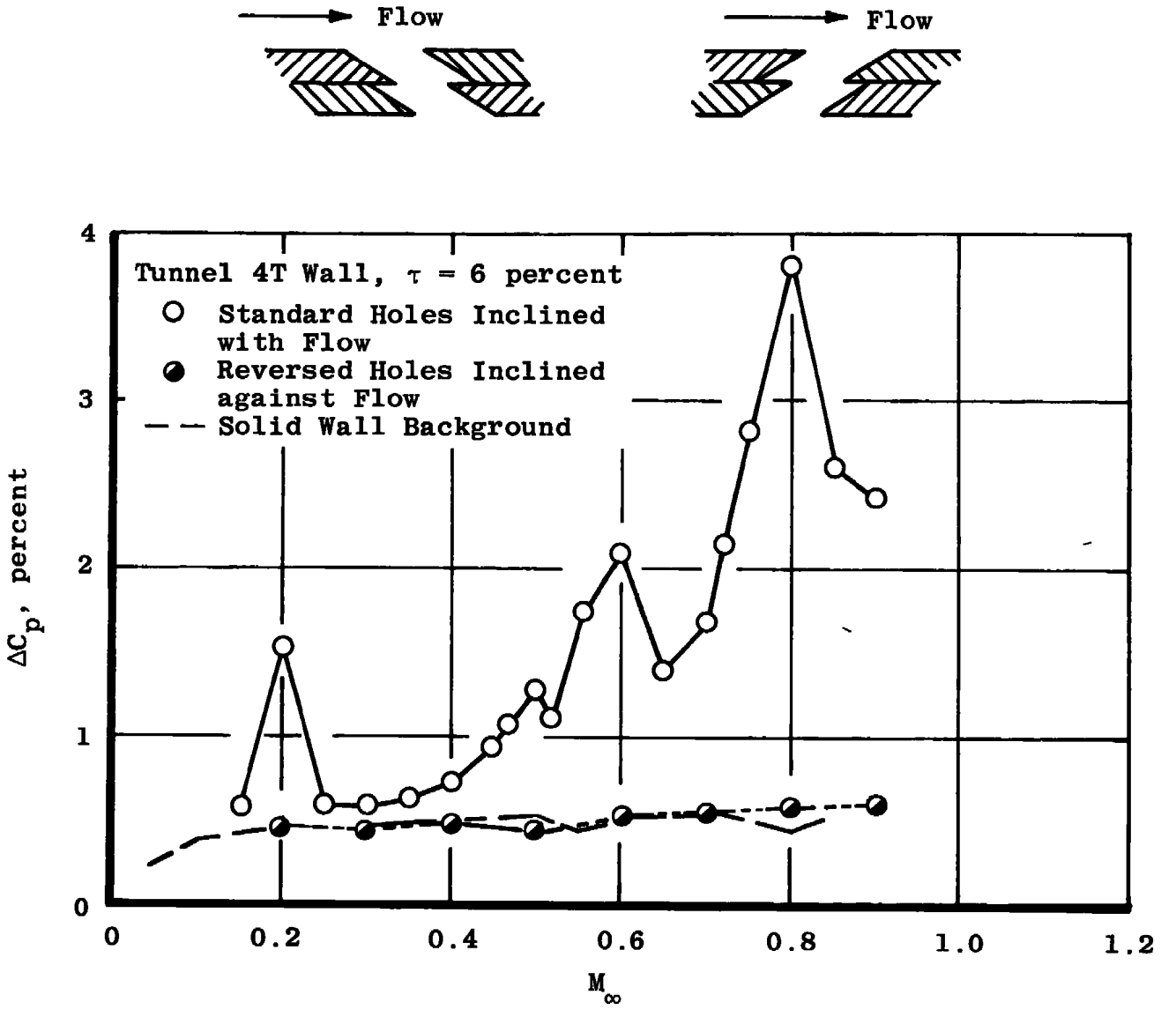

Figure 34. Effect on noise production from Tunnel 4T wall samples of reversing hole inclination direction.

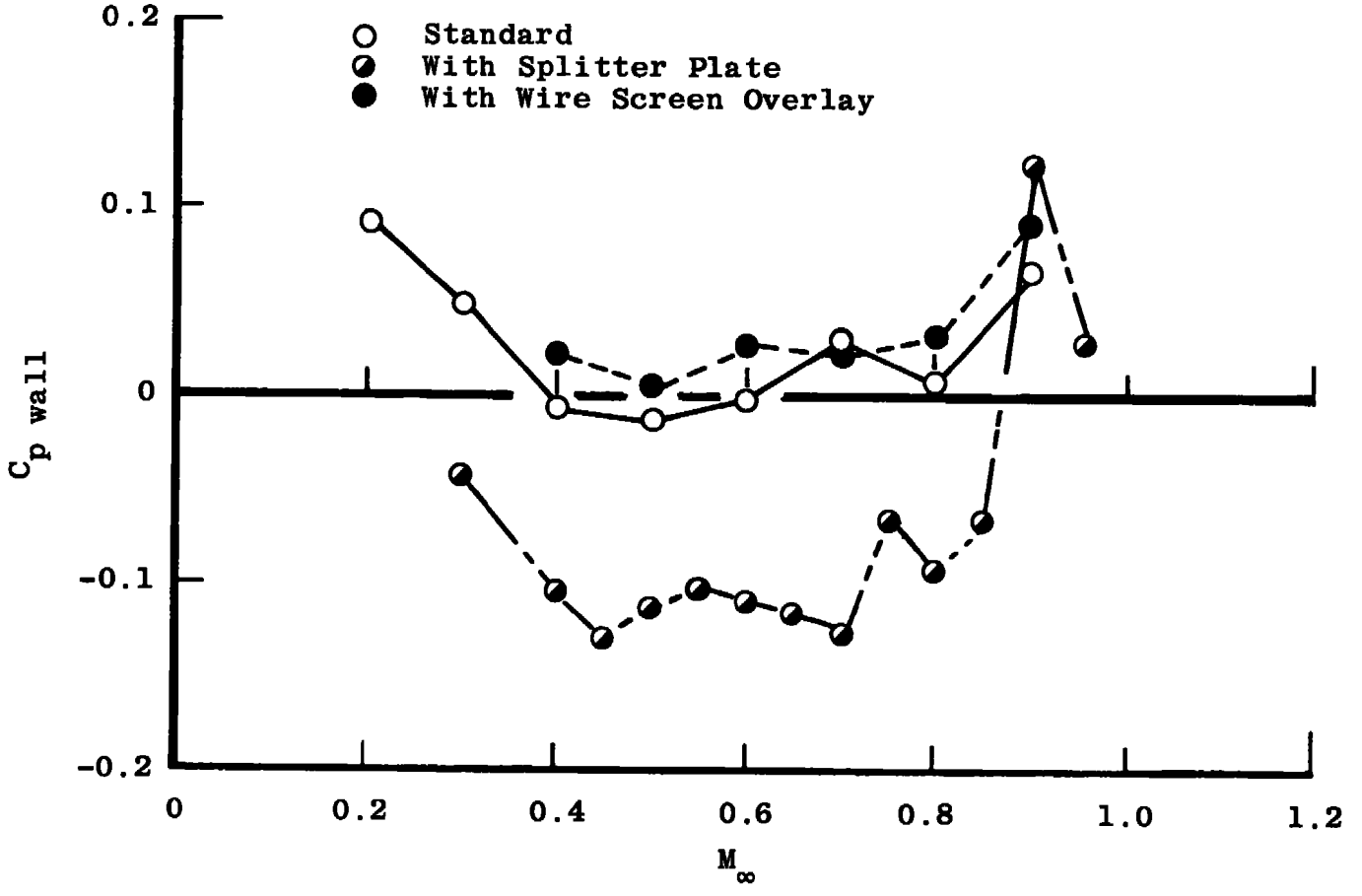

a. Porosity, τ = six percent

Figure 35. Differential pressures across Tunnel 4T wall samples.

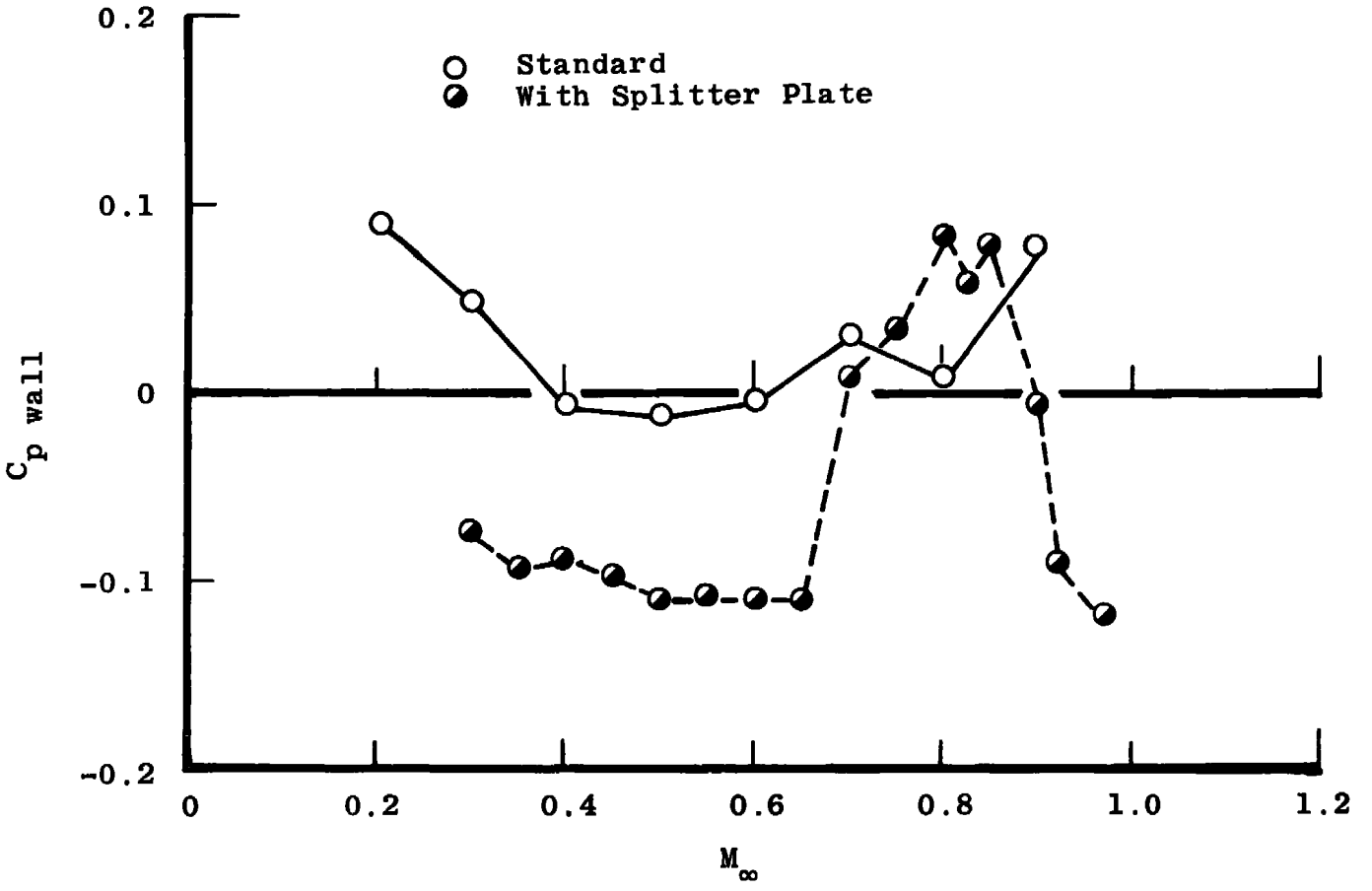

b. Porosity, τ = four percent
Figure 35. Continued.

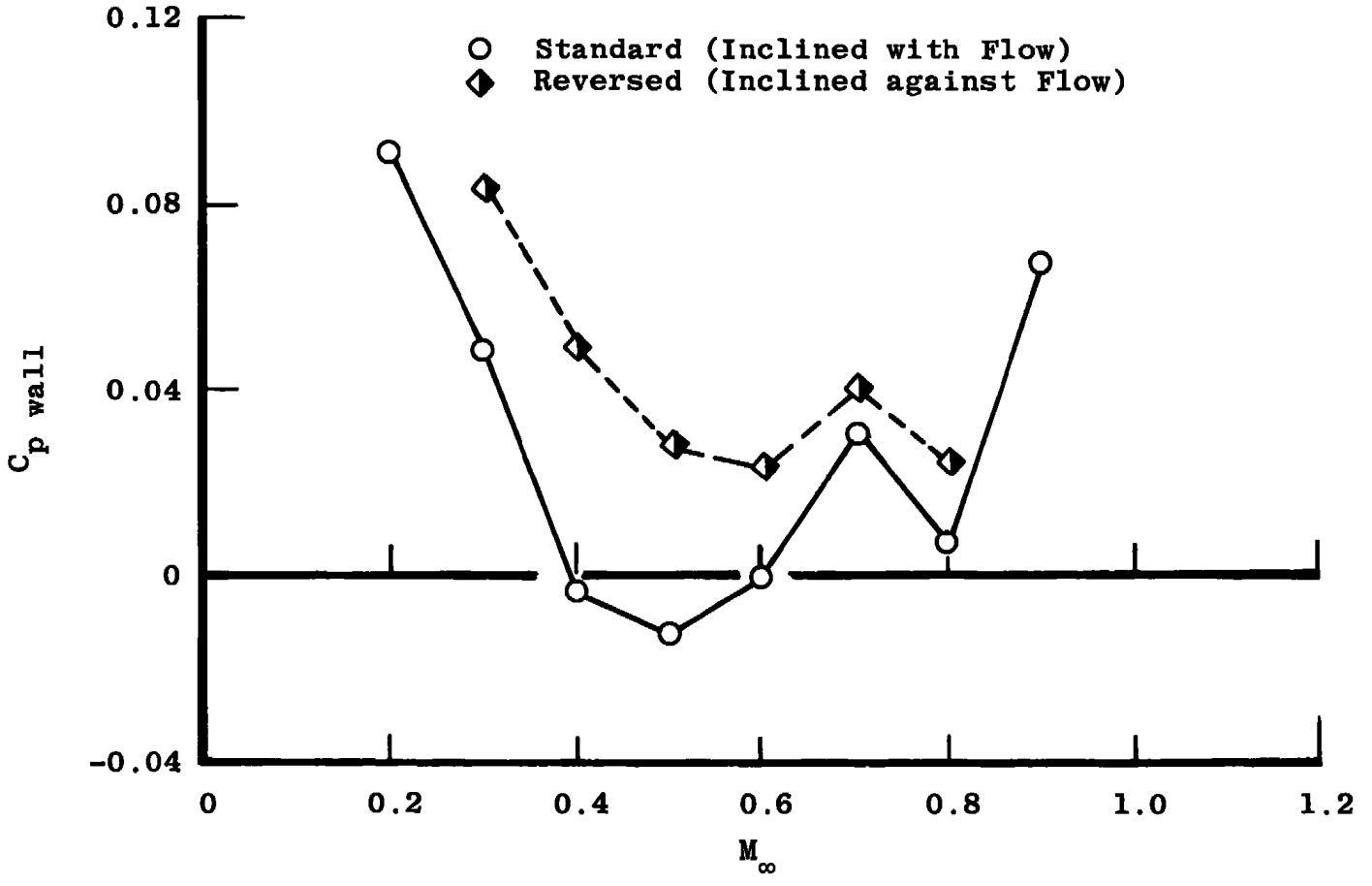

c. Porosity, τ = six percent, reversed inclination angle

Figure 35. Concluded.

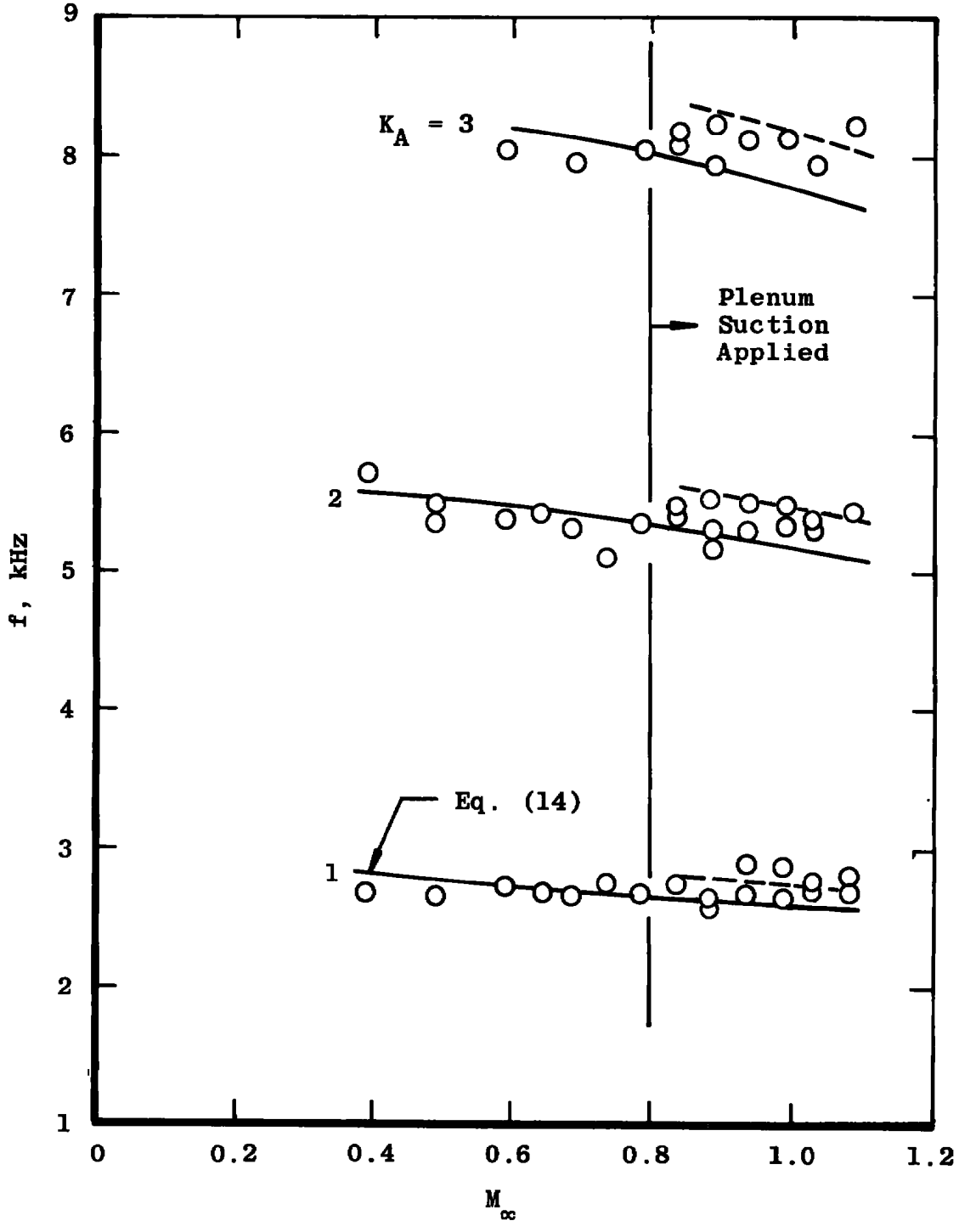

a. Measured frequencies

Figure 36. Frequencies from longitudinal baffled slots.

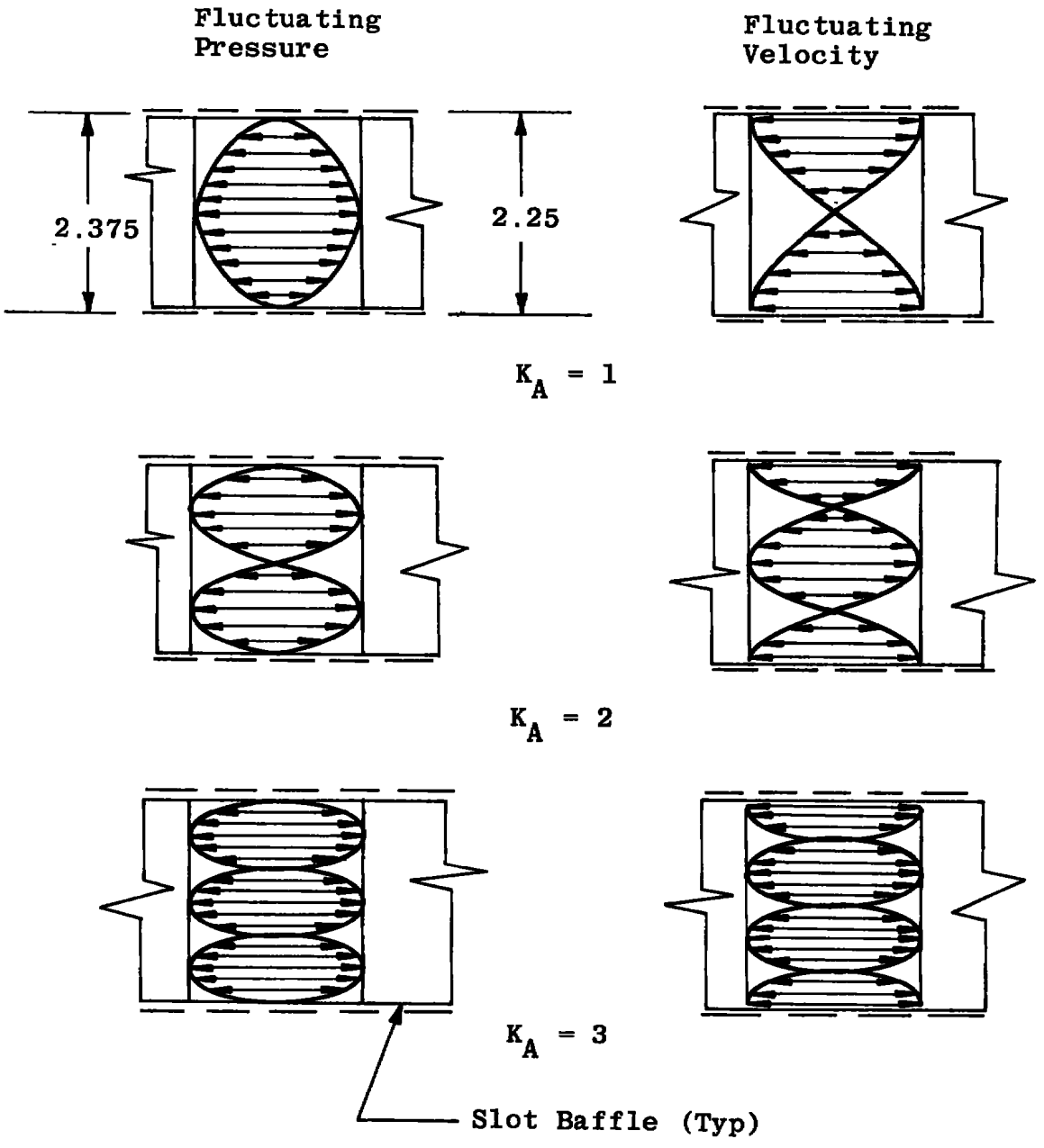

b. Suggested standing wave patterns
Figure 36. Concluded.

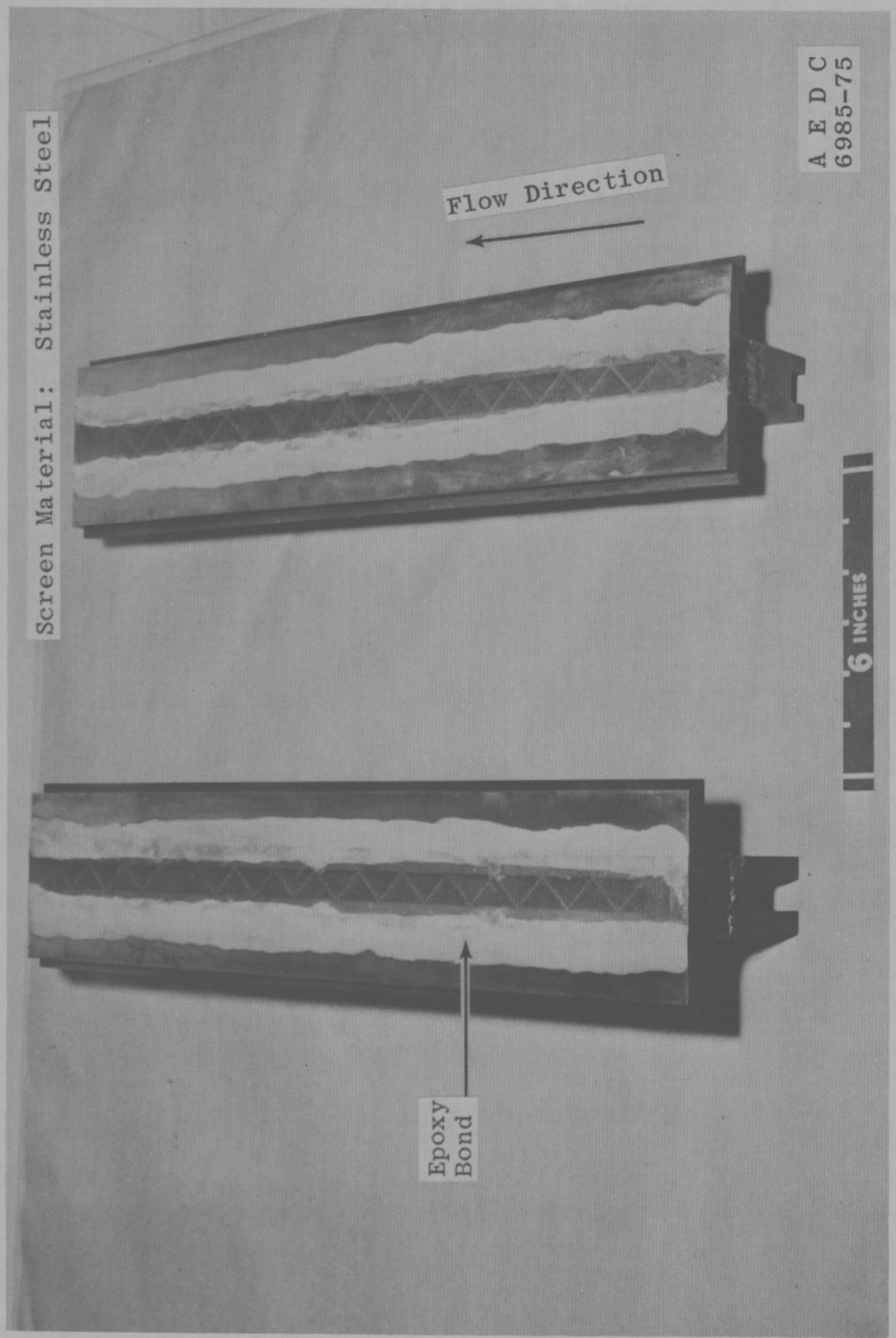

Figure 37. Wire screen overlay installation on baffled slots.

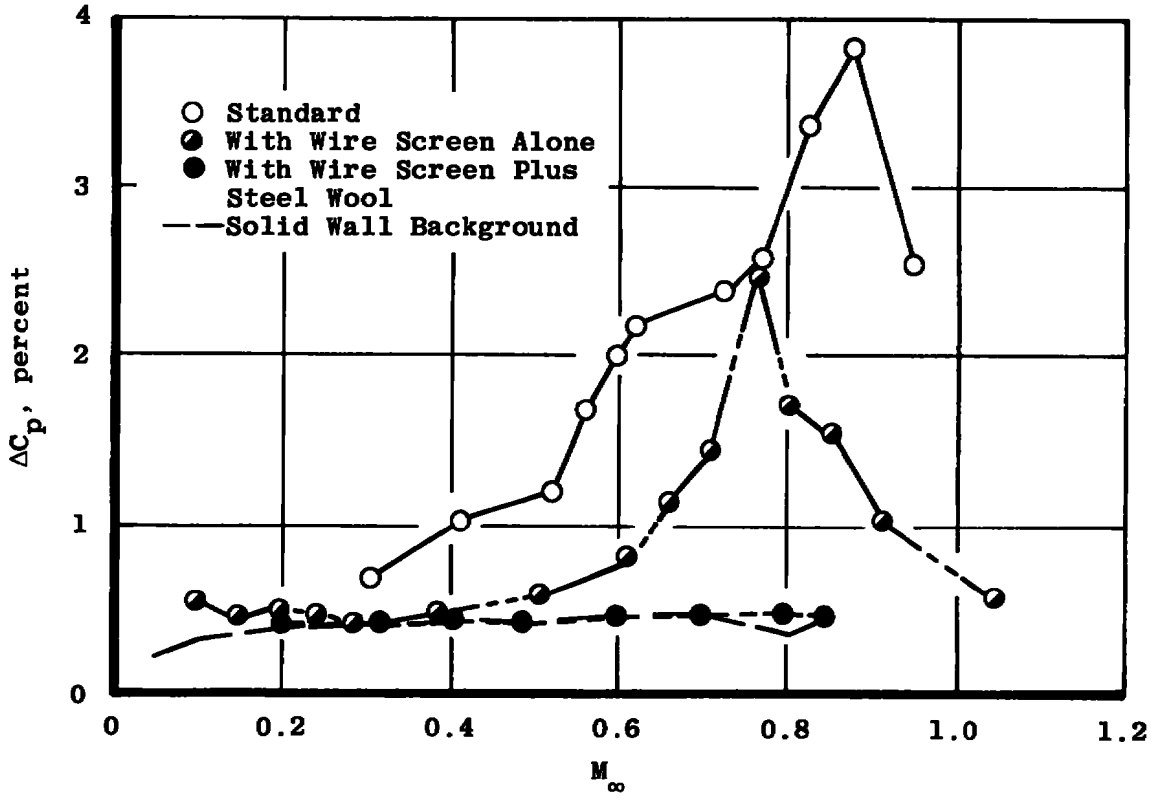

Figure 38. Noise levels from longitudinal baffled slots.

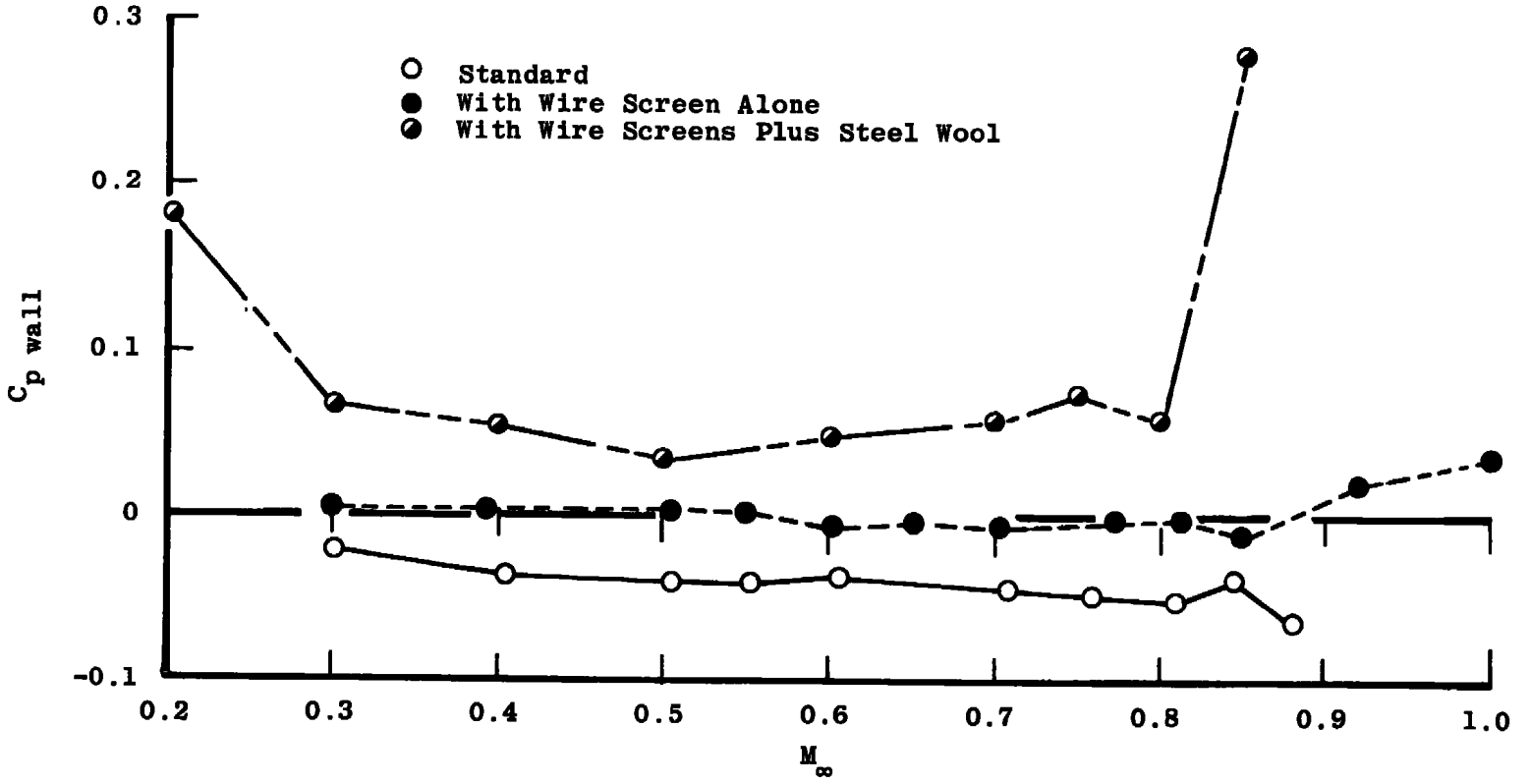

Figure 39. Wall differential pressures across longitudinal baffled slots.

Table 1. Position Schedule for Rod Walls

Porosity, τ, percent	Distance Movable Rods Are Depressed, in.*
0	0
1	0.019
2	0.026
4	0.037
6	0.046
10	0.060

*1/8-in.-diam Rods

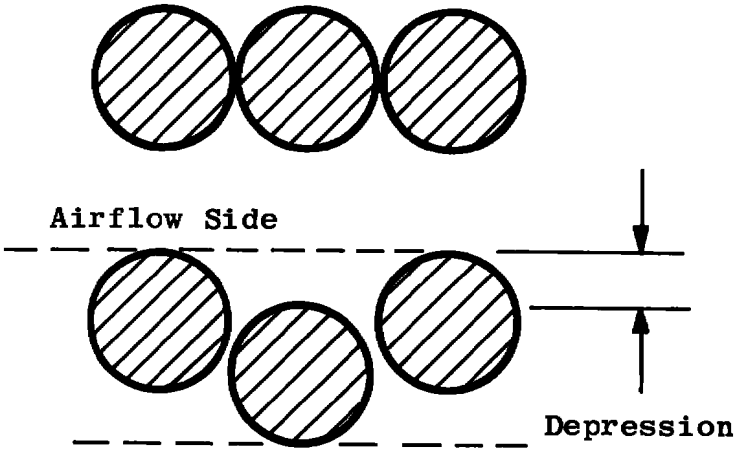

Section through Rods

Table 2. Test Summary

Wall Type	Characteristic Dimension, in.	Noise Suppression Measure	ΔC_{pmax}, percent	M_∞	Frequency, Hz
Longitudinal Tapered Slots	0.080 Maximum	None	0.60	0.75	None
Longitudinal Rods	0.125 Diameter	None	1.55	1.02	243
Longitudinal Baffled Slot	2.25 Depth	Standard	3.85	0.88	2,700
		Wire Screen Overlay	2.40	0.75	2,700
		Wires Screen Plus Steel Wool	0.55	0.80	None
Perforated Walls With Normal Holes - Thin Plate	0.50 Hole Diameter	Standard	4 .95	0.65	3,150
		Wire Screen Overlay	0.70	0.90	None
Perforated Walls with Normal Holes - Thick Plate	0.50 Hole Diameter	Standard	2.65	0.65	6,200
		Splitter Plate	5.95	0.60	6,200
		Wire Screen Overlay	0.70	0.90	None
Perforated Walls With Inclined Holes					
Tunnel 16T Samples	0.75 Hole Diameter	Standard	4.80	0.94	2.400
		Splitter Plate	1.05	0.78	2,400
		Wire Screen Overlay	0.63	0.94	None
Tunnel 4T Samples	0.50 Hole Diameter	Standard	4.25	0.90	1,900
		Splitter Plate	1.25	0.82	1,900
		Wire Screen Overlay	0.75	0.90	None
Tunnel 1T Samples	0.125 Hole Diameter	Standard	4.00	0.40	4,400
		Splitter Plate	0.63	0.81	None
		Wire Screen Overlay	0.48	0.60	None

NOMENCLATURE

C_f	Wall boundary-layer friction coefficient
$C_{p\ wall}$	Wall differential pressure coefficient
c_∞	Free-stream speed of sound
ΔC_p	Fluctuating pressure coefficient, percent
d	Hole diameter
db	Decibel, Ref. 0.0002 dynes/cm^2
f	Frequency, Hz
f_1	A particular frequency
f_2	Another frequency
h	Distance from leading to trailing edge of a circular hole in the axis of flow, h = d/cos θ
K_A	Acoustic mode number, 1,2,3,4,....
ℓ_{eff}	Effective length dimension of an organ pipe
M_∞	Free-stream Mach number
p_c	Plenum chamber static pressure
p_s	Wall static pressure in test section

p_t	Tunnel total pressure
$p'(t)$	Instantaneous pressure fluctuation
$\tilde{p}_{rms}$	Overall root-mean-square fluctuating pressure level (time-averaged value)
q_∞	Free-stream dynamic pressure
R	Gas constant for air
Re_θ	Reynolds number based on wall boundary-layer momentum thickness
S	Strouhal number (nondimensionalized frequency)
T	Averaging time, sec
T_s	Free-stream static temperature
T_t	Tunnel total temperature
t	Wall plate thickness
U_∞	Free-stream velocity
V_1	A particular volume
V_2	Another volume
x	Axial distance measured from start of nozzle contraction
γ	Ratio of specific heats for air

δ^*	Wall boundary-layer displacement thickness
θ	Hole inclination angle from normal, also boundary-layer momentum thickness
τ	Wall porosity (percent open area of a ventilated wall)